



PB99-175622

**Project Report
NASA/A-1**

An Assessment of the 60 km Rapid Update Cycle (RUC) with Near Real-Time Aircraft Reports

**R.E. Cole
C. Richard
S. Kim
D. Bailey**

15 July 1998

Lincoln Laboratory

MASSACHUSETTS INSTITUTE OF TECHNOLOGY

LEXINGTON, MASSACHUSETTS



**Prepared for the National Aeronautics and Space Administration
Ames Research Center, Moffett Field, CA 94035.**

**This document is available to the public through
the National Technical Information Service,
Springfield, Virginia 22161.**

REPRODUCED BY: **NTIS**
U.S. Department of Commerce
National Technical Information Service
Springfield, Virginia 22161

This document is disseminated under the sponsorship of the NASA Ames Research Center in the interest of information exchange. The United States Government assumes no liability for its contents or use thereof.

24 September 1998

ERRATA

Document: Project Report NASA/A-1, "An Assessment of the 60 km Rapid Update Cycle (RUC) with Near Real-Time Aircraft Reports," R.E. Cole, C. Richard, S. Kim, and D. Bailey, published 15 July 1998.

This report requires corrections on pages 27 and 32. All the pages within that range are provided for you to insert into your copy of the document.

Publications Office
MIT Lincoln Laboratory
244 Wood Street
Lexington, MA 02420-9108

PROTECTED UNDER INTERNATIONAL COPYRIGHT
ALL RIGHTS RESERVED.
NATIONAL TECHNICAL INFORMATION SERVICE
U.S. DEPARTMENT OF COMMERCE

.

.

.

4.3. Interpolation to Aircraft Position vs. Nearest Value

There are two approaches used to compute the modeled wind vector that is matched to each aircraft observation once a wind field is matched to the aircraft time. The simplest approach is to take the wind vector at the Terminal Winds grid point nearest the aircraft. In this approach the RUC wind field is interpolated to the TW grid using bi-linear interpolation so that both wind fields are on the same grid. A more sophisticated approach uses bi-linear interpolation in 3-D on the surrounding eight grid points to interpolate the winds to the aircraft position. The value of the extra complexity was not known. Table 7 shows the results on the entire year database. The benefit to TW is about a third of a m/s for the RMS vector error and slightly less for RUC, and the benefit is greater for the larger percentile errors. Given the substantial benefit relative to the modest increase in complexity of the second approach, the 3-D interpolation is justified for use in CTAS. For this report, only results using the 3-D interpolation are given, except in Table 7.

Table 7.
Comparison of Results Using Interpolation of Wind
to Aircraft Position vs. Using Nearest Wind Value
 Results are for 1,228,588 aircraft reports. Values are in m/s.

<u>variable</u>	<u>mean+/-std</u>	<u>RMSE</u>	<u>50%</u>	<u>75%</u>	<u>90%</u>	<u>95%</u>
<u>TW vector error</u>						
nearest	4.53±3.21	5.55	3.82	5.91	8.47	10.44
interpolated	4.26±2.95	5.18	3.64	5.54	7.85	9.61
<u>RUC vector error</u>						
nearest	5.85±3.76	6.96	5.14	7.62	10.52	12.73
interpolated	5.67±3.64	6.74	4.99	7.38	10.18	12.31

4.4. Performance Results Over All Reports

A number of statistics are computed over the entire year. These results provide information on the sorts of errors encountered by the aircraft. Since the aircraft are not uniformly distributed in space and time, these results are not necessarily an accurate or full account of the quality of the wind fields. Since a goal of this study is to determine the accuracy of the wind fields relative to CTAS, it is important to study the errors encountered as opposed to studying the fields in general. For example, the results are dominated by the aircraft at cruise altitudes, except for the results broken down by altitude. There are also more aircraft after May due to United Airlines turning on many of their aircraft in order to provide more numerous data on ascent and descent.

The results for the entire year are provided in Table 8. Over 1.2 million MDCRS are used on 343 days. Since the statistics are for (MDCRS - Model), a negative value for u error, v error, or speed error indicates that the model wind is larger than the MDCRS wind. The results show that RUC has small biases and the addition of recent MDCRS data reduces these biases. Both RUC and TW have a slight high bias in speed, -0.6 m/s and -0.4 m/s, respectively. However, these small biases are misleading, as seen in Section 4.5. The wind over the year averaged a little over 20 m/s from west southwest. By all measures, adding recent MDCRS to RUC improves performance both in the on-average measures and in the reduction of outliers.

As noted earlier, the errors in the MDCRS reports enter into the errors in Table 8. Table 9 provides the uncorrected RMS error estimates in RUC and TW, along with values that are corrected to remove the effects of the MDCRS errors. Both of the estimates of the MDCRS errors are used to show the effect of differing estimates of the MDCRS errors. For CTAS applications, 5 m/s is a significant headwind error. The RMS component errors for RUC are fairly close to 5 m/s even after correction, while the RMS component errors after adding recent MDCRS, at about 3.1 m/s, are well below 5 m/s.

In addition to bulk statistics, it is useful to consider the distribution of errors. Figure 6 provides a histogram of percent of MDCRS and count of MDCRS vs. vector error. The addition of recent

Table 8.
Comparison of 60 km RUC and 10 km TW

Results are for 1,228,588 aircraft reports.
(1,131,373 reports for % Speed Errors and Direction Errors)
Values are in m/s, except for % speed error, which is unitless,
and direction, which is in degrees.

variable	mean+/-std	RMSE	50%	75%	90%	95%
TW u error	-0.25±3.62	3.63	-0.27	1.84	4.03	5.59
TW v error	0.09±3.69	3.69	0.15	2.18	4.25	5.71
TW vector error	4.26±2.95	5.18	3.64	5.54	7.85	9.61
TW % speed error	-0.40±22.9	22.9	0.9	11.3	23.2	33.0
TW direction error	-0.01±16.1	16.1	-0.27	5.78	13.8	21.0
RUC u error	-0.22±4.61	4.62	-0.38	2.51	5.45	7.48
RUC v error	0.40±4.90	4.91	0.56	3.35	6.04	7.86
RUC vector error	5.67±3.64	6.74	4.99	7.38	10.18	12.31
RUC % speed error	-0.60±28.9	28.9	2.1	15.4	29.2	39.6
RUC direction error	-1.03±22.5	22.5	-1.24	6.78	17.29	27.36
wind speed	21.5±13.8	25.6	19.0	29.8	40.6	47.8
wind direction	252.6±67.9	261.5				

Table 9.
Comparison of 60 km RUC and 10 km TW RMS Errors
After Correction for MDCRS Errors
Corrected values using MDCRS RMS errors of 2.55 m/s and 2.78
m/s are given. Results are for 1,228,588 aircraft reports.
Values are in m/s.

variable	raw	corrected (2.55 m/s)	corrected (2.78 m/s)
TW u error	3.63	3.14	3.08
TW v error	3.69	3.23	3.09
TW vector error	5.18	4.51	4.37
RUC u error	4.62	4.25	4.20
RUC v error	4.91	4.58	4.48
RUC vector error	6.74	6.24	6.14

MDCRS is seen to reduce many of the vector errors greater than 5 m/s to less than 5 m/s. The number of very large vector errors also drops. The counts of vector errors in each bin above about 8 or 9 m/s is reduced by approximately half with the addition of recent MDCRS. Given the possible sensitivity of user acceptance to occasional incorrect CTAS guidance, the reduction in these very large errors due to the addition of recent MDCRS is very important.

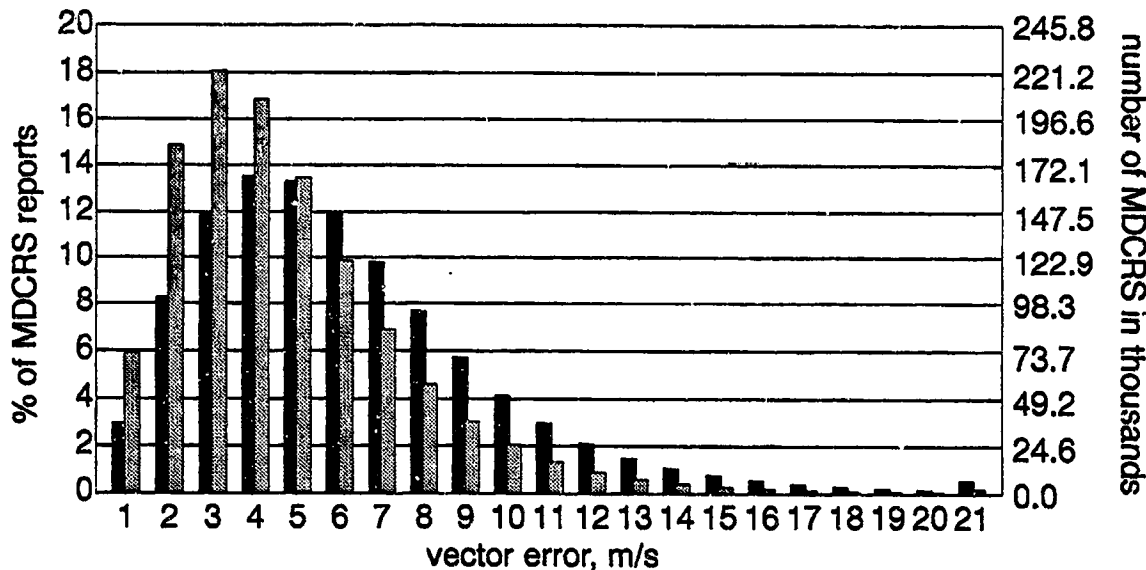


Figure 6. Histogram of the percent and number of MDCRS reports vs. RUC (black bar) and TW (gray bar) vector errors. Each bin labeled n contains errors between $n-1$ and n , except bin 21 which contains all errors 20 m/s and greater.

Another approach to examining these data is via a cumulative probability plot as in Figure 7. Here the percent of vector errors less than a value are plotted vs. that value. This allows the reader to set any vector error threshold and then to determine how often the vector errors are larger or smaller than this threshold. In Figure 7, RUC is seen to have 50 percent of its vector errors less than 5 m/s. Terminal Winds is seen to have 70 percent of its vector errors less than 5 m/s, or conversely, TW has 30 percent of its vector errors greater than 5 m/s. Terminal Winds has about half the number of errors as RUC for any threshold which is greater than about 6 m/s, again showing that the addition of recent MDCRS not only improves overall performance but also greatly reduces the potentially problematic outliers.

4.5. Performance Results vs. Wind Speed

Wind speed is one of the primary indicators of error magnitude. Figure 8 shows the RMS and 90th percentile vector error for various wind speeds. The errors rise monotonically with wind speed. For wind speeds of zero to about 60 m/s, the rise in error is roughly linear, especially for TW. The increase in RUC error with wind speed is more nearly linear if the errors are corrected for the MDCRS errors since the correction is larger for smaller errors. The errors rise more rapidly for wind speeds above approximately 60 m/s. However, this may be due to sampling error; there are hundreds of thousands of samples from 5 m/s to 30 m/s, tens of thousands of samples from 35 m/s to 60 m/s, and dropping by about 50 percent for each bin thereafter to only 160 samples at 85 m/s.

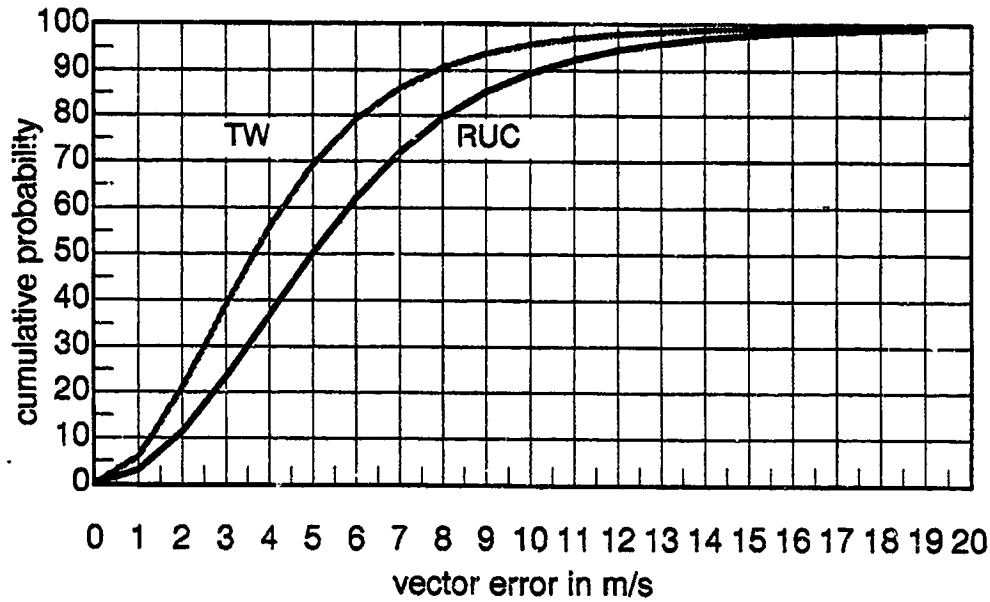


Figure 7. RUC and TW cumulative probability vs. vector error.

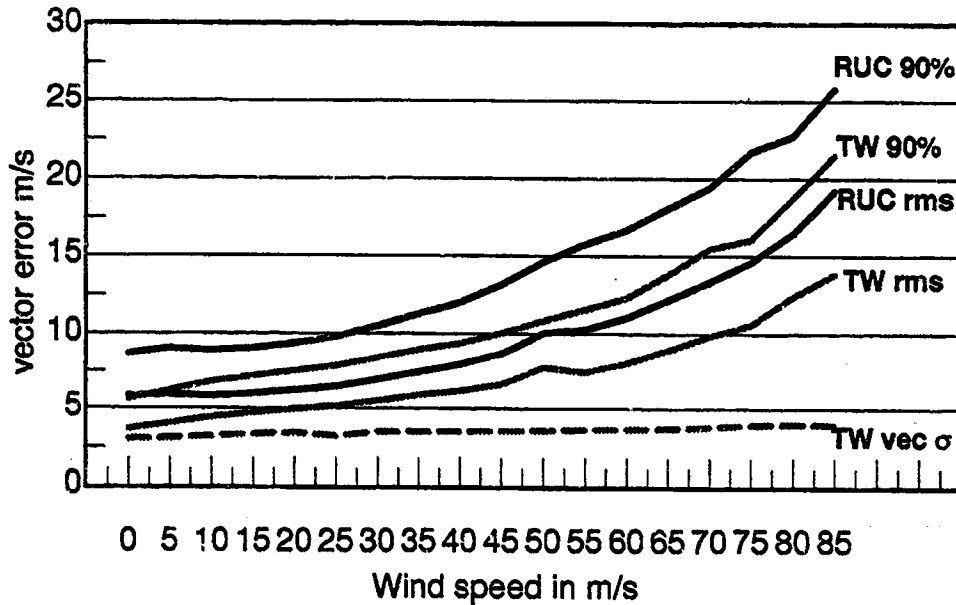


Figure 8. Vector error vs. wind speed. Both the RMS vector error and the 90th percentile error are shown. The TW estimate of the standard deviation of the vector error is shown by the dashed line.

Also plotted in Figure 8 is the mean of the TW estimates of the standard deviation of the vector error for each speed bin. These values are computed in the TW system for use in the interpolation, and these values are largely a function of data density at a given location. The relationship between these values and the actual computed vector errors is considered in the next section. Errors are expected to rise as these TW error estimates rise. Given that low wind speeds generally occur near the ground and high wind speeds generally occur aloft and that the data density may vary with altitude, the apparent relationship between vector errors and wind speed may reflect the influence of data density changes with altitude. However, as Figure 8 shows, there is very little change in the TW error

estimates with mean wind speed, although the change has the same trend as the vector errors vs. wind speed plots.

It is important to understand the nature of the error vs. speed results in Figure 8. Figure 9 shows the ratio of speed error to wind speed, with a change in sign so that a negative value indicates an underestimation. RUC underestimates the wind speed more than half the time for winds over 15 m/s and the underestimation grows with wind speed. This means that the errors in strong winds are not only very large but are systematic. The addition of recent MDCRS to RUC reduces the amount of underestimation by about half. When winds are strong, even the 90th percentile errors are negative, indicating that virtually all reported winds are too light. These results are especially problematic since they indicate that during strong winds the errors in RUC are large and highly correlated; these two attributes can interact to cause large errors in time-of-flight estimates. The addition of recent MDCRS to RUC greatly reduces both the magnitude of the errors and their correlation.

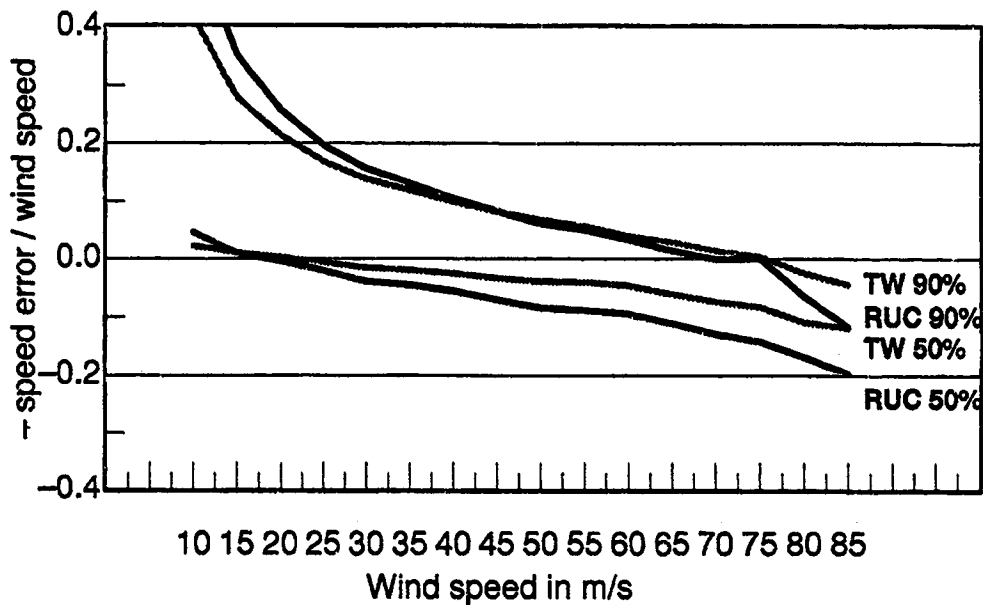


Figure 9. Speed error/wind speed vs. wind speed. Both the median and the 90th percentile percent speed error are shown.

4.6. Performance Results vs. TW Estimates of Error Variance

The TW algorithm uses a statistical interpolation technique. The interpolation technique provides error variance estimates for each wind component, and these estimates are used to derive TW estimates of the RMS vector error. These TW estimates of RMS error depend on error models for errors in RUC and in the MDCRS, as well as how these errors grow with distance and how these errors are correlated; they are a direct measure of information density. If the error models are perfect and the hypotheses underlying the theorems applied held, there would be perfect statistical agreement between the measured RMS vector errors and the TW estimates of RMS error. The achieved relationship between the measured estimates of the RMS vector error vs. the TW estimates of the RMS error is given in Figure 10 along with the mean wind speed vs. the TW estimate of RMS error. All the measures of error grow with the TW estimate of error for small values of the RMS error, but unfortunately so does the wind speed. This presumably occurs because these points are near the air-

port where air traffic is most dense and wind speeds lowest. After a TW estimate of RMS error of about 3 m/s, the mean wind speed is nearly constant. The RUC RMS error is also nearly constant, indicating that the wind speed is no longer a factor in the measured TW errors. In this region the TW RMS and 90th percentile errors continue to grow, indicating that the measured errors do grow with increasing TW estimate of RMS error or with decreasing data density. This relationship is stronger for the 90th percentile errors than for the RMS error. As expected, as the data density decreases, the TW errors converge to the RUC errors.

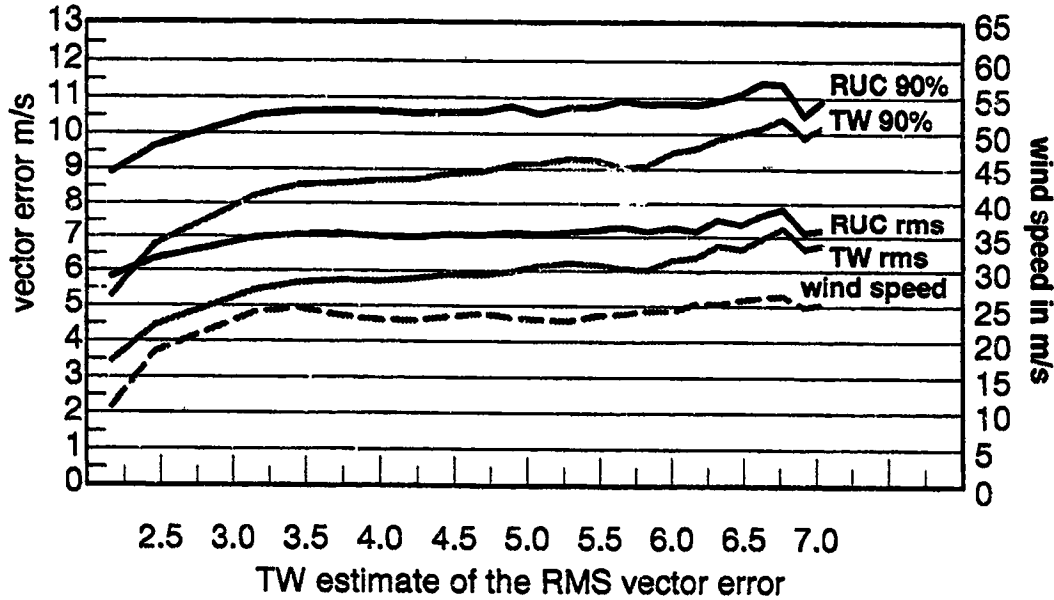


Figure 10. Vector error vs. TW estimate of the RMS vector. Both the RMS vector error and the 90th percentile error are shown, as is the mean wind speed vs. TW estimate of the RMS vector error.

The MDCRS errors partly obscure the relationship between TW vector errors and the TW estimates of the vector error in Figure 10. Figure 11 shows the measured RMS vector errors for RUC and TW corrected for the MDCRS errors (assuming a MDCRS error of 2.78 m/s) vs. the TW estimate of the RMS vector error. The horizontal and vertical scales in the figure are matched to highlight the relationship between the measured RMS vector errors and the TW estimates of the RMS vector error. The light gray line on the diagonal in Figure 11 gives the ideal relationship between the two values being plotted. There is some noise evident in the graph due to small sample sizes when the TW vector error estimates are above about 5 m/s. The dependence of the vector errors on wind speed is clearly evident at both ends of the graph. In the middle range of TW estimates of the RMS vector error, where the mean wind speed is fairly constant, the measured TW RMS vector error rises with the TW RMS vector error estimate, i.e., error increases with decreasing data density. Interestingly, RUC also shows a slight relationship with the TW data density. A conjecture is that regions where TW had many MDCRS reports in the recent past, RUC also had dense data somewhat farther back in time when the model was run, and thus RUC performs better in the same regions that TW performs better. The TW error models that underlie the TW estimates of the RMS vector error do not account for the wind speed. Accounting for the wind speed in the error models may or may not give much improvement in wind field accuracy, but it should improve the the TW estimates of the errors.

TECHNICAL REPORT STANDARD TITLE PAGE

1. Report No. NASA/A-1	2. Government Accession No.	3. Recipient's Catalog No.	
4. Title and Subtitle An Assessment of the 60 km Rapid Update Cycle (RUC) with Near Real-Time Aircraft Reports		5. Report Date 15 July 1998	6. Performing Organization Code
		8. Performing Organization Report No. NASA/A-1	
7. Author(s) R.E. Cole, C. Richard, S. Kim, and D. Bailey		10. Work Unit No. (TRAVIS)	
9. Performing Organization Name and Address MIT Lincoln Laboratory 244 Wood Street Lexington, MA 02420-9108		11. Contract or Grant No. NASA Ames	
		13. Type of Report and Period Covered Project Report	
12. Sponsoring Agency Name and Address National Aeronautics and Space Administration Ames Research Center Moffett Field, CA 94035		14. Sponsoring Agency Code	
15. Supplementary Notes This report is based on studies performed at Lincoln Laboratory, a center for research operated by Massachusetts Institute of Technology, under Contract to NASA Ames Research Center.			
16. Abstract NASA is developing the Center-TRACON Advisory System (CTAS), a set of Air Traffic Management (ATM) Decision Support Tools (DST) to enable controllers to increase airspace capacity and flight efficiency. A crucial component of the CTAS, or any ATM DST, is the computation of the time-of-flight of aircraft along flight path segments which requires accurate knowledge of the wind through which the aircraft are flying. CTAS currently uses wind information from the Rapid Update Cycle (RUC), a numerical prediction model run operationally by the National Weather Service (NWS) National Center for Environmental Prediction (NCEP). There exists near real-time wind observations from commercial aircraft that can be used to increase the accuracy of the RUC wind forecasts via the FAA Integrated Terminal Weather System (ITWS) Terminal Winds (TW) algorithm. This report presents a study based on the application of the ITWS TW algorithm as an improvement to the baseline PUC product. Terminal Winds generally does not support the full Center airspace; the domain of the prototype MIT/LL ITWS TW system was increased to cover the Denver Center airspace to support this study. This study has three goals: 1) determine the errors in the baseline 60-km resolution RUC forecast wind fields relative to the needs of en route DSTs such as CTAS, 2) determine the benefit of using the TW algorithm to refine the RUC forecast wind fields with near real-time Meteorological Data Collection and Reporting System (MDCRS) aircraft reports, and 3) identify factors that influence wind field errors in order to improve accuracy and estimate errors in real time. The data for this study were collected over a one-year period for the Denver Center airspace and over one million verification observations were used. This study is part of a larger effort funded by NASA which includes the NOAA/FSL.			
17. Key Words winds analysis air traffic management CTAS		18. Distribution Statement This document is available to the public through the National Technical Information Service, Springfield, VA 22161.	
19. Security Classif. (of this report) Unclassified	20. Security Classif. (of this page) Unclassified	21. No. of Pages 76	22. Price



ABSTRACT

The National Aeronautics and Space Administration (NASA) is developing the Center-TRACON Advisory System (CTAS), a set of Air Traffic Management (ATM) Decision Support Tools (DST) for en route (Center) and terminal (TRACON) airspace designed to enable controllers to increase capacity and flight efficiency. A crucial component of the CTAS, or any ATM DST, is the computation of the time-of-flight of aircraft along flight path segments. Earlier NASA studies show that accurate knowledge of the wind through which the aircraft are flying is required to estimate time-of-flight accurately. There are currently envisioned to be two sources of wind data for CTAS:

- The Rapid Update Cycle (RUC) for the Center airspace, a numerical model developed by the National Oceanic and Atmospheric Administration (NOAA) Forecast System Laboratory (FSL) and run operationally by the National Weather Service (NWS) National Center for Environmental Prediction (NCEP), and
- The Integrated Terminal Weather System (ITWS) Terminal Winds (TW) for the TRACON airspace, developed at MIT Lincoln Laboratory under funding from the Federal Aviation Administration (FAA).

The ITWS TW system takes in RUC data and refines the RUC forecasts with local measurements of the wind.

This report presents a study based in part on the application of the TW algorithm to the Center airspace as a value added improvement to the baseline RUC product. Terminal Winds generally does not support the full Center airspace; the domain of the prototype MIT/LL ITWS TW system was increased to cover the Denver Center airspace to support this study. The domain of the FAA operational ITWS TW may not extend more than 30 nautical miles beyond a given TRACON. This study is part of a larger effort funded by NASA which includes the NOAA/FSL.

This study has three goals: (1) determine the errors in the baseline 60 km resolution RUC forecast wind fields relative to the needs of en route DSTs such as CTAS, (2) determine the benefit of using the TW algorithm to refine the RUC forecast wind fields with near real-time Meteorological Data Collection and Reporting System (MDCRS) reports, and (3) identify factors that influence wind field errors in order to improve accuracy and estimate errors in real time.

The errors in the 60 km resolution RUC wind fields and the RUC wind fields augmented with near real-time MDCRS data via the TW algorithm are examined statistically over a one-year data set. The addition of the recent MDCRS data is seen to significantly improve the RMS vector error and the 90th percentile vector error (a statistic that captures extreme errors that may have a critical impact on the acceptability of en route DSTs advisories). The addition of the MDCRS data also reduces the number of hours of sustained large errors and reduces the correlation among errors.

The errors in the wind fields are seen to increase with increasing wind speed, in part due to an underestimation of wind speed which increases with increasing wind speed. The errors in the TW wind fields are seen to decrease with increasing numbers of MDCRS reports. The TW system, as part of its wind field estimation, produces an estimate of the error variance for each estimate of the wind. A relationship is shown to exist between the magnitude of the actual errors in the TW wind field and the TW estimates of the error variance. Different types of weather are also seen to influence wind field accuracy.

•

•

•

•

EXECUTIVE SUMMARY

The National Aeronautics and Space Administration (NASA) is developing the Center-TRACON Automation System (CTAS), a set of Air Traffic Management (ATM) Decision Support Tools (DST) for en route (Center) and terminal (TRACON) airspace designed to enable controllers to increase capacity and flight efficiency. A crucial component of the CTAS, or any ATM DST, is the computation of the time-of-flight of aircraft along flight path segments. Early NASA flight tests of the en route elements of CTAS discovered that variations in wind prediction error have a significant impact on the accuracy and value of en route DST advisories for ATC clearances.

There are currently envisioned to be two sources of wind data for CTAS:

- The Rapid Update Cycle (RUC) for the Center airspace, a numerical model developed at the National Oceanic and Atmospheric Administration (NOAA) Forecast Systems Laboratory (FSL) and run operationally by the National Weather Service (NWS) National Center for Environmental Prediction (NCEP), and
- The Integrated Terminal Weather System (ITWS) Terminal Winds (TW) for the TRACON airspace, developed at MIT Lincoln Laboratory under funding from the FAA.

The ITWS TW system takes in RUC data and refines the RUC forecasts with local measurements of the wind.

In light of the earlier NASA results on the effect of wind prediction errors, NASA initiated a collaborative effort with MIT/LL and NOAA/FSL to determine the variations in wind prediction accuracy and the impact of these variations on typical en route ATM operations; explore methods and algorithms to improve wind prediction accuracy (e.g., RUC improvements and real-time updates of RUC with recent observations via the TW algorithm); and develop wind error prediction models to support real-time ATM DST probabilistic analyses of trajectory/conflict prediction accuracy.

This report presents a study based on the application of the TW algorithm to the Center airspace as a value added improvement to the baseline RUC product. Terminal Winds generally does not support the full Center airspace; the domain of the prototype MIT/LL ITWS TW system was increased to cover the Denver Center airspace to support this study. The domain of the FAA operational ITWS TW may not extend more than 30 nautical miles beyond a given TRACON.

The goals of this study are to (1) determine the errors in the baseline 60 km resolution RUC forecast wind fields relative to the needs of en route DSTs such as CTAS, (2) determine the benefit of using the TW algorithm to refine the RUC forecast wind fields with near real-time Meteorological Data Collection and Reporting System (MDCRS) reports and identify factors that influence wind field errors in order to improve accuracy and estimate errors in real time.

To determine wind field accuracy, the wind fields are compared to a data set of aircraft reports from the MDCRS that are not included in the wind fields to which they are compared. More than one million MDCRS reports collected from 1 August 1996 to 1 August 1997 are used. These MDCRS reports are collected in a region approximately 1300 km on a side and centered on the Denver International Airport. Wind vector errors of 7 m/s – 10 m/s (approximately 10 knots – 15 knots of headwind error) are significant to CTAS.

Computed over the entire one-year data set, the RMS vector error for RUC is 6.74 m/s, which is reduced to 5.18 m/s for TW. The median vector error for RUC is 4.99 m/s, while incorporating recent MDCRS reduces these errors to 3.64 m/s, respectively. The 90th percentile RUC and TW vector errors are 10.18 m/s and 7.85 m/s, respectively. Also, it is seen that 11 percent of the RUC vector errors are greater than 10 m/s and this is reduced to four percent by the addition of the recent MDCRS data. The addition of recent MDCRS via the TW algorithm provides a significant improvement in these on-average wind field accuracy statistics.

Large errors are especially detrimental to CTAS if they are sustained over a large portion of the grid and over a long period of time. Examining the 50th percentile hourly vector error shows that out of the 7023 hours in the data set there are 829 hours when the hourly median RUC vector error is 7 m/s or more, and that adding recent MDCRS data to RUC reduces this number of hours to 124. There are 46 hours in the data set when the hourly median RUC vector error is 10 m/s or more, and adding recent MDCRS reduces this number of hours to 1. The addition of recent MDCRS data to the RUC wind field data provides a very large reduction in large sustained errors.

Another factor in whether or not wind field errors are detrimental to CTAS is their correlation in time and space. All else being equal, the wind field with the least correlation among errors will provide the smallest trajectory errors. Examining the correlation of errors for level flight over 20 minutes at 400 knots shows that errors in the RUC winds have correlation coefficients of approximately 0.45, and the addition of recent MDCRS reduces these coefficients to 0.23. The correlation of errors for a descending flight over 10 minutes at 400 knots shows that errors in the RUC winds have correlation coefficients in the range of 0.29 – 0.39, and the addition of recent MDCRS reduces these coefficients to 0.11.

United Airlines increased the frequency of their MDCRS reports from May through August of 1997 to support this study. This allows the study of TW wind field errors vs. number of MDCRS reports, where the number of MDCRS reports is varied from less than the current normal to greater than the current normal. The results show that relative to the current normal level of MDCRS, the extra MDCRS reports reduce the TW RMS vector error by about 0.3 m/s and reduce the TW 90th percentile vector error by about 0.5 m/s. This is considered to be a significant improvement.

The errors in both the RUC wind fields and the TW wind fields are seen to increase with increasing wind speed, in part due to an underestimation of wind speed which increases with increasing wind speed. A relationship is shown to exist between the errors in the TW wind field and the local data density. These relationships to wind errors warrant greater examination.

Different types of weather are also seen to influence wind field accuracy. Altocumulus lenticularis, indicative of mountain waves, is associated with a decrease in wind field errors, while precipitation, towering cumulus, and thunder are associated with an increase in wind field errors. Precipitation provides the best signal for increased wind field errors of the four simple weather types studied. The combination of thunder and towering cumulus did not provide a significantly better signal than thunder alone. The combination of thunder and precipitation provided the best signal of increased wind field errors of all the weather types and combinations.

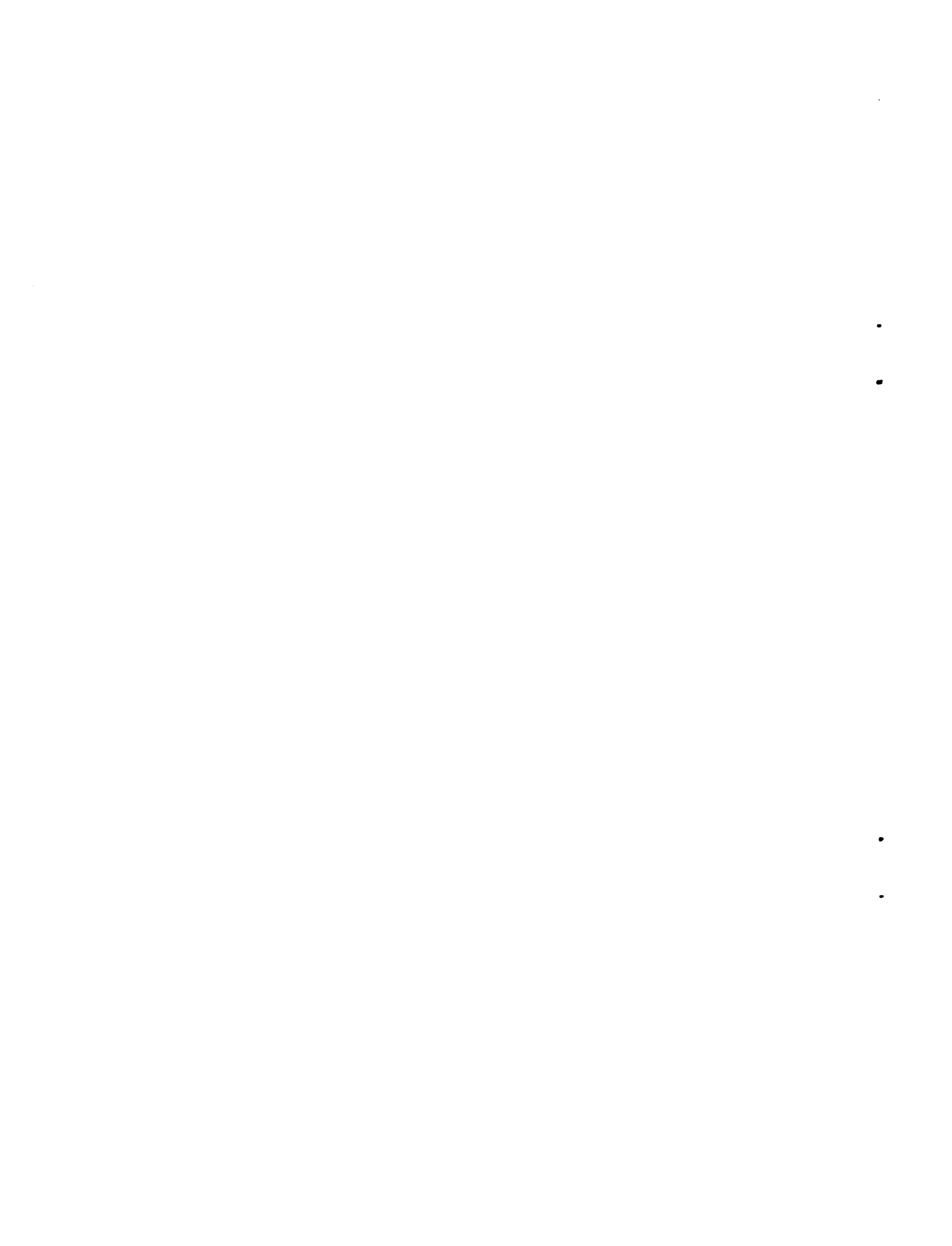
ACKNOWLEDGMENTS

This work, part of a collaborative effort between NASA, MIT/LL, and NOAA/FSL, was funded by the Center-TRACON Advisory System-Flight Management System (CTAS-FMS) Integration activity within NASA's Terminal Area Productivity Program. Matt Jardin and Steve Green of NASA Ames provided valuable coordination and insight into the meteorological sensitivities of ATM en route DSTs and made significant contributions to the design of the study. Barry Schwartz and Stan Benjamin made significant contributions to the design of the study and generously provided both the MDCRS data used in the study and the hourly weather-type analysis. We would like to thank United Airlines, and Carl Knable, in particular, for generously agreeing to increase the observation rate on many United aircraft. The extra United Airlines data were very valuable.



TABLE OF CONTENTS

<u>Section</u>	<u>Page</u>
Abstract	iii
Executive Summary	v
Acknowledgments	vii
List of Illustrations	xi
List of Tables	xii
1. Introduction	1
2. The Terminal Winds System	5
2.1. Introduction to the TW Product	5
2.2. Design Considerations	5
2.3. TW System Overview	6
2.4. Analysis Overview	8
2.5. TW Interpolation Technique	10
3. Methodology	15
3.1. Data Collection	15
3.2. MDCRS Characteristics	15
3.3. Table Generation	18
3.4. Generation of Statistics	18
4. Statistical Results	21
4.1. Aircraft Accuracy	22
4.2. Restriction to Locations and Times when TW is not a Pass Through of RUC	26
4.3. Interpolation to Aircraft Position vs. Nearest Value	27
4.4. Performance Results Over All Reports	27
4.5. Performance Results vs. Wind Speed	29
4.6. Performance Results vs. TW Estimates of Error Variance	31
4.7. Performance Results vs. Altitude	33
4.8. Performance vs. Month	34
4.9. Performance vs. Day	34
4.10. Performance vs. Weather Type	35
4.11. Performance vs. Number of MDCRS	39
4.12. Performance vs. Maximum Allowed Number of MDCRS per Analysis Point	40
4.13. Performance vs. Separation in Time of MDCRS Reports and Wind Fields	40
4.14. Performance vs. Separation in the Vertical of MDCRS Reports and Wind Field Levels	41
4.15. Analysis of Sustained Errors	43
4.16. Error Correlation Lengths	44
5. Conclusions	57
5.1. Baseline Performance and Benefits from Adding MDCRS to RUC	57
5.2. Factors Useful in Real-Time Estimation of Error Magnitude	58
5.3. Possible Future Work	58
Glossary	61
References	63



LIST OF ILLUSTRATIONS

Figure	Page
1. Conceptual Overview Diagram for the Terminal Winds System.	7
2. Data processing modules for the 10 km Terminal Winds Analysis.	9
3. Distribution of MDCRS Reports for 1 April, 1997.	17
4. Distribution of MDCRS Reports for 1 May, 1997.	17
5. Correction to RMS Error Estimates due to Errors in MDCRS vs. RMS Error.	25
6. Histogram of the Percent and Number of MDCRS Reports vs. RUC (black bar) and TW (gray bar) Vector Errors.	29
7. RUC and TW Cumulative Probability vs. Vector Error.	30
8. Vector Error vs. Wind Speed.	30
9. Speed Error/Wind Speed vs. Wind Speed.	31
10. Vector Error vs. TW Estimate of the RMS Vector.	32
11. RMS Vector Error Corrected for MDCRS Errors vs. TW Estimate Of the RMS Vector Error.	33
12. Vector Error vs. Altitude.	34
13. Vector Error vs. Month.	35
14. TW and RUC Mean Vector Error \pm One Standard Deviation vs. Day.	36
15. TW RMS and 90th Percentile Vector Error vs. Data Density.	40
16. Vector error vs. Time After the Hour.	42
17. Vector Error vs. Vertical Interpolation Distance.	42
18. Histogram of the Percent and Number of Hours vs. RUC (black bar) and TW (gray bar) 25th Percentile Hourly Vector Errors.	44
19. RUC and TW Cumulative Probability vs. 25th Percentile Hourly Vector Error.	44
20. Histogram of the Percent and Number of Hours vs. RUC (black bar) and TW (gray bar) Hourly Median Vector Errors.	45
21. RUC and TW Cumulative Probability vs. Hourly Median Vector Error.	45
22. Histogram of the Percent and Number of Hours vs. RUC (black bar) and TW (gray bar) Hourly 75th Percentile vector Errors.	46
23. RUC and TW Cumulative Probability vs. Hourly 75th Percentile Vector Error.	46
24. RUC Error Correlation vs. Horizontal Separation.	50
25. RUC Error Correlation vs. Horizontal Separation.	50
26. TW Error Correlation vs. Horizontal Separation.	50
27. TW Error Correlation vs. Horizontal Separation.	50
28. RUC Error Correlation vs. Pressure Separation.	51
29. RUC Error Correlation vs. Pressure Separation.	51
30. TW Error Correlation vs. Pressure Separation.	51
31. TW Error Correlation vs. Pressure Separation.	51
32. RUC Error Correlation vs. Temporal Separation.	52
33. RUC Error Correlation vs. Temporal Separation.	52
34. TW Error Correlation vs. Temporal Separation.	52
35. TW Error Correlation vs. Temporal Separation.	52
36. RUC Error Correlation vs. Temporal Separation.	53

LIST OF ILLUSTRATIONS (Continued)

Figure	Page
37. RUC Error Correlation vs. Temporal Separation.	53
38. TW Error Correlation vs. Temporal Separation.	53
39. TW Error Correlation vs. Temporal Separation.	53

LIST OF TABLES

Table	Page
1. Scales of Analysis for RUC and Terminal Winds	7
2. Number of MDCRS, Binned by Analysis Level	16
3. Statistics for Maximum Separation of 1 Minute, 5 mb, 10 km	24
4. Statistics for Maximum Separation of 5 Minutes, 5 mb, 20 km	24
5. Correlation Coefficients for Errors in Same Aircraft Pairs	26
6. Comparison of Results Using All Reports vs. Using Reports when TW has at Least a Minimal Amount MDCRS Reports	26
7. Comparison of Results Using Interpolation of Wind to Aircraft Position vs. Using Nearest Wind Value	27
8. Comparison of 60 km RUC and 10 km TW	28
9. Comparison of 60 km RUC and 10 km TW RMS errors after correction for MDCRS errors	28
10. Performance in Different Types of Weather	38
11. Comparison of TW with a Maximum of 5 Observations per Grid Point and a Maximum of 10 Observations per Grid Point	41
12. Number of Hours with Hourly Nth Percentile Vector Errors Above Given Thresholds	47
13. Separation Limits for the Generation of Correlations	47
14. Fit Parameters for Error Correlation vs. Horizontal Separation	50
15. Fit Parameters for Error Correlation vs. Pressure Separation	51
16. Fit Parameters for Error Correlation vs. Temporal Separation	52
17. Fit Parameters for Error Correlation vs. Temporal Separation Using Six Parameters	53
18. Correlation of Errors for Nominal Separations Using Equation (11)	54
19. Comparison of 60 km RUC and 10 km TW after Correction for MDCRS Errors Using Equation (10)	55

1. INTRODUCTION

The National Aeronautics and Space Administration (NASA) is developing the Center-TRACON Advisory System (CTAS)[1][2], a set of Air Traffic Management (ATM) Decision Support Tools (DST) for en route (Center) and terminal (TRACON) airspace designed to enable controllers to increase capacity and flight efficiency. A crucial component of the CTAS, or any ATM DST, is the computation of the time-of-flight of aircraft along flight path segments. Early NASA flight tests of the en route elements of CTAS discovered that variations in wind prediction error have a significant impact on the accuracy and value of en route DST advisories for Air Traffic Control (ATC) clearances[3][4].

There are currently envisioned to be two sources of wind data for CTAS:

- The Rapid Update Cycle (RUC)[5][6] for the Center airspace, a numerical model developed at the NOAA Forecast Systems Laboratory (FSL) and run operationally by the NWS National Center for Environmental Prediction (NCEP), and
- The Integrated Terminal Weather System (ITWS)[7][8][9] Terminal Winds (TW)[10][11][12] for the TRACON airspace, developed at MIT Lincoln Laboratory under funding from the Federal Aviation Administration (FAA).

The ITWS TW system takes in RUC data and refines the RUC forecasts with local measurements of the wind. In light of the earlier NASA results on the effect of wind prediction errors, NASA initiated a collaborative effort with MIT/LL and the National Oceanic and Atmospheric Administration (NOAA)/Forecast System Laboratory (FSL)[13] to determine the variations in wind prediction accuracy and the impact of these variations on typical en route ATM operations; explore methods and algorithms to improve wind prediction accuracy (e.g., RUC improvements and real-time updates of RUC with recent observations via the TW algorithm); and develop wind error prediction models to support real-time ATM DST probabilistic analyses of trajectory/conflict prediction accuracy.

This report presents a study based on the application of the Terminal Winds algorithm to the Center airspace as a value-added improvement to the baseline RUC product. Terminal Winds generally does not support the full Center airspace; the domain of the prototype MIT/LL ITWS TW system was increased to cover the Denver Center airspace to support this study. The domain of the FAA operational ITWS TW may not extend more than 30 nautical miles beyond a given TRACON.

The RUC is a mesoscale numerical weather prediction model that incorporates aircraft measurements from the Meteorological Data Collection and Reporting System (MDCRS)[14], balloon soundings, and other sensor data and solves equations of atmospheric physics to predict the evolution of various atmospheric parameters. The RUC data in this study use a grid with a horizontal resolution of 60 km and a vertical resolution of 50 mb. The RUC is run every three hours, and each run produces a set of hourly forecasts. A new version of the RUC that uses a 40 km horizontal resolution and runs every hour is in development. In this study, RUC always refers to the operational 60 km resolution model. The timing of the RUC data collection and the running of the model results in the forecasts usually being available about three hours after the model run time, although occasionally it is later. The post-processing of the RUC data in this study used the assumption that the RUC data are always available by three hours after the run time; the forecasts used in this study are always the three-, four-, and five-hour forecasts. The data used to initialize

each model run are collected in a three-hour period starting two hours prior to the nominal run time and ending one hour after the nominal run time. This results in the measurement data in the initialization of the model being at least two hours old by the time of the three-hour forecast, increasing to being five hours old at the time the next forecast cycle is available.

The ITWS TW is a data assimilation system that uses a RUC wind forecast as an initial estimate and refines the initial estimate using recent local measurements of the wind. These local measurements can come from surface observing systems, Doppler weather radars, and MDCRS. The ITWS TW system produces two wind fields: one with a horizontal resolution of 10 km and an update every 30 minutes and one with a horizontal resolution of 2 km and an update every five minutes. The TW system has been running operationally in the Lincoln ITWS testbeds since 1991. In particular, the ITWS system collects MDCRS that are not yet included in the RUC model and uses them in the refinement of the RUC forecast fields. The data collection period for TW extends up to the run time. In this study, the TW algorithm uses only these MDCRS reports to refine the RUC forecast wind fields to the 10 km resolution grid every 30 minutes. The 2 km resolution analyses are not examined in this study. While the terms TW and TW errors are used throughout this study, no Doppler weather radar data are used. The term TW in this report is shorthand for "RUC augmented with recent MDCRS reports via a limited version of the ITWS TW algorithm."

This study has three goals:

1. Determine the errors in the baseline 60 km resolution RUC forecast wind fields relative to the needs of en route DSTs such as CTAS;
2. Determine the benefit of using the TW algorithm to refine the RUC forecast wind fields with near real-time Meteorological Data Collection and Reporting System (MDCRS) reports;
3. Identify factors that influence wind field errors to improve accuracy and estimate errors in real-time.

To determine wind field accuracy, the wind fields are compared to a data set of independent wind measurements. These independent measurements of the wind come from the MDCRS reports. More than one million MDCRS reports collected during a one-year period starting 1 August 1996 are used. These MDCRS reports are collected in a region approximately 1300 km on a side and centered on the Denver International Airport. This is roughly the Denver Center airspace. All MDCRS reports are independent of the RUC three-, four-, and five-hour forecasts since they have not yet been included in these fields. The MDCRS reports are also not included in any TW field generated before the MDCRS are taken, so the TW fields are independent of the MDCRS as well. The difference between each MDCRS report and the most recent prior TW field and the difference between each MDCRS report and the RUC forecast used in that TW field are computed and kept in a table, along with the location and time of the report. The resulting values in the table are then used to compute the desired statistics.

The viewpoint taken in this study is that the distribution of errors in the wind fields is not directly at issue. Rather, it is important to model the errors expected to be encountered by CTAS in computing aircraft time-of-flight as opposed to modeling random errors throughout the entire airspace. This is done by simply assuming that each MDCRS report is independent from any other MDCRS report; the distribution of MDCRS in this study is the likely distribution of aircraft for which CTAS will have to compute time-of-flight. This means, for several reasons, that the re-

ported accuracy statistics are not direct measures of the overall accuracy of RUC or TW. For example, this study shows that wind field errors are greater at higher altitudes. Since there are more MDCRS reports at higher altitudes, this tends to elevate the estimates of the RMS error in the wind fields relative to the RMS error that would be computed if the evaluation uniformly sampled the wind fields or if the evaluation corrected for the nonuniform sampling. On the other hand, errors in regions of high aircraft density are also heavily represented in the statistics in this report, and these errors are in regions where both RUC and TW have their densest input data. Therefore, these regions can be expected to have smaller errors than the errors in otherwise similar regions.

This report provides several types of analyses. The errors in the MDCRS reports influence the results. A study of the errors in the MDCRS is presented first so that the influence of these errors on later statistics can be evaluated. Wind field accuracy statistics are given for on-average accuracy; for example, mean, RMS, and median values. For some of the on-average studies, the distributions of errors vs. magnitude of the error is also provided. Statistics for the tails of the error distribution are also given; for example the 90th percentile error. The statistics are provided for the entire data set and some are provided for the data set subdivided in various ways; for example, by altitude, by time of year, and by data density. Also given are statistics for the sort of sustained errors for which CTAS might have trouble computing accurate time-of-flight estimates; for example, hourly median error, and error correlation lengths. The third goal is addressed by examining the relationship between wind field errors and various wind field parameters; and by examining the relationship between wind field errors and different types of weather.

The impact of wind field errors on CTAS depends on aircraft speed and trajectory accuracy requirements. The generation of meter times is less sensitive to wind errors than the generation of conflict advisories and clearance advisories. Generating conflict and clearance advisories require computing time-of-flight over approximately 20 minutes. For a ground speed of 420 knots (7 nautical miles per minute), a constant along-track error of 10 knots results in a 29 seconds or 3.3 nmi error in estimated time-of-flight. En route separation minima are typically 5 nmi, and the 3.3 nmi is a significant fraction of the desired aircraft separation. When conflict calculations are performed for aircraft converging from different directions, the errors tend to be of different sign; one aircraft is earlier than expected and the other is later than expected, resulting in a combined error which is larger than the error for a single aircraft. In this situation, a constant 10 knot along-track error could significantly degrade the conflict prediction accuracy of en route DSTs (such as CTAS) when generating ATC clearance advisories. Similarly, a constant 20 knot along-track error gives rise to a trajectory error, even for a single aircraft, that is greater than the desired spacing. Wind errors are rarely constant, or completely correlated, along a flight path, so along-track errors will generally result in smaller time-of-flight errors than in this simple example. However, this indicates that along-track errors with a magnitude of 10 knots are problematic, and along-track errors with a magnitude of 20 knots are very serious.

•

•

•

•

2. THE TERMINAL WINDS SYSTEM

This section describes the full ITWS TW system. Only a limited subset of this functionality is used for this study. Terminal Winds generally does not support the full Center airspace. The domain of the prototype MIT/LL ITWS TW system was increased to cover the Denver Center airspace to support this study. The domain of the FAA operational ITWS TW may not extend more than 30 nautical miles beyond a given TRACON.

2.1. Introduction to the TW Product

The Integrated Terminal Weather System acquires data from various FAA and NWS sensors and combines these data with products from other systems (e.g., NWS Doppler weather radars (NEXRAD) and numerical weather prediction forecasts from the RUC to generate a new set of safety and planning/capacity improvement weather products for the terminal area and adjacent en route airspace. Operational users of the ITWS products to date include pilots, controllers, TRACON supervisors, terminal and en route traffic flow managers, airlines, Flight Service Stations, and terminal automation systems. The ITWS production system is currently being built by Raytheon and will be deployed at 34 sites. These sites are generally the high-volume, heavily weather-impacted TRACONs. As products are refined and new products developed, advanced versions of ITWS are expected to be fielded.

The TW algorithm produces estimates of the horizontal winds in an airport region. The primary users of this data are CTAS and human air traffic controllers. The TW obtains wind information from four types of sources:

- National scale numerical forecast model: RUC
- Doppler radars: TDWR [15] and NEXRAD [16]
- Commercial aircraft: MDCRS
- Surface anemometer networks: Low Level Wind Shear Alert System (LLWAS) [17] and Automated Surface Observing System (ASOS) [18]

2.2. Design Considerations

There are a number of design considerations for a winds analysis system that will support aviation systems and operate with information from sensors in the terminal area. Ideally, users of the gridded analyses levy performance requirements for resolution, accuracy, and timeliness. However, the aviation systems that rely on these analyses were under development as TW was being developed and did not provide performance requirements. During development, the approach taken was to base resolution and timeliness on sensor characteristics, expected wind field phenomenology, and knowledge of aircraft response to changing winds gained during the development of the TDWR and LLWAS wind shear algorithms. The goal of minimizing the variance of the wind vector error was also taken.

Meteorological Doppler radars provide estimates of the wind velocity component along the radar beam (radial velocities) as well as measurements of return intensity (reflectivity). Doppler radars can not directly measure the wind velocity component perpendicular to the radar beam.

They provide accurate and dense measurements in regions with sufficient reflectors. Due to the highly non-uniform distribution of data, the errors in the Doppler data tend to be highly correlated. The analysis technique must be able to estimate the horizontal winds from these single component measurements. It also must account for the highly correlated errors and dynamic data distribution inherent in the Doppler data.

The airspace covered by the TW grid extends from the surface to 100 mb (approximately 50,000 ft. mean sea level (MSL)) and is divided into two regimes. The planetary boundary layer (PBL) contains the atmosphere near the earth's surface, and it often contains wind structures with spatial scales on the order of kilometers and temporal scales on the order of minutes. Above the PBL, wind structures typically have spatial scales of 10s of km and temporal scales of hours. Doppler radars provide high-resolution information in the PBL where small scale wind structures are expected. Above the PBL, Doppler information becomes more sparse, and RUC and MDCRS are important sources of additional information. A cascade-of-scales analysis is used to capture these different scales of atmospheric activity.

2.3. TW System Overview

The philosophy of the TW analysis system is that the national scale forecast model provides an overall picture of the winds in the terminal airspace, although painted in very broad strokes. The terminal sensors are then used to fill in detail and to correct the broad-scale picture. The corrections and added detail can be provided only in those regions with nearby data. What constitutes "nearby" depends on the spatial and temporal scales of the features to be captured in the analysis. The refinement of the broad-scale wind field is accomplished by averaging the model forecast with current data, using statistical techniques described later. This allows the analysis to transition gracefully from regions with a large number of observations to regions with very few observations or no observations at all. This also enables the analysis to cope gracefully with unexpected changes to the suite of available sensors.

To account for the different scales of wind features and the differing resolution of the information provided from the various sensors, the analysis employs a cascade-of-scales. This cascade-of-scales uses nested grids, with an analysis having a 2 km horizontal resolution and five-minute update rate nested within an analysis having a 10 km horizontal resolution and 30-minute update rate;¹ this in turn is nested within the RUC forecast with a 60 km horizontal resolution and 180 minute update rate² as shown in Table 1. The vertical resolution is currently 50 mb (about 400 m near the surface, increasing to about 1000 m at aircraft cruise altitudes). The vertical resolution is expected to be increased to 25 mb, which is the maximum vertical resolution the data will support. All of the data sources are used in the 10 km resolution analysis. Only the information from the Doppler radars and LLWAS are suitable for the 2 km resolution analysis.³

1. For this study, the domain of the 10 km analysis was increased from its nominal domain size of 240 km x 240 km.

2. RUC is scheduled to produce forecasts on a 40 km grid and with an update rate of 60 minutes in the near future.

3. ASOS data will also be included in the 2 km analysis when the ASOS update rates are increased as expected.

Table 1.
Scales of Analysis for RUC and Terminal Winds

	Horizontal Resolution	Update Rate	Domain Size ⁴	Max Altitude
RUC	60 km	180 min	national	100 mb
TW	10 km	30 min	240 km x 240 km	100 mb
TW	2 km	5 min	120 km x 120 km	500 mb

4. The domain of the 10 km resolution grid was increased from its nominal size to 1300 km x 1300 km for this study.

This cascade-of-scales is appropriate for the scales to be captured in the analysis, the different scales of information contained in the observations, and provides a uniform level of refinement at each step of the cascade. The domain sizes are dictated by the domain of CTAS for the 10 km resolution grid and by the coverage of the Doppler radars for the 2 km resolution grid.

A conceptual picture of the TW system is provided in Figure 1. The two gridded analysis modules are shown as gray boxes. The data shown entering each subalgorithm from the top are used to produce each cycle's initial estimate of the current wind field. The national domain fore-

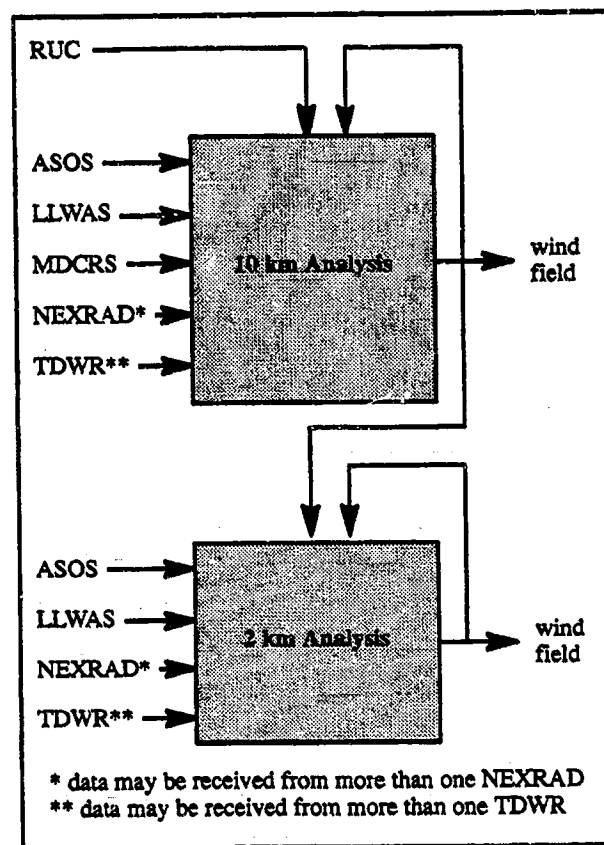


Figure 1. Conceptual overview diagram for the TW System.

cast model, RUC, provides national scale information for use in forming the 10 km resolution initial estimate, and the 10 km resolution analysis provides coarse scale information for use in forming the 2 km resolution initial estimate. Gridded information flows from the coarser scale to the finer scale. In addition, each interpolation step is shown feeding back its previous output to be used in producing the initial estimate of the current wind field. The observational data sources used in the refinement of the initial estimate are shown feeding data into the subalgorithms from the left. In each gridded analysis module, the refinement of the initial estimate in the least squares analysis provides a refinement of larger scale information and a refinement of its previous output.

2.4. Analysis Overview

Figure 2 provides a high-level overview of the processing steps in the 10 km and 2 km resolution analyses. Each analysis takes in wind information, computes grid-specific attributes of the wind information, performs data quality editing, and interpolates the wind information to the analysis grid to produce estimates of the wind field using a statistical technique (Optimal Estimation, described in detail below). Each analysis is triggered to run at specific times relative to the ITWS system clock. The 2 km resolution analysis runs every five minutes and the 10 km resolution analysis runs every 30 minutes. The following are the top-level functions in the analysis step:

1. Prepare initial estimate: This function provides an initial estimate of the current wind field and is executed each time the analysis module is executed. If available, a large-scale wind field, RUC for the 10 km analysis or the 10 km analysis for the 2 km analysis, is bi-linearly interpolated to the analysis grid.⁵ The last analysis is smoothed to remove transient wind features.⁶ If there is a large scale wind field, it is merged with the smoothed last analysis to form the initial estimate of the current wind field; otherwise, the smoothed last analysis is used as the initial estimate. The estimated height above MSL of each grid point is adjusted to bring the RUC height field into agreement with the pressure reported at the airport.⁷
2. Prepare radar data: This function maps all of the radial velocity data from one radar to the analysis grid and performs the initial data quality processing. The reflectivity information from the same radar is used in data quality editing. The radial velocity values from each set of tilt data are passed through a median filter to remove data outliers and to smooth the data appropriately for each grid resolution, resampled to the projection of the analysis grid, and then linearly interpolated in the vertical to --

5. For example, RUC is available only on the hour; no RUC data are used directly in the initial estimate for the analyses run on the half hour. The previous RUC data do get included through the last analysis, although averaged with observations if they are available. The initial estimate is built point by point, and when a new RUC is available, if the last analysis value at a given point is essentially the previous RUC value it is discarded in favor of the new RUC value.

6. At start-up, there is no previous TW wind field, so only RUC (or a default wind field, if need be) is used to form the initial estimate.

7. The adjustment of the height field is not done in this study due to the lack of surface observations.

form the final radial wind estimates. One instance of the prepare radar data function runs for each radar.

3. Prepare vector data: This function processes the ASOS, LLWAS, and MDCRS data into a standard data structure and assembles these data structures into a list. Pressure is computed from the initial estimate height field for each observation having a missing pressure measurement. Both ASOS and LLWAS wind data are smoothed temporally using a weighted mean.
4. Data quality edit: This function provides data quality editing. Each wind observation, vector or radial, is compared to a reference wind field, and observations dissimilar to the reference wind field are discarded. The reference wind field is the interpolated large-scale wind field if available; otherwise, it is the smoothed previous analysis.
5. Interpolate winds: This function refines the initial estimate field to agree with the observations in a least squares sense to produce the output wind field.

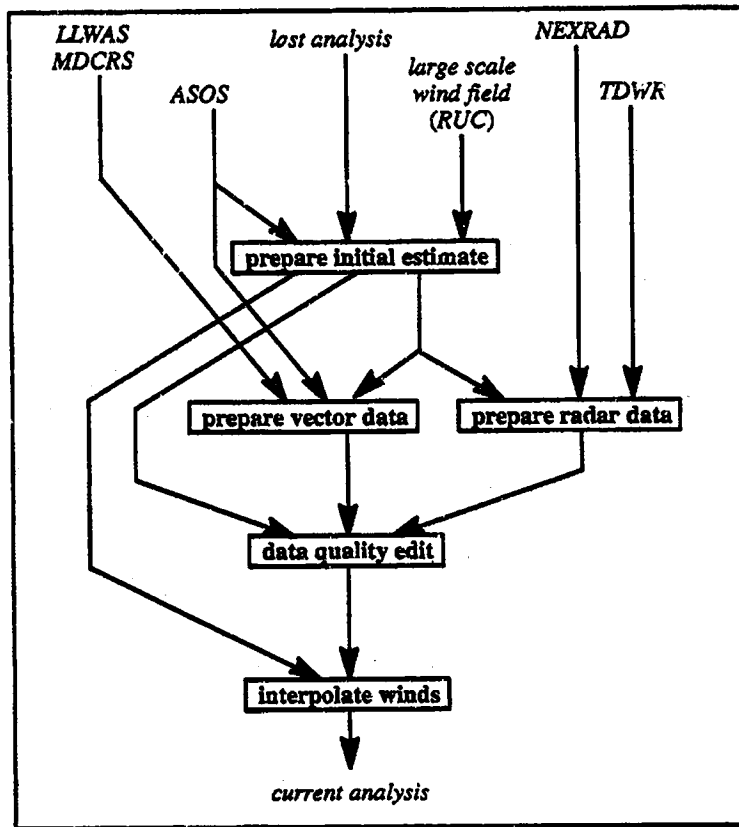


Figure 2. Data processing modules for the 10 km TW analysis. The 2 km analysis is similar, except that the 10 km analysis replaces the RUC.

2.5. TW Interpolation Technique

A state-of-the-art analysis technique for producing gridded fields from non-Doppler meteorological data analysis is Optimal Interpolation (OI)[19][20]. Optimal Interpolation is a statistical interpolation technique that under certain hypotheses gives an unbiased minimum variance estimate. The idea is to use observations to perturb an initial estimate. Differences between the observations and the initial estimate at the observation location are computed (Δ_j for the j th observation). The Δ_j terms are averaged in a least square sense to form a perturbation field which is then added back to the initial estimate. If the observations, as has traditionally been the case, are sparse relative to the desired resolution of the wind analysis, this provides a method to adjust the overall wind field without smoothing over the detail, or pattern of winds, in the initial estimate, which would occur if the sparse data are analyzed directly. This method ties the errors in the output field to the errors in the initial estimate, which is a reasonable trade-off when data are sparse. Standard OI applications require observations to provide both a u and a v wind component, which Doppler radars do not provide.

In traditional multi-Doppler wind analysis, radars are sited so that they cover the region of interest with significantly different viewing angles[21]. At a given location, each radar then provides an estimate of a different wind component. If two radars are used, a simple change of coordinates to eastward and northward results in an estimate of the horizontal winds at that location in standard form. If three or more radars are used, the resulting system of equations is overdetermined and the horizontal wind can be estimated using least squares techniques. When the geometry is good and each radar has sufficient return power, the resulting wind estimates are very accurate. However, at locations without returns from at least two radars, this method cannot be used. At locations where the radars are looking in nearly the same direction, the solution to the equations is numerically unstable and the method again cannot be used. An operational system using existing radars cannot count on good Doppler returns where they are desired, nor can the system count on favorable radar siting.

We apply the Gauss-Markov Theorem[22] to develop an analysis to jointly analyze both vector quantities and single component quantities and to provide for a smooth transition between an analysis of differences from the initial estimate in data poor regions to a direct analysis of data in data rich regions. It is the ease with which the Gauss-Markov Theorem allows for such properties that motivated its use. This technique provides a new capability which is important since increasing numbers of Doppler weather radars are being deployed.

The TW analysis accounts for the differing quality of the wind information as well as errors arising from data age and using data at locations removed from the location at which the data are collected (displacement errors). The analysis also accounts for correlated errors in a manner similar to Optimal Interpolation. Highly correlated displacement errors arise frequently due to the nonuniform distribution of data from the Doppler radars. If these correlated errors are not accounted for, these data dominate the analysis to a degree greater than is warranted by their information content.

The TW analysis technique has the following properties:

1. Multi-Doppler quality winds are automatically produced in regions where multi-Doppler analyses are numerically stable.

2. TW is numerically stable in regions where multi-Doppler analyses are not numerically stable.
3. Small gaps in multi-Doppler radar coverage are filled to produce near multi-Doppler quality winds in these gaps.
4. The analysis directly analyzes data in data rich regions and analyzes differences from the initial estimate in data sparse regions.
5. The analysis produces smooth transitions between regions with differing densities of data.

Throughout this section the following notation is used:

- r denotes a radial wind component
- u denotes an east wind component
- v denotes a north wind component
- superscript a denotes an analyzed quantity
- superscript i denotes a initial estimate quantity
- superscript o denotes an observed quantity
- subscripts denote location, o denoting an analysis location

To apply the Gauss-Markov Theorem, the problem must be posed in the form

$$Ax = d, \text{ where} \quad (1)$$

$$x = (u_o^a, v_o^a)^T, \text{ is the unknown horizontal wind vector}$$

and d contains the initial wind estimate and information derived from observations in a window centered on the analysis location. The size of the window adjusts dynamically based on local data density. The form of the matrix A depends on the type of data, vector and/or radial, to be analyzed. The Gauss-Markov Theorem states that the linear minimum variance unbiased estimate of $(u_o^a, v_o^a)^T$ is given by

$$(u_o^a, v_o^a)^T = (A^T C^{-1} A)^{-1} A^T C^{-1} d, \quad (2)$$

if each element of d is unbiased and if C is the error covariance matrix for the elements of d . The error covariance of the solution is

$$(A^T C^{-1} A)^{-1}. \quad (3)$$

When the data window contains m vector observations and n Doppler observations, equation (1) has the form:

$$\begin{pmatrix} 1 & 0 \\ 0 & 1 \\ \vdots & \vdots \\ \vdots & \vdots \\ 1 & 0 \\ 0 & 1 \\ \cos \theta_1 & \sin \theta_1 \\ \vdots & \vdots \\ \vdots & \vdots \\ \cos \theta_n & \sin \theta_n \end{pmatrix} \begin{pmatrix} u_o^a \\ v_o^a \end{pmatrix} = \begin{pmatrix} u_o^b \\ v_o^b \\ \vdots \\ u_m^o - (u_m^i - u_o^i) \\ v_m^o - (v_m^i - v_o^i) \\ r_1^o - (r_1^i - r_o^i) \\ \vdots \\ \vdots \\ r_n^o - (r_n^i - r_o^i) \end{pmatrix}$$

The terms of the form $(f_m^i - f_o^i)$ are estimates of the displacement error in the variable f that arise from taking a measurement at location m and using that measurement as an estimate at location o . This is just the change in f between these two locations. The actual change is not known, so it is estimated from the initial estimate of the field f . The initial estimate of the radial wind component is computed from the initial estimates of u and v . The resulting estimates of the form $f_m^o - (f_m^i - f_o^i)$ are unbiased estimates of the variable f at the analysis location provided the observations are unbiased relative to the observation locations. This is true even if the initial estimate has a bias, since differencing the initial estimate removes the bias.

In data rich regions, a small data window is employed which results in small displacement distances. This coupled with the fact that the initial estimate is smoothed prior to applying the Gauss–Markov Theorem causes the displacement error terms to be near zero in data rich regions: the observations in data rich regions are analyzed directly. This allows the analysis to incorporate the full richness of detail in the observations and largely decouples the errors in the output field from the errors in the initial estimate. In data poor regions, large data windows are used and the displacement terms come into full play. While the form of the analysis using the displacement error correction is different from the form classical OI takes, it is equivalent: each is simply a different method of solving the same least square problem, assuming a consistent set of error models.

In practice, the error covariance matrix C is not known and must be estimated. There are two types of errors to estimate. The first is the error that arises from imperfect sensors and an imperfect initial estimate. The second is the error due to an imperfect correction of the displacement error. Our error models are based on the following simplifying assumptions:

1. Observations are unbiased.
2. Sensor errors from different observations are uncorrelated.
3. Errors in u and v components, measured or initial estimate, are uncorrelated.
4. Displacement errors and sensor errors are uncorrelated.
5. Displacement errors are functions solely of the horizontal, vertical, and temporal distance of the observation from the analysis point.

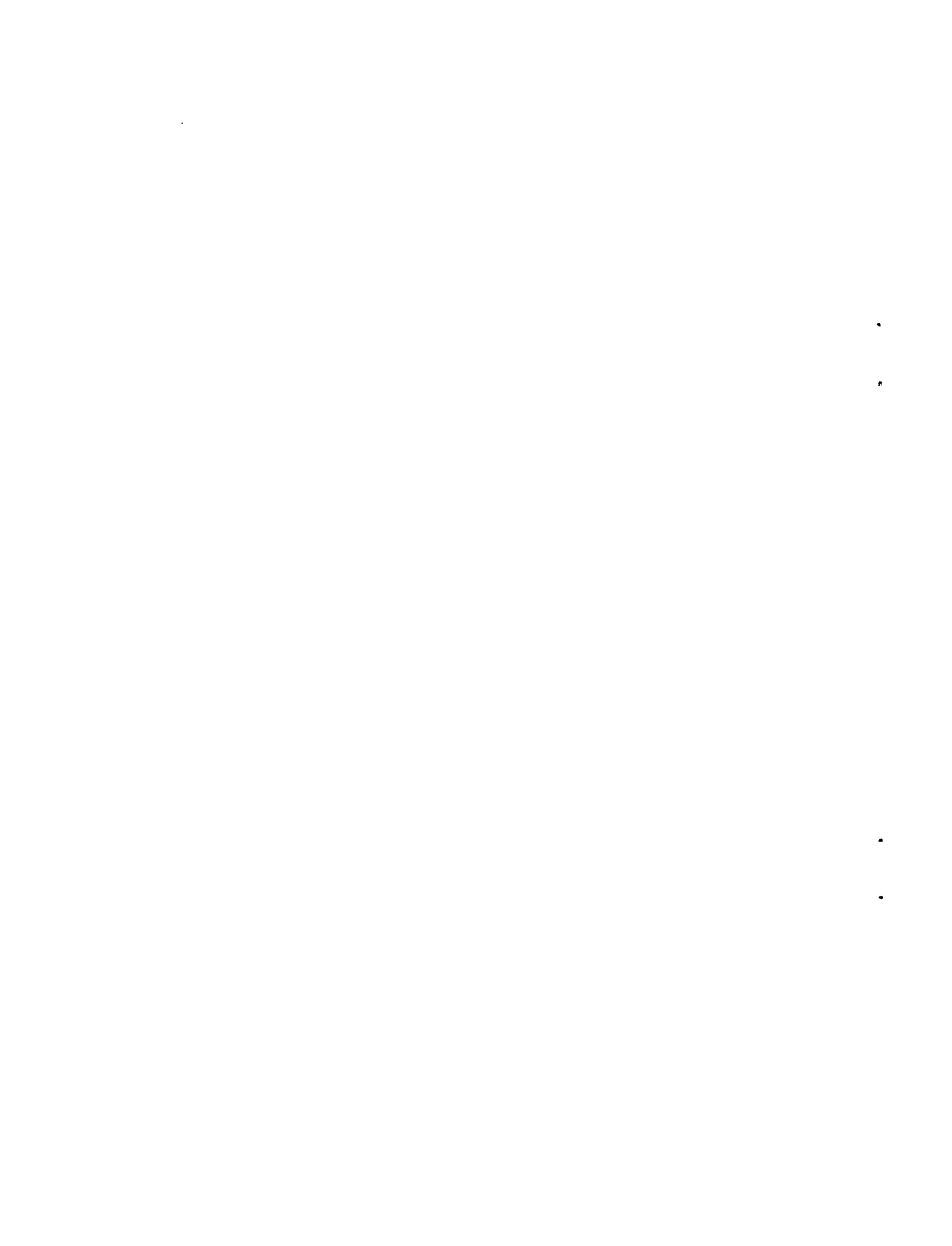
These assumptions have been tested on our data set and are found to hold relatively well.

With these assumptions, the error covariance matrix C decomposes into the sum of a sensor error covariance matrix and a displacement error covariance matrix. The sensor error covariance matrix is diagonal, and the sensor error variances are reasonably well known. The remaining task is the estimation of the displacement error covariance matrix.

The initial displacement error variance models are linear functions of the displacements, horizontal, vertical, and temporal, between the observation location and the analysis location. The initial displacement error correlation model for two like components is a decreasing exponential function of the displacement between two observation locations. The displacement error covariance model for two non-orthogonal, non-parallel components must take into account the angle between the two components. The angle between the observed component and the u axis is denoted by θ , with east at 0° , and north at 90° , and the displacement error in observation j is denoted by δ_j^o . Then the displacement error covariance for two observations is given by the following equation:

$$\text{Cov}(\delta_1^o, \delta_2^o) = \cos(\theta_1 - \theta_2) [\text{Var}(\delta_1^o) \text{Var}(\delta_2^o)]^{1/2} \text{Cor}(\delta_1^o, \delta_2^o) \quad (4)$$

Unlike the multiple Doppler analysis, the TW analysis is always numerically stable due to the inclusion of the initial estimate wind. The inclusion of a (u, v) data point provides two component estimates at right angles, giving a maximum spread of azimuth angles. Since the Doppler data are usually much more numerous than the other data, the TW solution closely matches the multiple Doppler solution at locations where the multiple Doppler problem is well conditioned. Otherwise, the analysis gives a solution that largely agrees with the radar observations in the component measured by the radars. The remaining component is derived from the vector estimates.



3. METHODOLOGY

3.1. Data Collection

The data for this study are collected from a region roughly 1300 km on a side and centered on the Denver International Airport (latitudes between 34.88 degrees and 44.82 degrees, longitudes between -97.86 degrees and -112.00 degrees). This airspace encompasses the Denver Center airspace. The data were collected for 343 days between 1 August 1996 and 1 August 1997.

The MDCRS data are collected at the NOAA Forecast Systems Laboratory and provided to Lincoln Laboratory via the Internet. Each MDCRS report contains the wind speed and direction, an aircraft ID, measurement location, the time the measurement was taken, and the time the measurement was received. Also included are data quality flags.

The experimental RUC data are downloaded over the Internet from a server at NCEP shortly after the data are generated. These data are on the grid and in the variables that the 60 km resolution RUC model uses to solve its equations of atmospheric physics. These variables are transformed into the isobaric variables used in the study using software written by the developers of RUC and made available to Lincoln Laboratory. After transformation, the RUC data variables are those expected to be available through operational NCEP channels. These variables are on the RUC 60 km horizontal resolution grid, with a vertical spacing of 50 mb. The RUC runs every three hours, starting at 00Z, and produces a set of hourly forecasts. The three-hour, four-hour, and five-hour forecasts are used. These forecasts represent the data that are usually available in time for use in ITWS.

The TW data are generated off line using archived RUC data and archived MDCRS data. The TW is run at 10 minutes and 40 minutes after each hour. The TW grid has a horizontal resolution of 10 km and a vertical resolution of 50 mb. The RUC data are fed into the TW system at 10 minutes after the hour. The 10 minute offset is used in the real-time ITWS to allow for RUC processing and transmission delays. Each MDCRS report is fed into the TW system based on the time it was received. The 2 km resolution grid is not used in this study.

3.2. MDCRS Characteristics

The MDCRS measurements represent the winds averaged over a period of 0.1 seconds. The vast majority of the MDCRS data come from four airlines: United Airlines (UA), Delta Airlines (DL), United Parcel Service (UP), and Northwest Airlines (NW). The MDCRS data are collected and disseminated using various strategies. For example, DL aircraft collect data every five minutes, and the data are immediately transmitted. But NW aircraft collect data with temporal separations that alternate between six and seven minutes, and the observations are held until six observations have been taken before the data are transmitted. United Airlines and United Parcel Service aircraft use less consistent strategies. Some of the UA and UP data are collected every minute, and some of the UA and UP data are collected every eight or nine minutes. The UA and UP data are usually, but not always, held by the aircraft until four observations are made before being transmitted.

Starting 1 May 1997, a number of UA aircraft began collecting one-minute data in support of this study. Before 1 May, the number of UA reports averaged about 1000 per day from about 10 aircraft in the 13,000 x 1300 km region of interest. After 1 May, the number of UA reports averaged about 5000 UA reports per day from over 160 aircraft, with many of the additional aircraft collecting data every minute. The number of reports per day from DL and NW is fairly constant, at about 1400 per day for DL and about 500 per day for NW. The number of UP reports per day varies greatly, from a low of about 50 to a high of about 1500.

The (approximate) maximum lag between the data collection time and the time the data were received is 20 minutes for UA, 30 minutes for UP, and 20 minutes for NW. The DL data have almost no lag between the time the data are collected and the time the data are received.

The MDCRS reports are available at all altitudes, but there are many more at cruise altitudes than at other altitudes, as shown in Table 2. As can be seen in Figure 3 and Figure 4, the MDCRS data are relatively uniformly distributed in the horizontal at cruise altitudes. Below cruise altitudes, the MDCRS reports are largely restricted to standard descent and ascent corridors into and out of Denver, although some descent and ascent corridors into other airports also show up, most notably at Albuquerque and Salt Lake City.

Table 2.
Number of MDCRS, Binned by Analysis Level

Level (MB)	Nominal Altitude MSL		Number (K)
	Feet	Meters	
100	53,190	16,210	0.0
150	44,760	13,640	0.1
200	38,770	11,820	501.5
250	34,000	10,360	317.2
300	30,070	9160	75.3
350	2,6630	8120	62.3
400	23,580	7190	27.5
450	20,810	6340	49.1
500	18,290	5580	26.0
550	15,960	4870	25.4
600	13,800	4210	25.5
650	11,780	3590	26.5
700	9880	3010	27.5
750	8090	2470	27.9
800	6390	1950	33.2
850	4780	1460	3.3
900	3240	990	0.1

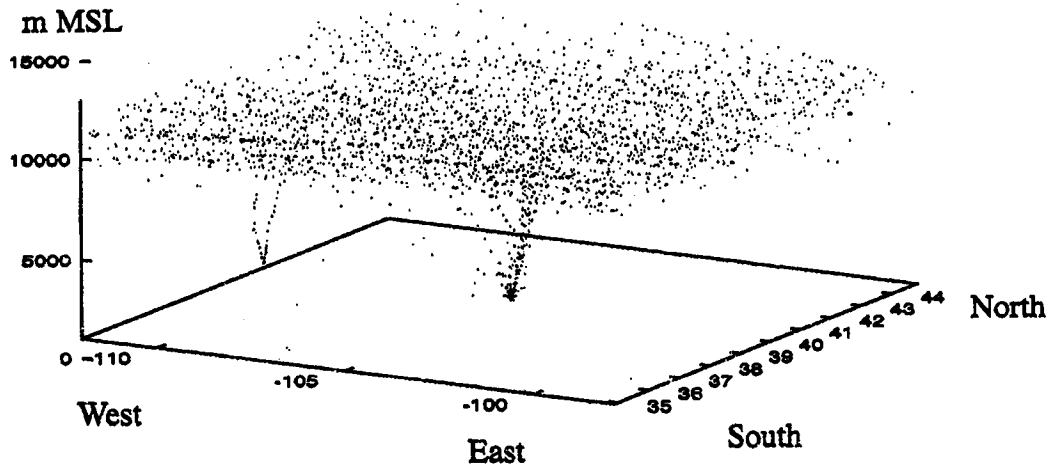


Figure 3. Distribution of MDCRS reports for 1 April 1997. This day has 2904 MDCRS. This is prior to United Airlines increasing their reporting rate.

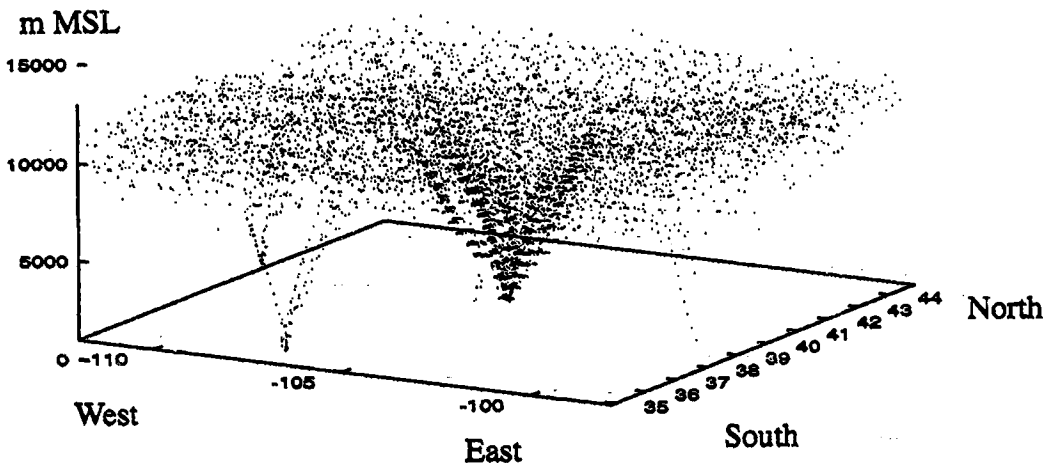


Figure 4. Distribution of MDCRS reports for 1 May 1997. This day has 8125 MDCRS. This is after United Airlines increased their reporting rate.

All MDCRS reports go through a simple validation process. First, each MDCRS arrives with two or three quality control (QC) flags that are produced by FSL: an "error type" flag, a "corrected" flag, and a "roll" flag. The error type flag indicates if there is a known error in one of the reported variables; for example, in the temperature or wind. The corrected flag indicates if any correction to the data has been made; for example, some aircraft are known to provide reports with the wind direction in error by 180 degrees, and these values are corrected for the known error. The roll flag indicates that the aircraft is in a steep turn. Only reports with an error type flag indicating no error are used. No corrected reports are used in this study. The roll flag is not used to determine which reports are used. The second data quality step is to check the data

values to see if they are within acceptable ranges. For example, is the wind direction between zero and 360 degrees? Finally, FSL keeps a list of aircraft ID for those aircraft that have produced suspect reports in the past. The data from these aircraft were examined. In all but one case, the number of suspect observations is small enough to have negligible impact on the results, and these data are left in the data set. The data for one aircraft, N520UA, contained numerous reports with significant errors, and all the data from this aircraft are removed from the data set.

3.3. Table Generation

The differences between each MDCRS measured wind vector component and the corresponding RUC and TW wind component estimates are generated and stored in tables. These differences represent estimates of the errors in the wind fields at the aircraft locations. The performance measures are generated from these tables. Each MDCRS report is matched to the most recent previous TW wind field, provided that the most recent TW wind field is not more than 30 minutes old. Likewise, each MDCRS is matched to the RUC wind field for the previous hour, provided RUC is available that hour. This RUC wind field is the one used as input in the TW wind field that matches this MDCRS. Using this method, each MDCRS report is matched to RUC and TW wind fields that do not yet contain the report. Thus, each MDCRS provides an independent estimate of the accuracy of a RUC wind field and an independent estimate of the improvement to that RUC wind field due to the addition of MDCRS. The differences between the MDCRS and the TW and the differences between MDCRS and the RUC wind estimates are then computed and stored along with auxiliary data in the table. Data for approximately 1.5 million MDCRS reports are in the tables, although not all are used in generating the performance statistics.

Two methods of computing the wind error estimates for each MDCRS are used. The first simply uses the wind estimate at the TW grid point nearest the MDCRS location. The RUC data are bi-linearly interpolated in the horizontal to the TW grid, so both RUC and TW are on the same grid. The second method uses bi-linear interpolation in three dimensions to interpolate the wind fields to the aircraft location. Temporal interpolation is not used in either case. The results from both methods are included in the table.

The auxiliary data in the table for each MDCRS are the following: the aircraft ID, the measured u and v wind components, the time of the measurement, the latitude and longitude of the measurement, the atmospheric pressure at which the measurement was taken, and the TW error variance estimate at the grid point nearest the measurement. This latter term is an estimate of the quality of the TW data in the region near the aircraft, and it is generated as part of the TW analysis process.

3.4. Generation of Statistics

The performance statistics are generated from the tables described above. Only data with results for both RUC and TW in the tables are used. This ensures that both RUC and TW are compared to a common MDCRS verification data set. The software to generate the statistics is written in Statistical Analysis Software (SAS). A number of different types of performance mea-

tures are generated, and the data are subdivided into a number of different classifications; for example, by altitude and by wind speed.

The statistics found in the results section are as follows:

1. **Mean.** The sum of the data values divided by the number of data values.
2. **Root Mean Square (RMS).** The square root of the sum of the squares of the data values divided by the square root of the number of data values.
3. **Standard deviation.** The RMS value of the differences between the data values and the mean of the data values. This measures the spread of the data values about their mean.
4. **RMS Error (RMSE).** The RMS value of the differences between the data values and zero. This is similar to the standard deviation but measures the spread of the data values about zero.
5. **Variance.** The standard deviation squared.
6. **Percentile.** The Nth percentile value, P, of a set of values is the smallest value for which N percent of the values in the set are less than P.
7. **Correlation.** Correlation measures how nearly two sets of data are related linearly. Correlation values range from -1 to 1 . The absolute value of the correlation measures how nearly the relationship is linear, with zero being no linear relationship to 1 when the relationship is exactly linear. The sign gives the slope of the linear relationship.

•

•

•

•

4. STATISTICAL RESULTS

There are three preliminary subsections before the bulk of the performance statistics are presented. The first subsection contains results of a study of the accuracy of the MDCRS wind measurements. The values of (MDCRS-wind field) are used to estimate the errors in the modeled wind fields. However, the MDCRS have their own errors, and these errors contaminate the estimates of the errors in the modeled wind fields. Following this are two subsections comparing performance results for two restrictions of the data in the table containing the (MDCRS-wind field) error estimates. Section 4.2 compares results when all error estimates are used to results when only error estimates in which TW has at least some data in addition to RUC are used. An important goal of this study is to determine the benefit of adding recent MDCRS to RUC via the TW system. Including error estimates when TW is merely a pass through of RUC does not support this goal. After this section, the results are for error estimates only when TW had at least a minimal amount of MDCRS to work with. This comparison provides information on how the results of the remaining subsections might differ if the error estimates were included for cases when TW is a pass through of RUC. Section 4.3 compares results using two different methods to generate the wind field estimate that is compared to the MDCRS measured wind. In method one, the TW wind field value is the value at the TW grid point nearest the aircraft location, and the RUC wind field value is generated by bi-linear interpolation in two dimensions to the TW grid point nearest the aircraft location. In method two, each wind field value is generated by bi-linear interpolation in three dimensions to the aircraft location. The extra complication of the second method provides a significant increase in accuracy and is used exclusively in the other subsections.

The on-average behavior of the errors, such as measured by mean and RMS, provide standard measures of performance. While these standard measures are important, for the purposes of understanding errors relative to the needs of ATM DSTs they need to be used in conjunction with additional measures such as error correlation length. The results for u and v components largely tell the same story as the results for vector errors. The results for the mean, standard deviation, RMS, and median errors likewise each tell largely the same story. The usual practice in this report will be to provide the results for the RMS vector error, except as noted. The individual RMS u and v wind component errors can be estimated very closely by dividing the RMS vector error by the square root of two; that is, the square of the individual RMS errors is nearly the square of the RMS vector error. However, this does not hold for the outliers; for example, the 90th percentile errors. Errors in m/s can be converted to knots by multiplying by 1.9438, or converted approximately by doubling. Thus, an RMS vector error measured in m/s can be converted, approximately, to an RMS headwind error in knots by multiplying by 1.4 (approximately the square root of two). When considering these results it is useful to keep in mind that a sustained headwind error of about 10 knots (roughly corresponding to a vector error of about 7 m/s) is problematic for CTAS.

Perhaps more important than on-average performance for a fielded FAA ATC system is the number of times when the system provides incorrect guidance. The ATC personnel are very quick to simply walk away from a system that is not extremely reliable, and with good reason; it takes very few go-arounds or other problems to negate the benefits gained otherwise. For this reason, measures of large errors are also provided. A human evaluation of the MDCRS data that is used for confirmation of the accuracy of the wind fields reveals that some small percentage of reports, probably less than one percent, are not credible. For this reason, percentile errors are reported only up to the 95th percentile. The 90th percentile value is generally chosen for the figures to represent "worst case"

systematic errors. The 90th percentile error is both robust to the errors in the MDCRS data set and represents a level at which errors are still numerous enough, if large, to cause CTAS problems; very large but very rare errors may not affect CTAS trajectory calculations.

Results are also given for various breakouts of the data set; for example, by wind speed, by data density, and by altitude. The goal is to determine what variables might be used to estimate the errors in a modeled wind field in real time. These results show that wind speed and data density are related to wind field errors, but the exact nature of the relationship is difficult to see as the wind speed and data density tend to move in concert; in the data set, the regions of high winds tend to be the regions with the least data, and vice versa. A detailed analysis of the relationship between these variables and the errors is beyond the scope of this report.

Even if errors are small on average, there are expected to be periods of time and regions of space where errors are large. Errors sustained over time or space are more likely to lead to incorrect CTAS guidance than are sporadic errors. Error correlation length is another way to quantify sustained errors and plays an important role in determining how errors affect CTAS performance. Errors that are correlated tend to add together when computing aircraft time-of-flight, and errors that are uncorrelated tend to cancel; all else being equal, the wind field with the shorter error correlation length will lead to better time-of-flight estimations. Error correlation length is not directly related to RMS errors. Given two wind fields, one can have the larger RMS error but also have the shorter error correlation length.

The addition of recent MDCRS to RUC improves the mean errors and their standard deviation as well as the RMS errors. It also reduces the number of large errors in each study performed for this report. The improvements are generally operationally significant to CTAS.

4.1. Aircraft Accuracy

The goal of this study is to determine statistical parameters of the wind field accuracy. The MDCRS reports that are not yet included in the wind fields provide an independent source of confirmation of the correct winds at the locations of the aircraft. However, one problem in comparing MDCRS to modeled wind fields is that errors in the MDCRS become enmeshed with the errors in the wind field. Since the MDCRS used in the comparisons are independent of the wind fields, the variance of (MDCRS-model) is the sum of the error variances of each term:

$$\text{var}(MDCRS\text{-}model) = \text{var}(MDCRS\text{-}truth) + \text{var}(model\text{-}truth) = \sigma_{AC}^2 + \sigma_f^2 \quad (5)$$

where the terms σ_{AC} and σ_f are the standard deviation of the error in the aircraft reports (MDCRS) and the standard deviation of the error in the modeled wind (RUC or TW), respectively. The term $\text{var}(MDCRS\text{-}model)$ can be estimated directly from the large set of (MDCRS-model) values. The term $\text{var}(MDCRS\text{-}truth)$ can be estimated indirectly, as described below. The desired term, $\text{var}(model\text{-}truth)$, can then be estimated from the first two terms.

Here it is important to be careful to define what is meant by truth, or the true wind. The wind can be considered to be composed of wind features with various length scales. Features that are very small relative to the response of a sensor or the needs of a particular user of the information may be considered noise despite the fact that in some other sense they may be real. In this case features that are so small that they do not affect the computation of aircraft trajectories are considered to be

noise. The error variance in the MDCRS reports is the sum of the sensor error variance relative to the scales MDCRS intends to measure (0.1 sec average winds) and the variance in the wind due to features that are sub-scale relative to CTAS. The error variance of the MDCRS relative to the needs of CTAS is estimated. Some information on the contribution to that error from wind features that are real, but sub-scale to CTAS, is also provided.

Given a large set of pairs of aircraft observations, with each aircraft in the pair at nearly the same location and time, the variance in the difference between the two nearly coincident random measurements is estimated by:

$$\text{var}(ac1 - ac2) = \text{var}(ac1 - \text{truth} + \text{truth} - ac2) = \text{var}(ac1 - \text{truth}) + \text{var}(ac2 - \text{truth}), \quad (6)$$

provided that the errors in the two aircraft reports are uncorrelated. The issue of correlated error is addressed later.

Assuming that on average any random aircraft is no better or worse than another random aircraft, the last equation is:

$$\begin{aligned} \text{var}(ac1 - ac2) &= 2 * \text{var}(ac - \text{truth}), \text{ or} \\ \text{var}(ac - \text{truth}) &= \text{var}(ac1 - ac2) / 2 \end{aligned} \quad (7)$$

Given a large set of aircraft observation pairs, the value $\text{var}(ac1 - ac2)$ can be estimated, and from this value, the value $\text{var}(ac - \text{truth})$ can be estimated. Using this process, both measurement errors and wind features smaller than the separation of the aircraft used to make the pairs are included in the error variance estimate.

Error variance estimates are computed for two sets of separation limits. The first set allows a maximum separation of one minute; 10 km in the east and north directions and 5 mb in the vertical (at cruise altitudes 1 mb is about 24 meters). The second set allows a maximum separation of five minutes; 20 km in the east and north directions and 5 mb in the vertical. The temporal and spatial separation limits are linked by the speed of the aircraft: at cruise speeds, one minute of flying time is approximately 10–15 km. In practice, due to preferred aircraft altitudes and the search method used to find aircraft pairs, the average separations in time and in the vertical are much smaller than the maximum limits, as seen in Table 3 and Table 4.

The set of tighter separation limits used in the results presented in Table 3 represents the finest separation limits that gives a usable number of aircraft pairs, and thus gives results that are as close as possible, given the MDCRS data set, to the actual measurement errors uncontaminated by small-scale wind features. The results from the second set give a set of error estimates better coupled to the scales of wind features that affect trajectory analyses. However, even these separations may be smaller than the features that affect CTAS. If so, the reported MDCRS errors are an underestimate of the errors relative to CTAS. The second set also has the benefits of more stable error estimates due to the greater number of aircraft pairs and of having approximately the same number of same-aircraft pairs and different-aircraft pairs. The difference in the two estimates for the two separation criteria provides information on the portion of the error variance due to small-scale wind features; in principle, these two estimates can be used to extrapolate back to a separation distance of zero, so that the error estimate is devoid of contamination by sub-scale winds.

Table 3.
Statistics for Maximum Separation of 1 Minute, 5 mb, 10 km
Separation Statistics for Pairs of Aircraft:

variable	all pairs	same AC	different AC
	mean+/-std	mean+/-std	mean+/-std
number of pairs:	23,303	15,272	8,031
Δtime (minutes):	0.47±0.50	0.33±0.47	0.72±0.45
Δpressure (mb):	1.07±1.39	1.42±1.56	0.42±0.53
Δeast distance (km):	3.27±2.92	3.03±2.93	3.71±2.86
Δnorth distance (km):	2.27±2.49	1.55±1.93	3.63±2.84
Variance Estimates of ac1-ac2 Components, (m/s)²:			
u variance	3.41	1.74	6.59
v variance	3.35	1.76	6.37
RMS Error Estimate for Single Aircraft, m/s:			
u RMS error	1.31	0.93	1.81
v RMS error	1.29	0.94	1.78
vector RMS error	1.84	1.32	2.55

Table 4.
Statistics for Maximum Separation of 5 Minutes, 5 mb, 20 km
Separation statistics for pairs of aircraft:

variable	all pairs	same AC	different AC
	mean+/-std	mean+/-std	mean+/-std
number of pairs:	44,123	21,869	22,254
Δtime (minutes):	0.90±0.83	0.57±0.62	1.01±0.95
Δpressure (mb):	0.76±1.16	1.09±1.48	0.44±0.55
Δeast distance (km):	6.89±5.79	6.25±5.83	7.52±5.68
Δnorth distance (km):	5.02±5.18	2.56±3.16	7.44±5.62
Variance Estimates of ac1-ac2 Components, (m/s)²:			
u variance	4.78	2.12	7.38
v variance	5.16	2.15	8.11
RMS Error Estimate for Single Aircraft, m/s:			
u RMS error	1.55	1.03	1.92
v RMS error	1.61	1.04	2.01
vector RMS error	2.23	1.46	2.78

Equation (6) is an equality if and only if the errors in the two aircraft observations are independent. This is expected to be the case if the two observations come from different aircraft. If the observations come from the same aircraft, any bias is in each measurement and the errors are not independent. In differencing the values from the same aircraft, the biases cancel, leading to a low estimate of the error variances. Given the increased reporting frequency of the United and UPS aircraft, the data set contains a large number of closely spaced observations from the same aircraft.

The maximum, mean, and standard deviations of the aircraft separations used in estimating the MDCRS error variance are given in Table 3 and Table 4. The corresponding variance estimates for (ac1-ac2) and the resulting estimates for the error variance of the MDCRS reports are also given in Table 3 and Table 4.

The effect of the MDCRS errors on RMS error estimates based on differences between MDCRS and the modeled winds depends on the the magnitude of the errors in the wind fields. The amount that should be subtracted from a raw RMS error estimate to correct for MDCRS errors for a given raw estimate is given in Figure 5. These corrections are based on equation (5) and apply only to RMS error estimates. The smaller the errors in the wind field, the greater the correction to account for the MDCRS errors. Since TW is more accurate than RUC, the RMS error estimates for TW are over estimated to a greater extent in the statistics than are the RMS error estimates for RUC. For this reason, the actual improvement due to the inclusion of MDCRS is greater than shown in the uncorrected results. Because there is some uncertainty in the exact value of the MDCRS errors relative to the needs of CTAS and because the corrections apply only to RMS errors, the results in this report are for uncorrected errors unless otherwise specified.

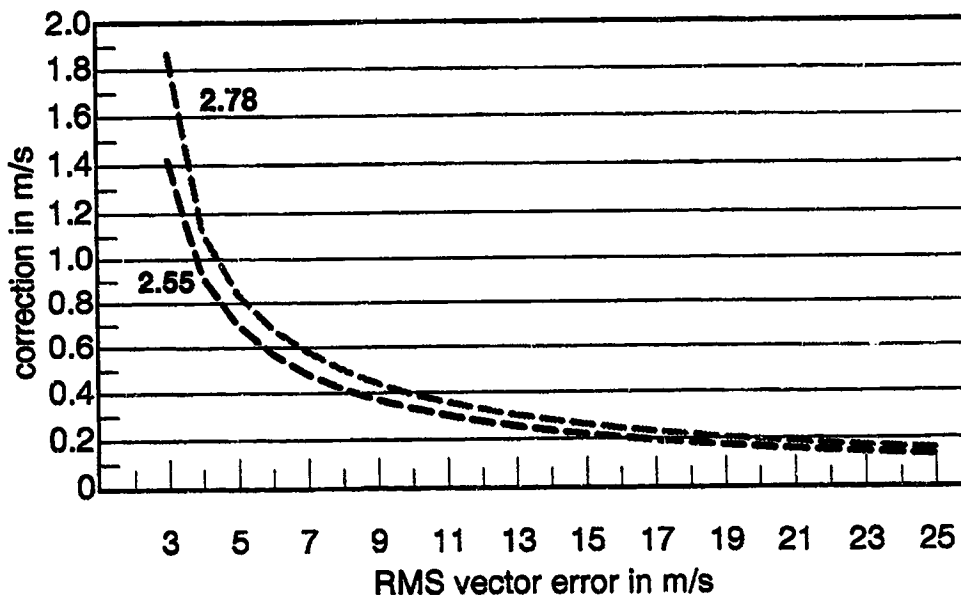


Figure 5. Correction to RMS error estimates due to errors in MDCRS vs. RMS error. The correction using a MDCRS error of 2.78 m/s is shown in gray and the correction using an MDCRS error of 2.55 m/s is shown in black.

Equation (8) gives the relationship between the variance estimate derived from pairs of the same aircraft and the variance estimate derived from pairs of different aircraft, where the term *correlation* is the correlation in errors in the same-aircraft pairs.

$$var_same = var_diff * (1 - correlation) \quad (8)$$

Table 5 shows the results from applying equation (8) to the data in Table 3 and Table 4. In each case, the resulting correlation coefficient is slightly larger than 0.7, showing that a very large portion of the errors in the MDCRS reports are biases that persist at least as long as the separations used in forming the aircraft pairs used in the analysis.

The above analysis is concerned with the statistical properties of the errors in the MDCRS reports, or on average errors, and assumes that the MDCRS reports are reasonable measurements with errors distributed about zero or at least distributed about some offset or bias. Examining the reports by hand shows that some small subset of the reports have other types of errors. Occasionally, re-

**Table 5.
Correlation Coefficients for Errors
in Same Aircraft Pairs**

<u>variable</u>	<u>from Table 3</u>	<u>from Table 4</u>
correlation in u error:	0.736	0.713
correlation in v error:	0.724	0.735

ported altitudes have very large discontinuities: an aircraft drops hundreds of mb for a moment and then jumps back to its original altitude. These are clearly erroneous reports. Large discontinuities in the wind values are also occasionally seen. It is difficult to know whether or not these are incorrect measurements or are due to strong, small-scale wind features. An automated search through the data set of MDCRS reports has not been done, but it appears that these sorts of problems affect well under one percent of the reports. The small fraction of reports that do not fit the statistical models underlying the analyses should not adversely affect the results.

4.2. Restriction to Locations and Times when TW is not a Pass Through of RUC

An important goal of this study is to understand the value of adding recent MDCRS to RUC via the ITWS Terminal Winds algorithm. For this reason, statistics are computed only for those aircraft observations where TW is not merely a pass through of RUC data unless specifically noted. Table 6 gives a comparison of vector errors using all aircraft and vector errors using only those aircraft at locations where TW is not a pass through of RUC. The first thing to note is that about 11 percent of the aircraft are at locations where TW is a pass through of RUC. The RMS vector error in TW is increased by about 0.2 m/s if all aircraft are included, and the 90-percentile vector error increases by about 0.3 m/s. This should be kept in mind when considering overall vector errors in TW, since after this point the only results reported are for aircraft where TW is not a pass through of RUC, except where explicitly noted. This restriction has almost no effect on the RUC performance results.

**Table 6.
Comparison of Results Using All Reports vs. Using Reports When TW
Has at Least a Minimal Amount MDCRS Reports. Values are in m/s
number of reports used: all = 1,387,776, restricted = 1,228,588,
dropped = 159,188 or 11.5%**

<u>variable</u>	<u>mean+/-std</u>	<u>RMSE</u>	<u>50%</u>	<u>75%</u>	<u>90%</u>	<u>95%</u>
<u>TW vector error</u>						
all	4.42±3.12	5.41	3.76	5.74	8.17	10.04
restricted	4.26±2.95	5.18	3.64	5.54	7.85	9.61
<u>RUC vector error</u>						
all	5.69±3.69	6.78	4.99	7.39	10.22	12.39
restricted	5.67±3.64	6.74	4.99	7.38	10.18	12.31

4.3. Interpolation to Aircraft Position vs. Nearest Value

There are two approaches used to compute the modeled wind vector that is matched to each aircraft observation once a wind field is matched to the aircraft time. The simplest approach is to take the wind vector at the Terminal Winds grid point nearest the aircraft. In this approach the RUC wind field is interpolated to the TW grid using bi-linear interpolation so that both wind fields are on the same grid. A more sophisticated approach uses bi-linear interpolation in 3-D on the surrounding eight grid points to interpolate the winds to the aircraft position. The value of the extra complexity was not known. Table 7 shows the results on the entire year database. The benefit to TW is about a third of a m/s for the RMS vector error and slightly less for RUC, and the benefit is greater for the larger percentile errors. Given the substantial benefit relative to the modest increase in complexity of the second approach, the 3-D interpolation is justified for use in CTAS. For this report, only results using the 3-D interpolation are given, except in Table 7.

Table 7.
Comparison of Results Using Interpolation of Wind
to Aircraft Position vs. Using Nearest Wind Value
 Results are for 1,228,588 aircraft reports. Values are in m/s.

<u>variable</u>	<u>mean+/-std</u>	<u>RMS</u>	<u>50%</u>	<u>75%</u>	<u>90%</u>	<u>95%</u>
<u>TW vector error</u>						
nearest	4.53±3.21	5.55	3.82	5.91	8.47	10.44
interpolated	4.26±2.95	5.18	3.64	5.54	7.85	9.61
<u>RUC vector error</u>						
nearest	5.85±3.76	6.96	5.14	7.62	10.52	12.73
interpolated	5.67±3.64	6.74	4.99	7.38	10.18	12.31

4.4. Performance Results Over All Reports

A number of statistics are computed over the entire year. These results provide information on the sorts of errors encountered by the aircraft. Since the aircraft are not uniformly distributed in space and time, these results are not necessarily an accurate or full account of the quality of the wind fields. Since a goal of this study is to determine the accuracy of the wind fields relative to CTAS, it is important to study the errors encountered as opposed to studying the fields in general. For example, the results are dominated by the aircraft at cruise altitudes, except for the results broken down by altitude. There are also more aircraft after May due to United Airlines turning on many of their aircraft in order to provide more numerous data on ascent and descent.

The results for the entire year are provided in Table 8. Over 1.2 million MDCRS are used on 343 days. The results show that RUC and TW have a slight low bias in the u component and RUC has a slight high bias in the v component. The RUC direction bias is only -1 degree, and the addition of recent MDCRS data reduces this bias to essentially zero. Both RUC and TW have a slight low bias in speed, -0.6 m/s and -0.4 m/s, respectively. The wind over the year averaged a little over 20 m/s from west southwest. By all measures, adding recent MDCRS to RUC improves performance both in the on-average measures and in the reduction of outliers.

As noted earlier, the errors in the MDCRS reports enter into the errors in Table 8. Table 9 provides the uncorrected RMS error estimates in RUC and TW, along with values that are corrected to

Table 8.
Comparison of 60 km RUC and 10 km TW
 Results are for 1,228,588 aircraft reports.
 (1,131,373 reports for % Speed Errors and Direction Errors)
 Values are in m/s, except for % speed error, which is unitless,
 and direction, which is in degrees.

variable	mean+/-std	RMSE	50%	75%	90%	95%
TW u error	-0.25±3.62	3.63	-0.27	1.84	4.03	5.59
TW v error	0.09±3.69	3.69	0.15	2.18	4.25	5.71
TW vector error	4.26±2.95	5.18	3.64	5.54	7.85	9.61
TW % speed error	-0.40±22.9	22.9	0.9	11.3	23.2	33.0
TW direction error	-0.01±16.1	16.1	-0.27	5.78	13.8	21.0
RUC u error	-0.22±4.61	4.62	-0.38	2.51	5.45	7.48
RUC v error	0.40±4.90	4.91	0.56	3.35	6.04	7.86
RUC vector error	5.67±3.64	6.74	4.99	7.38	10.18	12.31
RUC % speed error	-0.60±28.9	28.9	2.1	15.4	29.2	39.6
RUC direction error	-1.03±22.5	22.5	-1.24	6.78	17.29	27.36
wind speed	21.5±13.8	25.6	19.0	29.8	40.6	47.8
wind direction	252.6±67.9	261.5				

Table 9.
Comparison of 60 km RUC and 10 km TW RMS Errors
After Correction for MDCRS Errors
 Corrected values using MDCRS RMS errors of 2.55 m/s and 2.78
 m/s are given. Results are for 1,228,588 aircraft reports.
 Values are in m/s.

variable	raw	corrected (2.55 m/s)	corrected (2.78 m/s)
TW u error	3.63	3.14	3.08
TW v error	3.69	3.23	3.09
TW vector error	5.18	4.51	4.37
RUC u error	4.62	4.25	4.20
RUC v error	4.91	4.58	4.48
RUC vector error	6.74	6.24	6.14

remove the effects of the MDCRS errors. Both of the estimates of the MDCRS errors are used to show the effect of differing estimates of the MDCRS errors. For CTAS applications, 5 m/s is a significant headwind error. The RMS component errors for RUC are fairly close to 5 m/s even after correction, while the RMS component errors after adding recent MDCRS, at about 3.1 m/s, are well below 5 m/s.

In addition to bulk statistics, it is useful to consider the distribution of errors. Figure 6 provides a histogram of percent of MDCRS and count of MDCRS vs. vector error. The addition of recent MDCRS is seen to reduce many of the vector errors greater than 5 m/s to less than 5 m/s. The number of very large vector errors also drops. The counts of vector errors in each bin above about 8 or 9 m/s

is reduced by approximately half with the addition of recent MDCRS. Given the possible sensitivity of user acceptance to occasional incorrect CTAS guidance, the reduction in these very large errors due to the addition of recent MDCRS is very important.

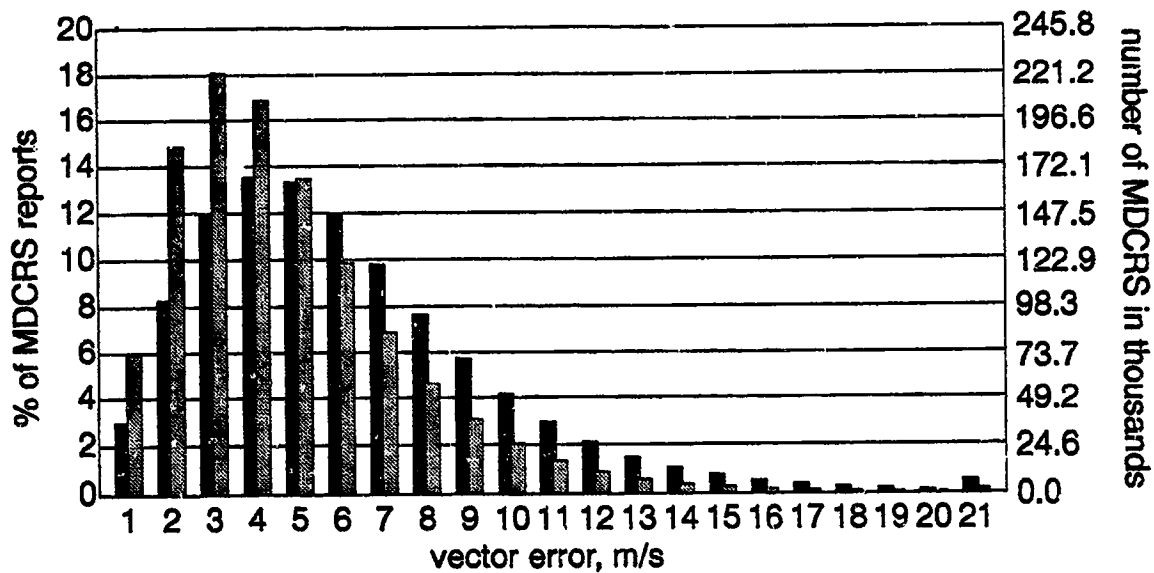


Figure 6. Histogram of the percent and number of MDCRS reports vs. RUC (black bar) and TW (gray bar) vector errors. Each bin labeled n contains errors between $n-1$ and n , except bin 21 which contains all errors 20 m/s and greater.

Another approach to examining these data is via a cumulative probability plot as in Figure 7. Here the percent of vector errors less than a value are plotted vs. that value. This allows the reader to set any vector error threshold and then to determine how often the vector errors are larger or smaller than this threshold. In Figure 7, RUC is seen to have 50 percent of its vector errors less than 5 m/s. Terminal Winds is seen to have 70 percent of its vector errors less than 5 m/s, or conversely, TW has 30 percent of its vector errors greater than 5 m/s. Terminal Winds has about half the number of errors as RUC for any threshold which is greater than about 6 m/s, again showing that the addition of recent MDCRS not only improves overall performance but also greatly reduces the potentially problematic outliers.

4.5. Performance Results vs. Wind Speed

Wind speed is one of the primary indicators of error magnitude. Figure 8 shows the RMS and 90th percentile vector error for various wind speeds. The errors rise monotonically with wind speed. For wind speeds of zero to about 60 m/s, the rise in error is roughly linear, especially for TW. The increase in RUC error with wind speed is more nearly linear if the errors are corrected for the MDCRS errors since the correction is larger for smaller errors. The errors rise more rapidly for wind speeds above approximately 60 m/s. However, this may be due to sampling error; there are hundreds of thousands of samples from 5 m/s to 30 m/s, tens of thousands of samples from 35 m/s to 60 m/s, and dropping by about 50 percent for each bin thereafter to only 160 samples at 85 m/s.

Also plotted in Figure 8 is the mean of the TW estimates of the standard deviation of the vector error for each speed bin. These values are computed in the TW system for use in the interpolation,

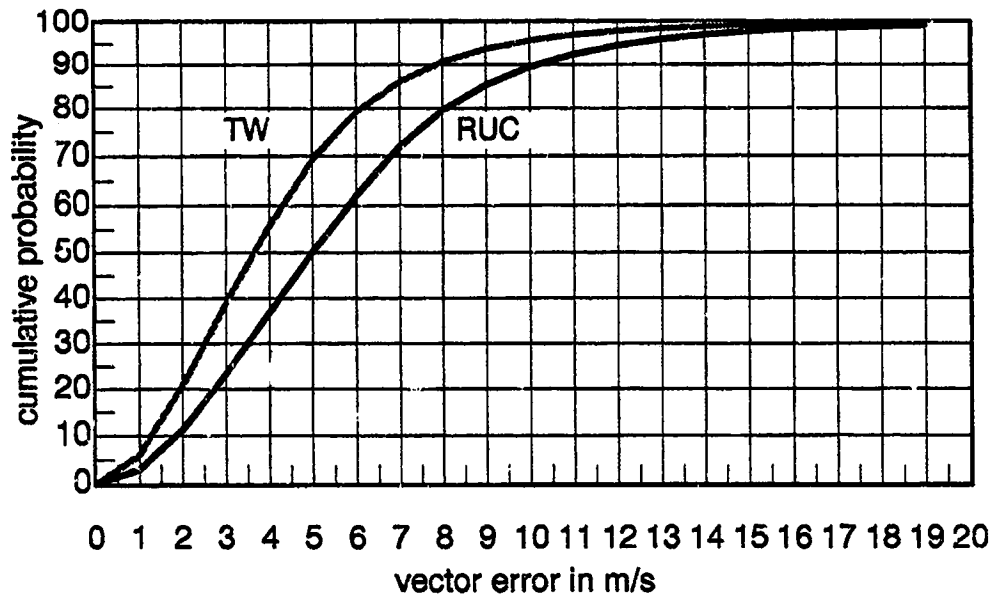


Figure 7. RUC and TW cumulative probability vs. vector error.

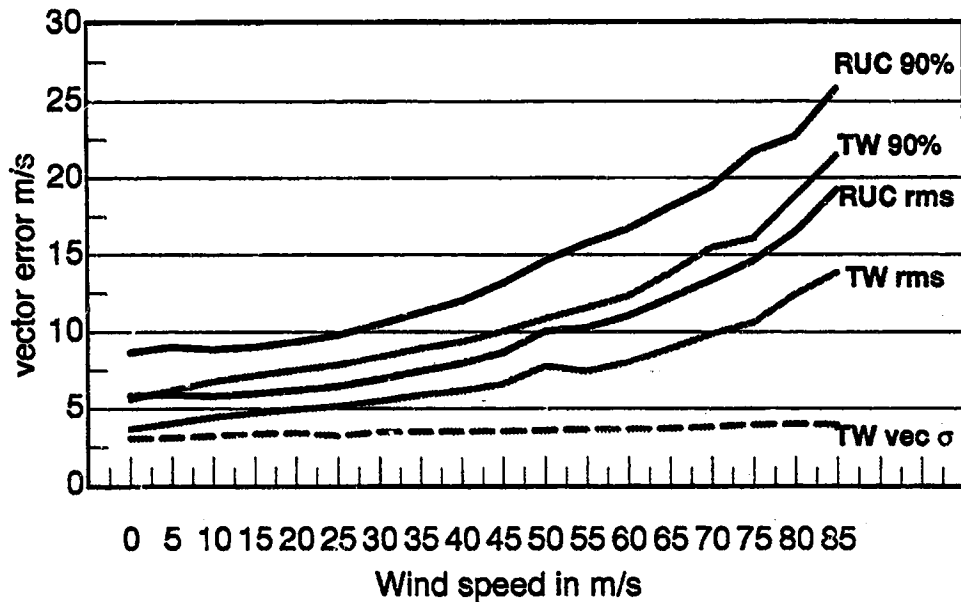


Figure 8. Vector error vs. wind speed. Both the RMS vector error and the 90th percentile error are shown. The TW estimate of the standard deviation of the vector error is shown by the dashed line.

and these values are largely a function of data density at a given location. The relationship between these values and the actual computed vector errors is considered in the next section. Errors are expected to rise as these TW error estimates rise. Given that low wind speeds generally occur near the ground and high wind speeds generally occur aloft and that the data density may vary with altitude, the apparent relationship between vector errors and wind speed may reflect the influence of data density changes with altitude. However, as Figure 8 shows, there is very little change in the TW error estimates with mean wind speed, although the change has the same trend as the vector errors vs. wind speed plots.

It is important to understand the nature of the error vs. speed results in Figure 8. Figure 9 shows the ratio of speed error to wind speed. In this figure it is seen that RUC, on average, underestimates the wind speed and that this underestimation is greatest when the wind speed is highest. This means that the errors in strong winds are not only very large but are systematic. The addition of recent MDCRS to RUC reduces the amount of underestimation by about half. When winds are strong, even the 90th percentile errors are negative, indicating that virtually all reported winds are too light. These results are especially problematic since they indicate that during strong winds the errors in RUC are large and highly correlated; these two attributes can interact to cause large errors in time-of-flight estimates. The addition of recent MDCRS to RUC greatly reduces both the magnitude of the errors and their correlation.

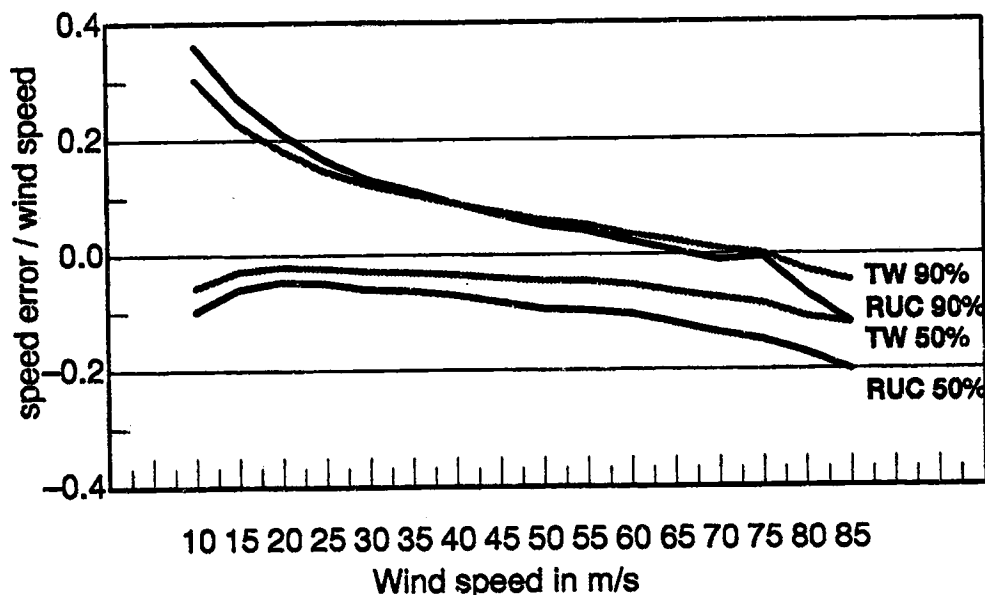


Figure 9. Speed error/wind speed vs. wind speed. Both the median and the 90th percentile percent speed error are shown.

4.6. Performance Results vs. TW Estimates of Error Variance

The TW algorithm uses a statistical interpolation technique. The interpolation technique provides error variance estimates for each wind component, and these estimates are used to derive TW estimates of the RMS vector error. These TW estimates of RMS error depend on error models for errors in RUC and in the MDCRS, as well as how these errors grow with distance and how these errors are correlated; they are a direct measure of information density. If the error models are perfect and the hypotheses underlying the theorems applied held, there would be perfect statistical agreement between the measured RMS vector errors and the TW estimates of RMS error. The achieved relationship between the measured estimates of the RMS vector error vs. the TW estimates of the RMS error is given in Figure 10 along with the mean wind speed vs. the TW estimate of RMS error. All the measures of error grow with the TW estimate of error for small values of the RMS error, but unfortunately so does the wind speed. This presumably occurs because these points are near the airport where air traffic is most dense and wind speeds lowest. After a TW estimate of RMS error of

about 3 m/s, the mean wind speed is nearly constant. The RUC RMS error is also nearly constant, indicating that the wind speed is no longer a factor in the measured TW errors. In this region the TW RMS and 90th percentile errors continue to grow, indicating that the measured errors do grow with increasing TW estimate of RMS error or with decreasing data density. This relationship is stronger for the 90th percentile errors than for the RMS error. As expected, as the data density decreases, the TW errors converge to the RUC errors.

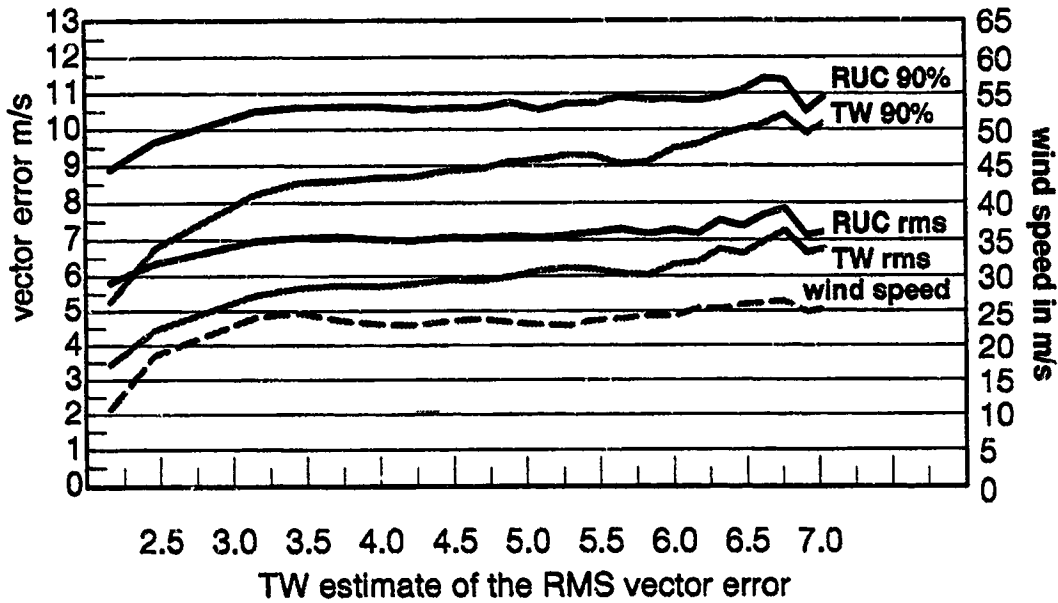


Figure 10. Vector error vs. TW estimate of the RMS vector. Both the RMS vector error and the 90th percentile error are shown, as is the mean wind speed vs. TW estimate of the RMS vector error.

The MDCRS errors partly obscure the relationship between TW vector errors and the TW estimates of the vector error in Figure 10. Figure 11 shows the measured RMS vector errors for RUC and TW corrected for the MDCRS errors (assuming a MDCRS error of 2.78 m/s) vs. the TW estimate of the RMS vector error. The horizontal and vertical scales in the figure are matched to highlight the relationship between the measured RMS vector errors and the TW estimates of the RMS vector error. The light gray line on the diagonal in Figure 11 gives the ideal relationship between the two values being plotted. There is some noise evident in the graph due to small sample sizes when the TW vector error estimates are above about 5 m/s. The dependence of the vector errors on wind speed is clearly evident at both ends of the graph. In the middle range of TW estimates of the RMS vector error, where the mean wind speed is fairly constant, the measured TW RMS vector error rises with the TW RMS vector error estimate, i.e., error increases with decreasing data density. Interestingly, RUC also shows a slight relationship with the TW data density. A conjecture is that regions where TW had many MDCRS reports in the recent past, RUC also had dense data somewhat farther back in time when the model was run, and thus RUC performs better in the same regions that TW performs better. The TW error models that underlie the TW estimates of the RMS vector error do not account for the wind speed. Accounting for the wind speed in the error models may or may not give much improvement in wind field accuracy, but it should improve the the TW estimates of the errors.

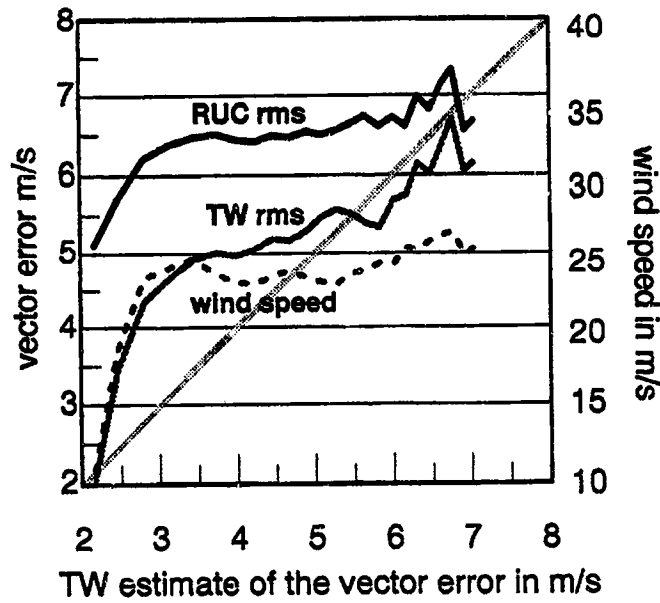


Figure 11. RMS vector error corrected for MDCRS errors vs. TW estimate of the RMS vector error. The mean wind speed vs. TW estimate of the RMS vector error is also shown.

4.7. Performance Results vs. Altitude

Another useful way to break down the error distribution is by altitude. The results over the year are dominated by the MDCRS at cruise altitudes so that important variations in the results, as aircraft descend to an airport, may be obscured. The RMS and 90th percentile vector errors for each of the 50 mb wind field levels are given in Figure 12. The vector errors are largest at cruise altitudes and near the ground. At both altitude extremes the RUC 90th percentile errors are well above the level at which en route DSTs may expect to have trouble (a vector error of 7 m/s or a headwind error of 10 knots). The addition of recent MDCRS to RUC greatly reduces the 90th percentile error; the 90th percentile error is improved by nearly 5 m/s at 750–800 mb. In the TRACON airspace, altitudes with pressures roughly greater than 500 mb or below approximately 18,000 ft. MSL, the addition of recent MDCRS to RUC brings the 90th percentile error down to about 7 m/s or lower. The addition of recent MDCRS to RUC is especially useful in the lower atmosphere; the RUC errors grow as the altitude drops while the TW errors are nearly constant in the lower atmosphere.

The errors above 300 mb dominate the error analyses performed over the entire data set due to the abundance of MDCRS reports at those altitudes. The wind speeds are greater at higher altitudes and decrease steadily towards lower altitudes, so the larger errors at higher altitudes are expected. Wind speeds are lower in the lower altitudes which does not explain the larger RUC errors there. The large RUC errors in the lower atmosphere may reflect difficulties in modeling the more complicated physics there. Errors can also be expected to vary with data density. The TW estimate of the RMS vector error stays between about 3 m/s and 4 m/s, and the measured TW RMS errors closely track the changes in the TW estimates of the RMS vector error across the entire spread of altitudes.

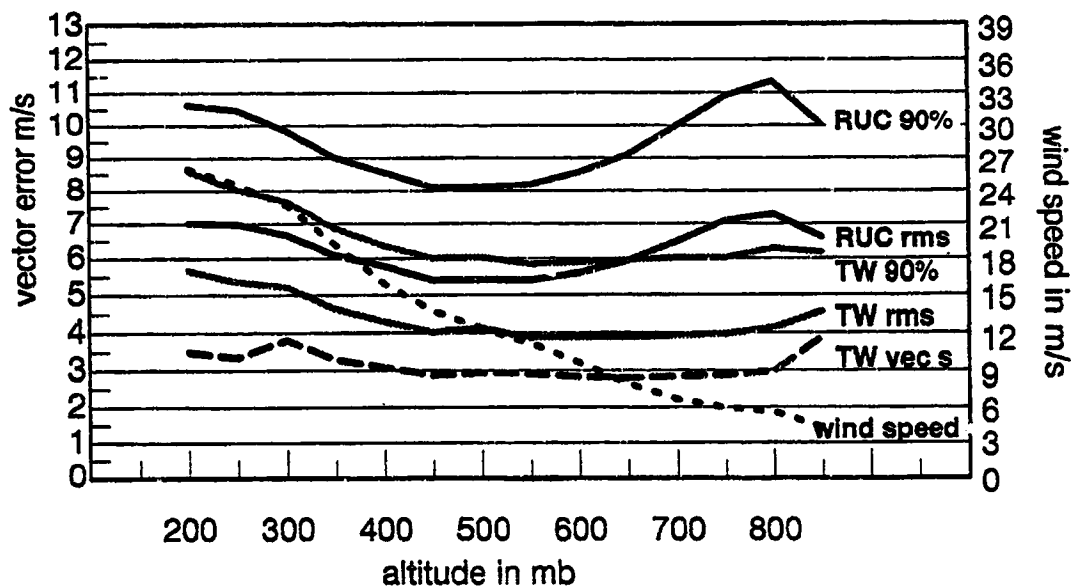


Figure 12. Vector error vs. altitude. Both the RMS vector error and the 90th percentile error are shown.

4.8. Performance vs. Month

The RMS and 90th percentile errors for RUC and TW for each month of the study are shown in Figure 13, along with the monthly mean wind speed and TW estimate of the monthly RMS vector error. The errors closely track the movements of the mean wind, with some minor exceptions. There is a slight dip in the errors in November that is not matched by a dip in wind speeds and a slight increase in the errors in April not matched by an increase in wind speeds. Given that the TW estimate of the RMS vector error changes very little over the year, the expectation is that the variation in the measured errors is driven by the changes in the wind speed.

4.9. Performance vs. Day

The mean vector error with error bars of one standard deviation are shown in Figure 14. The gaps are missing days. The results show that the addition of recent MDCRS to RUC improves both the mean error and the standard deviation. An analysis of each day shows that the addition of recent MDCRS to RUC provides an improvement in the mean error and in the standard deviation on all 343 days. There are many days where the RUC mean vector error plus one standard deviation is well above 10 m/s (nominally equivalent to a 14 knot headwind error), and there are three days where it is above 15 m/s (nominally equivalent to a 20 knot headwind error). Given that averaged over the year the RUC mean vector error plus one standard deviation is 9.31 m/s, this is not surprising, but this indicates that on some days the RUC errors can be expected to be large enough to have a significant operational impact on CTAS. The addition of recent MDCRS reduces the RUC mean vector error plus one standard deviation so that only on several days this value is above 10 m/s, and it is well below 15 m/s on all days.

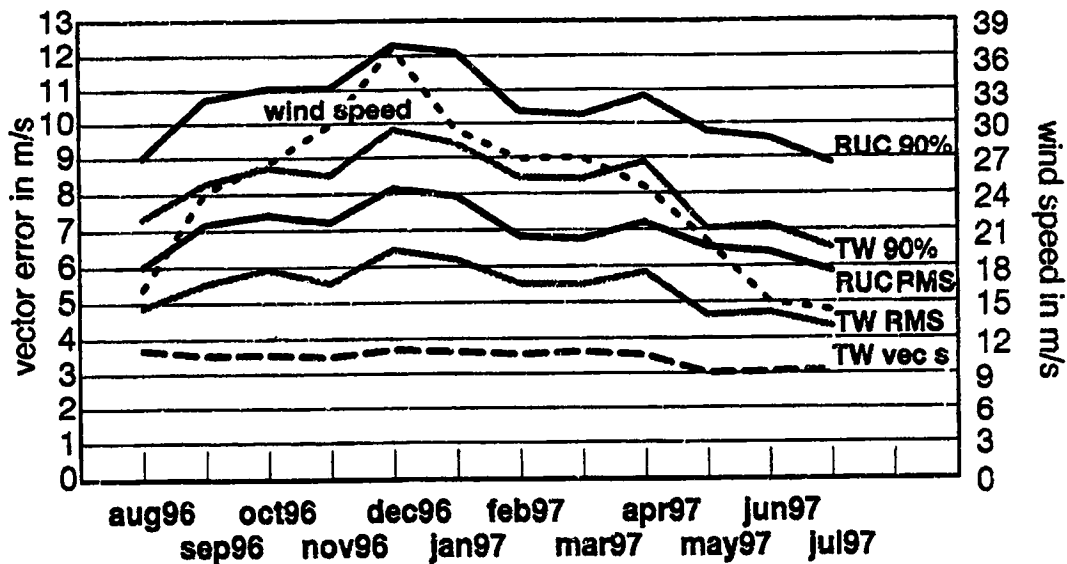


Figure 13. Vector error vs. month. Both the RMS vector error and the 90th percentile vector error are shown.

4.10. Performance vs. Weather Type

The statistical performance of RUC and TW are broken out for different types of weather. This part of the study is designed primarily by FSL and is adopted here for consistency of results. The weather classifications are as follows:

- Altocumulus (standing) lenticularis (ACSL), which is associated with mountain waves in the lee of the Rocky Mountains.
- Precipitation. Any type.
- Towering cumulus (TCU), which implies strong convection and strong vertical motions.
- Thunder, which is also associated with strong convection and strong vertical motions.
- Thunder and towering cumulus.
- Thunder and precipitation.

The determination of when the various weather phenomena exist in the Denver area is performed by searching the Denver Aviation Routine Weather Report (METAR) surface observations. The weather type classifications are treated as valid for a given hour and for the airspace within one degree of latitude and one degree of longitude of the Denver International Airport (DEN). The determination of when the various weather types are present (or not) is provided by FSL. The weather classifications are available for the year period, excluding the period of 12 October 1996 to 8 January 1997, for a total of 277 days. More than one type of weather can be present at the same time.

Although the weather observations are made at the surface, the effects of the weather may occur at different altitudes. If precipitation is occurring without TCU or thunder, it is generally a low-level

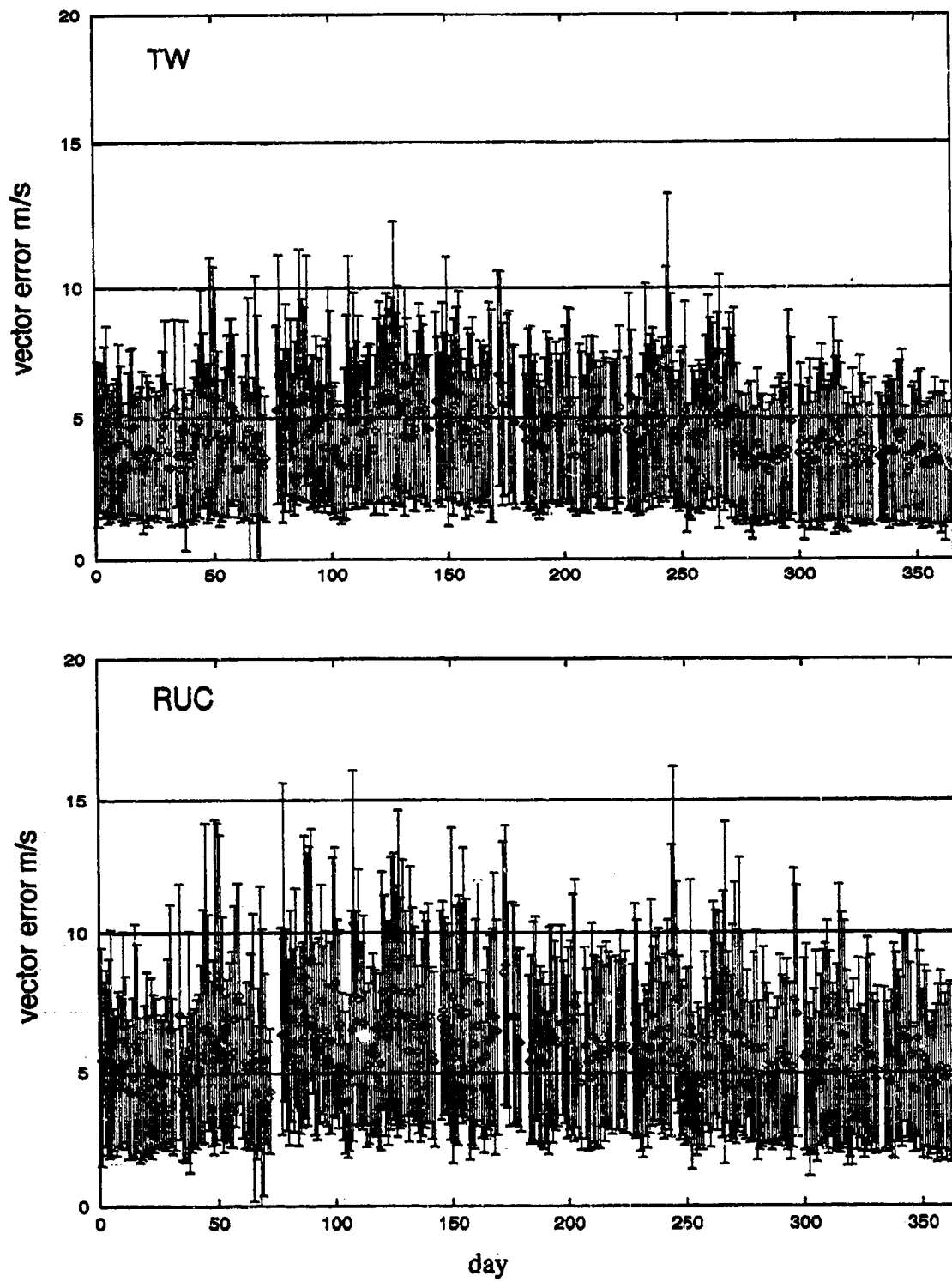


Figure 14. TW and RUC mean vector error \pm one standard deviation vs. day. Day 1 is August 1, 1996.

event (below 2 km). ACSL clouds are middle- or possibly upper-level features from about 2-6 km. Thunder and TCU are associated with convective activity, and each can cause strong wind shear up to the tropopause or about 12 km.

The statistics for the single weather classifications are computed by dividing all the MDCRS reports local to Denver into two sets for each weather classification: the set of MDCRS measurements taken during times when a given type of weather exists and the set of MDCRS measurements taken outside the times when a given type of weather exists. Note that possible altitude limits on the weather in question are not used in dividing the MDCRS into these two sets. The standard performance statistics are computed for these two sets. The performance is also computed for times when there are both thunder and towering cumulus and for times when there are both thunder and precipitation. In these two cases the MDCRS are divided into two sets: the set of MDCRS measurements taken when both types of weather exist and the set of MDCRS measurements taken when neither weather type exists. The MDCRS measurements taken when only one of the weather types exist are not used in these cases.

The statistics of primary importance are the statistics for the general case (all) and the statistics for a given weather classification. The statistics for the "no weather" case, for example, no precipitation, are included for completeness. The comparison of the RMS error and 90th percentile error for the general case vs. these statistics for a given weather case shows whether or not the weather type has a significant impact on the wind errors and whether or not it may be a useful real-time discriminate of expected errors. Because the number of MDCRS in each weather classification is relatively small, the "no weather" data sets are nearly the same as the full data set, and thus the statistics for the "no weather" cases are very close to the general case. For this reason, the "no weather" statistics are not particularly useful.

The results for each of the weather classifications, along with results for the entire data set, are given in Table 10. For each weather classification, the data set is partitioned into two sets: data collected during the time of the given weather and data collected outside the time of the given weather. Because the MDCRS reports are in the Denver area, many of the aircraft are descending to or ascending from the Denver airport, so the aircraft are generally at lower altitudes than in the general case. This results in lower average wind speed, which reduces the magnitude of the errors. Statistics for wind speed and the TW estimate of the RMS vector error are also provided in Table 10. An increase in wind speed is associated with an increase in wind field errors, as is an increase in the TW estimate of the vector error. These two influences on the magnitude of the vector errors are included to help discern whether a change in wind field accuracy for a given weather classification can be explained by other, more readily available factors.

A synopsis of the results follows:

1. Altocumulus (standing) lenticularis (ACSL) is associated with a modest decrease in the vector errors, an increase in wind speeds, and no significant change in the TW estimate of the RMS vector error. The decrease in errors is in opposition to the expected increase in errors due to the increase in wind speed. ACSL is a signal associated with a moderate decrease in wind field errors.

The benefit of the addition of recent MDCRS to RUC in wind field accuracy is about the same as in the general case.

Table 10.
Performance in Different Types of Weather

The basic weather categories are as follows: All reports, altocumulus (standing) lenticularis (ACSL), precipitation, towering cumulus (TCU), and thunder. Values are in m/s.

Weather type	number MDCRS	RUC RMS	TW RMS	RUC 90%	TW 90%	wind spd	wind std	TW σ RMS
All	216.1K	6.14	4.14	9.22	6.09	10.61	8.02	2.78
ACSL	2.4K	5.79	3.85	8.87	5.78	14.24	10.29	2.84
no ACSL	213.6K	6.15	4.15	9.22	6.10	10.57	7.98	2.79
Precipitation	12.6K	7.07	4.73	10.69	7.35	11.37	8.30	2.81
no Precip	203.4K	6.08	4.10	9.12	6.01	10.56	8.00	2.79
TCU	58.7K	6.27	4.22	9.62	6.48	8.74	5.59	2.56
no TCU	157.4K	6.09	4.11	9.07	5.95	11.31	8.65	2.86
Thunder	14.6K	6.96	4.65	10.59	7.17	9.13	5.32	2.50
no Thunder	201.5K	6.08	4.10	9.12	6.02	10.72	8.17	2.80
Thunder & TCU	13.6K	6.84	4.64	10.45	7.15	9.04	5.25	2.49
no Thun. or TCU	156.4K	6.08	4.11	9.05	5.94	11.31	8.66	2.86
Thun. & Prec.	3.9K	7.66	5.21	11.57	7.95	9.28	5.14	2.59
no Thun. or Prec	192.8K	6.05	4.08	9.07	5.97	10.64	8.11	2.80

- Precipitation is associated with a distinct increase in the vector errors, a slight increase in wind speed, and no significant change in the TW estimate of the RMS vector error. Given that the increase in wind speed is small, precipitation is a signal associated with significant increases in wind field errors.

The benefit of the addition of recent MDCRS to RUC in wind field accuracy is slightly greater, by about 0.2 m/s to 0.3 m/s, than in the general case, e.g. for the 90th percentile: 10.69 m/s vs. 7.35 m/s for an improvement of 3.34 m/s vs. the general case improvement of 3.13 m/s in the 90th percentile error.

- Towering cumulus (TCU) is associated with a small increase in the RMS vector error and is associated with a larger increase in the 90th percentile vector error. TCU is also associated with a small decrease in wind speed and a small decrease in the TW estimate of the RMS vector error. The effect of these later two influences largely cancel, so TCU is a signal associated with a moderate increase in wind field errors.

The benefit of the addition of recent MDCRS to RUC in wind field accuracy is about the same as in the general case.

- Thunder is associated with a large increase in the RMS vector error and in the 90th percentile vector error. Both the wind speeds and the TW estimate of the RMS vector error are reduced during times of thunder, and their effects largely cancel. Thunder provides a signal for significant increases in wind field errors.

The benefit of the addition of recent MDCRS to RUC in wind field accuracy is slightly greater, by about 0.3 m/s, than in the general case.

5. The combination of thunder and towering cumulus is associated with a large increase in the vector errors, similar to the increase seen with precipitation. This combination is also associated with a decrease in wind speed and a decrease in the TW estimate of the RMS vector error. The combination of towering cumulus and thunder is a signal for significant increases in wind field errors, but it is not a better signal than thunder alone.

The benefit of the addition of recent MDCRS to RUC in wind field accuracy is very slightly greater, by about 0.1 m/s to 0.2 m/s, than in the general case.

6. The combination of thunder and precipitation is associated with much larger increases in the vector errors than are seen for the other weather classifications. This combination is associated with a decrease in wind speed and is associated with a small decrease in the TW estimate of the RMS vector error. Of the weather classifications studied, the combination of thunder and precipitation provides the strongest signal for significant increases wind field errors.

The benefit of the addition of recent MDCRS to RUC in wind field accuracy is significantly greater, by about 0.5 m/s, than in the general case.

4.11. Performance vs. Number of MDCRS

One goal of the study is to determine the optimal rate of MDCRS reporting. This is related to the issue of errors vs. data density. In support of this study, after May 1, 1997 United Airlines increased the rate at which some of their aircraft reported the winds. The increased reporting brings the number of MDCRS reports per day from about 3500 to about 7800 per day. This gives the opportunity to run some days varying the number of MDCRS data from less than normal to greater than normal to determine the variation in performance with the number of MDCRS reports. Rerunning large numbers of days is time consuming, but some minimum number of days is needed for the results to be statistically significant. The 10 days, 97150–97159 (May 30 through June 8), are used as a compromise. These days are used simply because they provide 10 consecutive days while the United aircraft are providing data at a high rate. Recall that the wind speeds are lower than average during this period, so these are not particularly challenging days. The results on these 10 days may represent a conservative estimate of the benefits of the increase in the number of MDCRS reports. In this section, the statistics are computed by comparing the wind fields to all available MDCRS reports, even if the matched TW wind is a pass through of RUC.

There are four runs of TW in addition to the original run for each day. Additional runs of RUC are not available due to the difficulty in rerunning the RUC processing. The MDCRS data for each day are thinned in a naive way to remove observations from a time-ordered list of the MDCRS reports, and TW is run using the thinned list. Runs with 20, 40, 60, and 80 percent of the MDCRS are made. A percentage of 45 corresponds to the data rate without the increased United reporting. The original runs provide the data for 0 percent of the MDCRS (RUC only) and 100 percent of the MDCRS. The RUC data incorporated with the recent MDCRS by TW uses the full MDCRS data set. The resulting RMS vector errors and the 90th percentile vector errors are shown in Figure 15. The improvement in the RMS vector error is substantial up to 40 or 60 percent, and improvement

continues up to 100 percent. There is a substantial improvement in the 90th percentile error up to 60 or 80 percent, and the improvement continues up to 100 percent. Since the RUC data in this study uses the full MDCRS data set, the improvement shown here as the number of MDCRS increases is expected to be an underestimate of the improvement if RUC also used reduced MDCRS data sets.

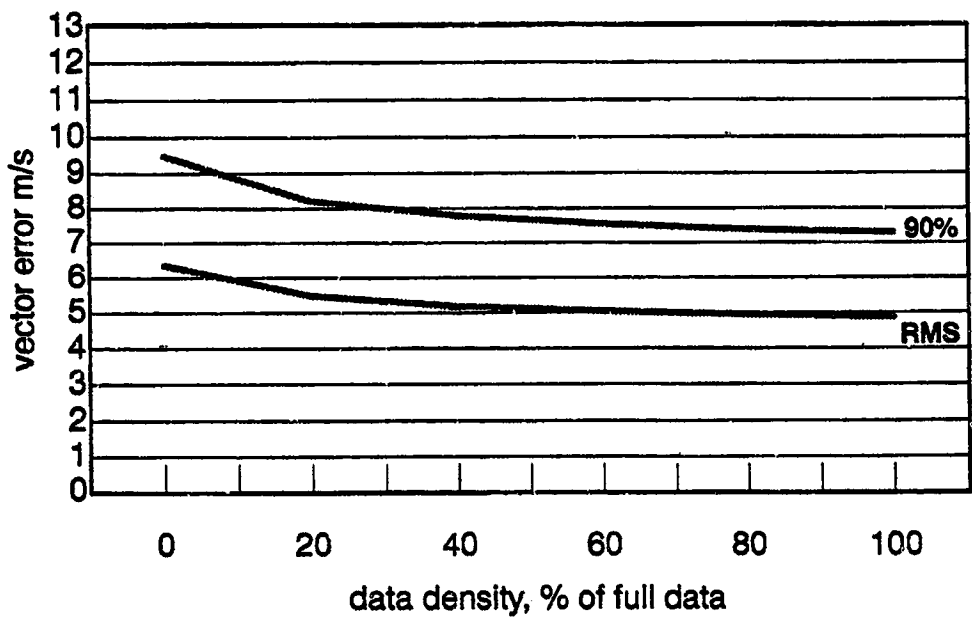


Figure 15. TW RMS and 90th percentile vector error vs. data density. The corresponding percentage without the increased United Airlines reporting is 45 percent.

4.12. Performance vs. Maximum Allowed Number of MDCRS per Analysis Point

In the TW algorithm, MDCRS near an analysis point are chosen for use in estimating the wind at that analysis point. The algorithm estimates the error variance of each MDCRS relative to the analysis point based on distance and age and then selects the *n* best MDCRS. The tradeoff is that averaging more data increases the accuracy if the data represent the wind at the analysis location, but gathering more observations for a given location requires searching farther from the location; which reduces the representativeness of the observations. The value of *n* for the run of the year's data is five. This is increased to 10 for the ten days used above. The results comparing the performance of TW using up to five MDCRS per analysis point and using up to 10 MDCRS per analysis point on these 10 days are given in Table 11. No improvement is seen from going from five observations per grid point to 10 observations per grid point.

4.13. Performance vs. Separation in Time of MDCRS Reports and Wind Fields

The performance results are computed by comparing MDCRS reports to the wind field for the most recent previous cycle, provided it exists. RUC wind fields are valid on the hour and TW wind fields are valid at 10 and 40 minutes after the hour. So, the MDCRS observation time can be up to 59 minutes after the time at which the wind field is valid for RUC, and the MDCRS observation time can be up to 29 minutes after the time at which the wind field is valid for TW. The (MDCRS-wind field) values are binned every five minutes by time from the last hour, and the resulting RMS and

Table 11.
Comparison of TW with a Maximum of 5 Observations per Grid Point
and a Maximum of 10 Observations per Grid Point
 Results are for 74,344 aircraft reports (66,485 for % speed error and direction error). Values are in m/s, except for % speed error, which is unitless, and direction, which is in degrees.

variable	mean+/-std	RMSE	50%	75%	90%	95%
5 obs/grid point:						
TW u error	-0.52±3.32	3.36	-0.45	1.39	3.30	4.67
TW v error	0.25±3.51	3.52	0.33	2.17	4.08	5.46
TW vector error	3.94±2.86	4.87	3.31	5.11	7.30	9.11
TW % speed error	-0.60±25.0	25.0	0.2	12.9	27.1	37.4
TW direction error	-0.56±18.9	18.9	-0.24	6.31	14.72	22.12
10 obs/grid point:						
TW u error	-0.50±3.34	3.38	-0.44	1.43	3.36	4.73
TW v error	0.24±3.54	3.55	0.31	2.19	4.12	5.52
TW vector error	3.97±2.87	4.90	3.34	5.13	7.35	9.14
TW % speed error	-0.60±25.3	25.3	0.1	13.0	27.3	37.5
TW direction error	-0.53±18.9	18.9	-0.19	6.39	14.87	22.55

90th percentile vector errors are shown in Figure 16. The errors in RUC rise slightly over the hour, from a low of 6.48 to a high of 6.88 m/s for the RMS vector error and from a low of 9.79 m/s to a high of 10.41 m/s for the 90th percentile vector error. The errors in TW show a similar rise between cycles, with minima as expected at 10 and 40 minutes after the hour. The maxima and minima of the TW cycle are 4.98 m/s and 5.34 m/s for the RMS vector error and 7.55 m/s and 18.21 m/s for the 90th percentile vector error. This indicates that there is some benefit to adding the recent MDCRS more frequently than every 30 minutes and that interpolation in time between RUC forecasts may be useful, as these modifications might reduce the errors by a couple tenths of a m/s. Wind speed did not play a factor since the mean wind speed is nearly constant for each time bin.

4.14. Performance vs. Separation in the Vertical of MDCRS Reports and Wind Field Levels

The performance results are computed using interpolation in the vertical between wind field levels to the MDCRS altitude. Both RUC and TW are available at pressure levels spaced 50 mb apart, giving rise to a maximum difference of 25 mb between the MDCRS and the closest wind field level. The MDCRS-wind field values are binned every five mb based on the separation of the MDCRS from the nearest wind field level. The resulting RMS and 90th percentile vector errors are shown in Figure 17. The mean wind in each bin is also shown and varies, presumably, because the distributions of preferred aircraft altitudes gives rise to a relationship between the bins and altitude. While the errors grow as the separation between MDCRS and wind field level grows, the resulting increase also closely follows the mean wind profile, making it difficult to separate the two effects. While there is not a clear benefit shown to going to a vertical resolution finer than 50 mb, it is expected that there is a benefit in sheared environments.

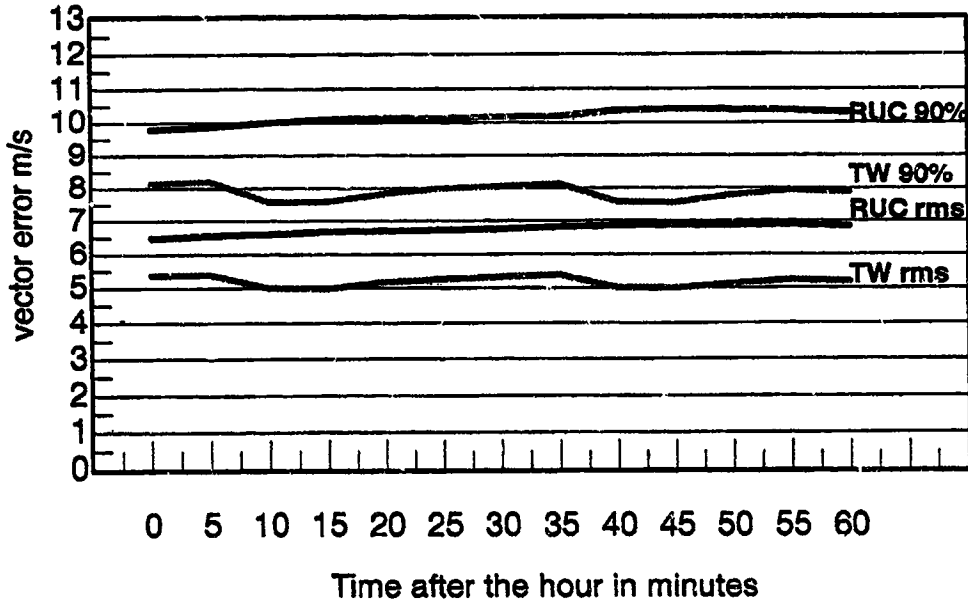


Figure 16. Vector error vs. time after the hour. Both the RMS vector error and the 90th percentile errors are shown. RUC updates on the hour, and TW updates at 10 and 40 min. after the hour. The MDCRS reports are compared to the most recent prior wind field.

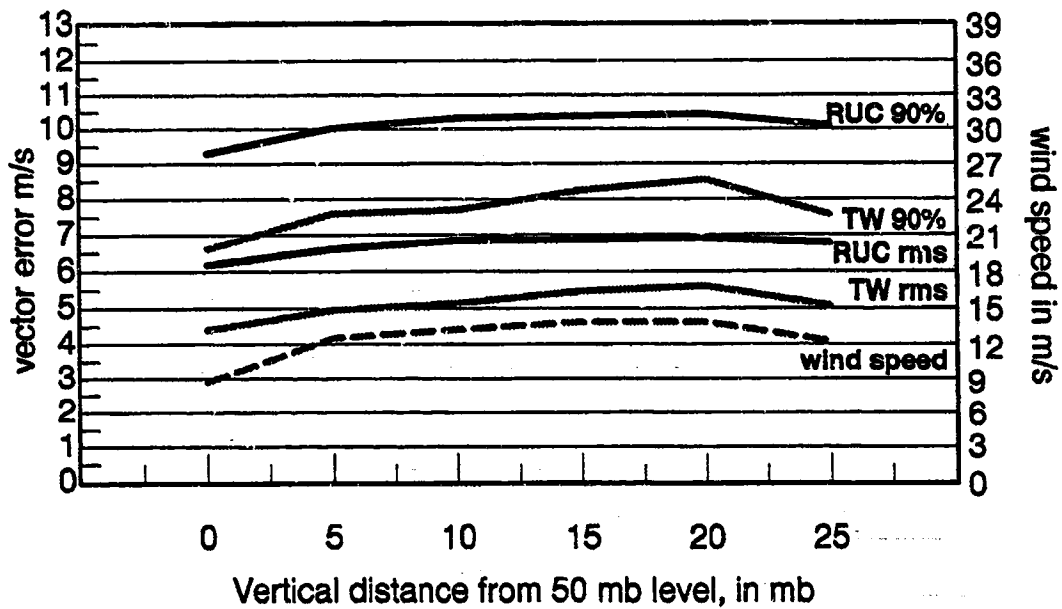


Figure 17. Vector error vs. vertical interpolation distance. Both the RMS vector error and the 90th percentile errors are shown. The relationship to mean wind speed is also shown.

4.15. Analysis of Sustained Errors

For wind errors to have a deleterious effect on CTAS they must be sustained and well correlated along the flight path. It would be useful to study this directly by looking at individual paths through the airspace. However, looking at errors along the track of a single aircraft is problematic due to the biases in the measurements from a single aircraft (as shown in Table 5). A detailed analysis of errors along flight paths is left for another study. This study examines the distribution of sustained errors without examining their correlation. It is implicitly assumed that sustained errors will tend to be correlated, but this is not directly shown.

To find errors which persist over time and space, the hourly 25th percentile vector error, the hourly 50th percentile error or median, and the hourly 75th percentile error are computed. For example, the hourly 25th percentile error is the value X for which 75 percent of all aircraft reports in a given hour are reporting errors greater than X . The hourly 75th percentile error is the value Y for which 25 percent of all aircraft in a given hour are reporting errors greater than Y . The data set contains 7023 hours of data.

The distributions of the hourly N th percentile vector errors are given in Figure 18, Figure 20, and Figure 22. Each error bin labeled n m/s contains errors between $n-1$ m/s and n m/s. Both the percent of hours with errors of given magnitude and the number of hours are given. Cumulative probability plots are also given (Figure 19, Figure 21, and Figure 23). The cumulative probability plots are especially useful in this context, as they let the reader estimate the number of hours with errors above any threshold. The exact number of hours for which the sustained vector errors are above 7 m/s (headwind error of approximately 10 knots), 10 m/s (headwind error of approximately 14 knots), and 15 m/s (headwind error of approximately 20 knots) are given in table Table 12.

Focussing on Table 12, it is seen that there are 42 hours during the year when 75 percent of the RUC vector errors are greater than 7 m/s and that the addition of recent MDCRS reduces that number to five hours. These 42 hours are evenly divided between nighttime and daytime and usually occur as an isolated hour. There are no hours when 75 percent of the RUC vector errors are greater than 10 m/s. There are many hours during the year when 50 percent of the RUC vector errors are greater than 7 m/s. The addition of recent MDCRS reduces the number of hours of such errors from 829 to 124. There are 46 hours during the year when 50 percent of the RUC vector errors are greater than 10 m/s, and the addition of recent MDCRS reduces the number of hours of such errors to one. These 46 hours are evenly divided between nighttime and daytime and usually occur as an isolated hour. Since a 10 m/s vector error corresponds to about a 14 knot headwind error, this is a significant reduction in sustained errors. Having even 25 percent of the aircraft experiencing large errors is potentially of operational concern for CTAS if the aircraft are concentrated along one or more flight paths as opposed to randomly scattered about. There are 45 hours during the year when 25 percent of the RUC vector errors are greater than 15 m/s, or a headwind error of approximately 20 knots. The addition of recent MDCRS reduces this number of hours to eight. These 45 hours are evenly divided between nighttime and daytime and usually occur as an isolated hour. Over the course of the year, 4160 hours, or more than half the hours in the study, have 25 percent of the RUC vector errors greater than 7 m/s or more. This number of hours is reduced to 1913, or by a factor of more than 50 percent, with the addition of recent MDCRS data.

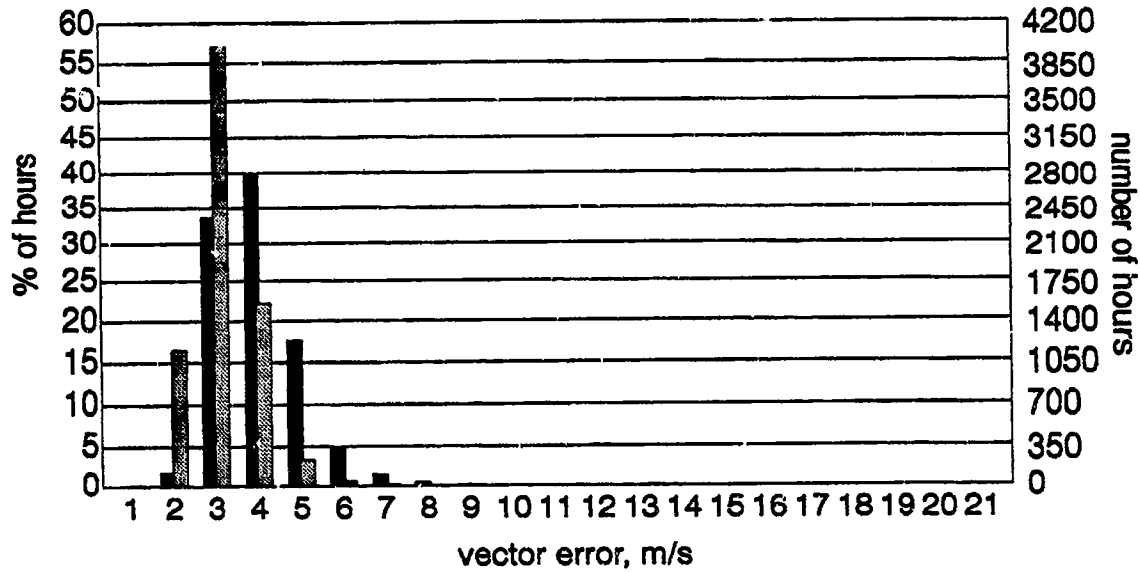


Figure 18. Histogram of the percent and number of hours vs. RUC (black bar) and TW (gray bar) 25th percentile hourly vector errors. Each bin labeled n contains errors between $n-1$ and n , except bin 21 contains all errors 20 m/s and greater.

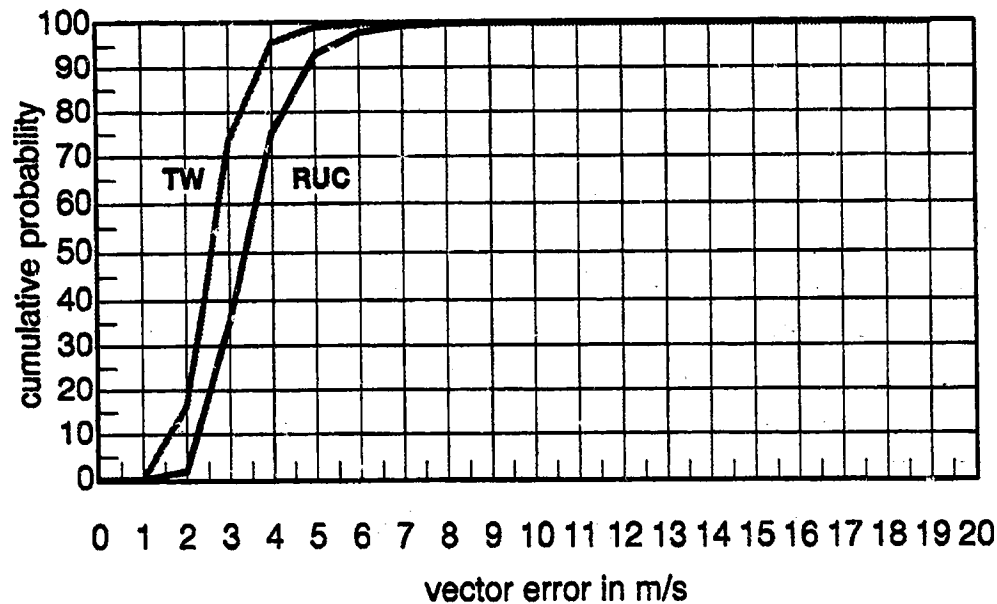


Figure 19. RUC and TW cumulative probability vs. 25th percentile hourly vector error.

4.16. Error Correlation Lengths

The computation of time-of-flight along a path requires computing a numerical integral. The path is broken into small segments, and the time-of-flight for each segment is computed. Then the times are summed to get the time-of-flight for the entire path. Each segment's time-of-flight has an error due to incorrect winds. Time-of-flight errors, which arise from correlated wind errors, will

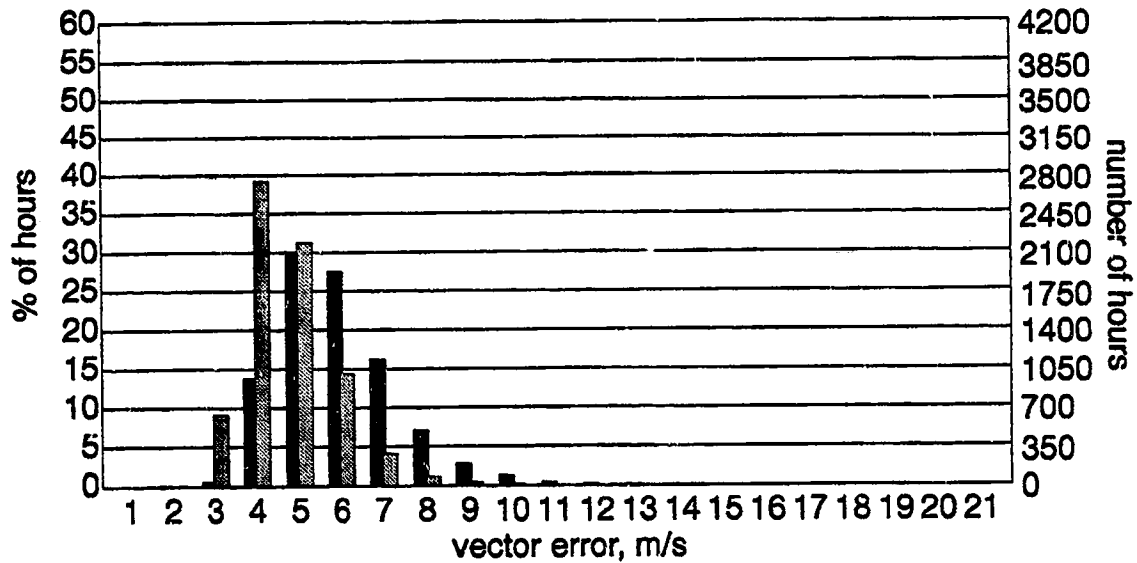


Figure 20. Histogram of the percent and number of hours vs. RUC (black bar) and TW (gray bar) hourly median vector errors. Each bin labeled n contains errors between $n-1$ and n , except bin 21 contains all errors 20 m/s and greater.

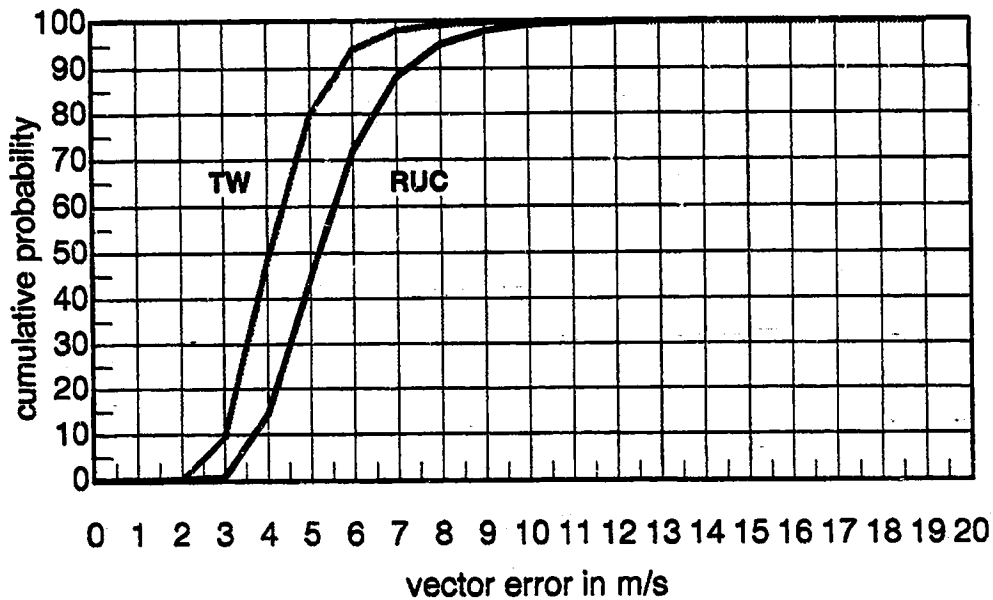


Figure 21. RUC and TW cumulative probability vs. hourly median vector error.

tend to be of the same sign, and when summed, these errors accumulate. Time-of-flight errors that arise from wind errors that are not correlated will often vary in sign, and when summed, these errors tend to cancel. Assuming the correlation in the wind errors decays exponentially, the correlation length of the error is the distance over which the correlation in the wind errors drops to a value of $1/e$. All else being equal, the wind field with the shorter correlation length will lead to more accurate time-of-flight estimates.

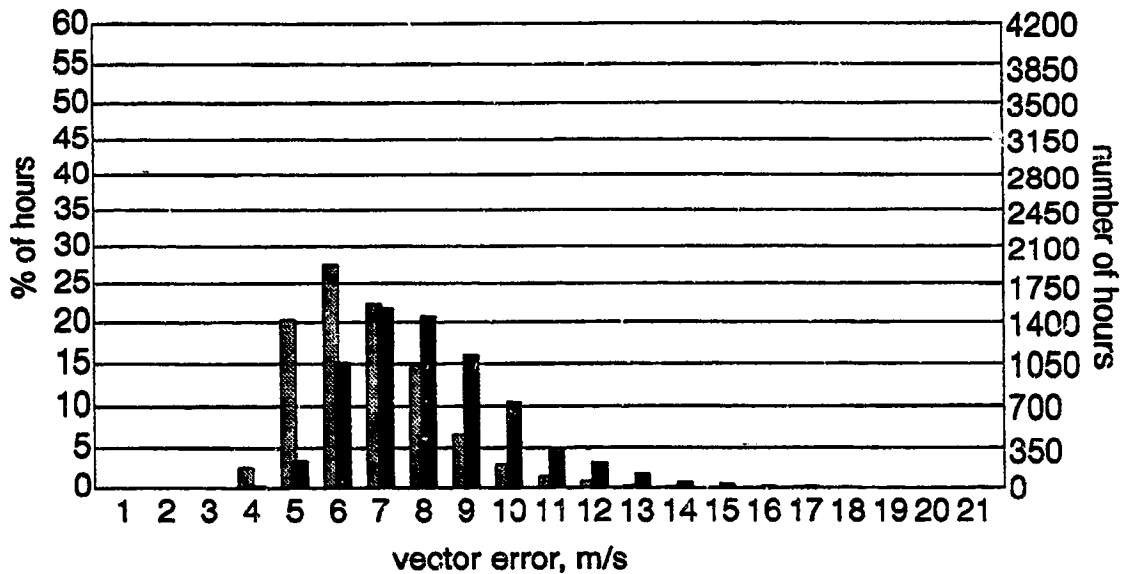


Figure 22. Histogram of the percent and number of hours vs. RUC (black bar) and TW (gray bar) hourly 75th percentile vector errors. Each bin labeled n contains errors between $n-1$ and n , except bin 21 contains all errors 20 m/s and greater.

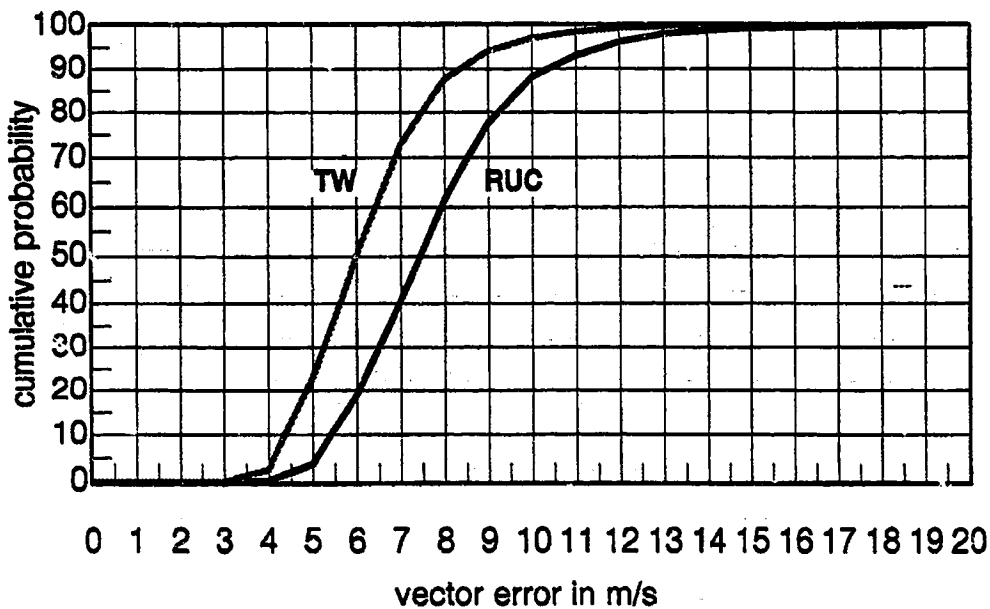


Figure 23. RUC and TW cumulative probability vs. hourly 75th percentile vector error.

The error correlation length is a very important parameter, along with some measure of average error, in performing simulations of time-of-flight calculation accuracy. Often the wind error is set to a constant value, perhaps the RMS error for an on-average scenario or 90th percentile error for a worst-case scenario. Setting the wind error to a constant is equivalent to setting the error correlation length to infinity, which allows no cancelation of errors. In reality, errors do cancel to some de-

Table 12.
Number of Hours with Hourly Nth Percentile Vector Errors
Above Given Thresholds
 Results are for 7023 Hours.

<u>variable</u>	<u>>7m/s</u>	<u>>10 m/s</u>	<u>>15 m/s</u>
RUC 25th percentile	42	0	0
TW 25th percentile	5	0	0
RUC 50th percentile	829	46	0
TW 50th percentile	124	1	0
RUC 75th percentile	4160	834	45
TW 75th percentile	1913	203	8

gree, and this can be modeled by using a wind error model that gives wind errors with the desired mean error, RMS error, and correlation length.

The error correlation lengths are influenced by data density and the amount of data averaging or smoothing in the data assimilation. For numerical models, the model physics plays an important role. For TW, which uses RUC in forming an initial estimate, the error correlation lengths inherited from RUC also play an important role. Large error correlation lengths can arise when the error in a given observation is spread over a large region. In TW, the spread of a given observation is tied to the local data density: in regions with numerous observations each observation influences a smaller region. Large error correlation lengths tend to arise in wind fields generated by processes that cause a region of grid point values to be correlated, such as forcing the wind and other values to strictly follow equations of large-scale physics, in which case an error becomes a regional bias. Shorter correlation lengths can arise from analyses where adjacent grid point values are more nearly independent (This approach can lead to other problems from the point of view of numerical models; however, these problems are not a concern to ATM DSTs.)

To estimate the correlation of errors as a function of separation distance, the aircraft are paired in much the same way as is done in the MDCRS accuracy study above. However, instead of requiring that the pair of aircraft be very close together in all three dimensions, the pair are required to be close together in only two dimensions. The data are then binned by the third dimension. To study the error correlation vs. horizontal separation, the MDCRS are paired so that both aircraft are at nearly the same altitude and time. The pairs are then sorted into bins containing pairs whose horizontal separation is a multiple of 20 km. The correlation among the wind field errors in each bin is then computed; bins with small separations have errors which are strongly correlated while bins with large separations have errors which are only weakly correlated. Correlations are computed independently for the u and v wind components. Correlations for vertical and temporal separations are computed similarly. The separation and binning criteria are listed in table Table 13.

Table 13.
Separation Limits for the Generation of Correlations

<u>variable</u>	<u>h corr.</u>	<u>p corr.</u>	<u>t corr.</u>
max horizontal, km	1500	20	20 km
max vertical, mb	5	600	5 mb
max temporal, minutes	2	2	2000
bin size	20 km	10 mb	15 minutes

After computing the correlations, a function of the form $f(x)=a \cdot \exp(-x/b)+c$ is fit to the data. The fit is done using least squares that accounts for the quality of the data. The value of sigma chosen for each correlation value is $1/\sqrt{\text{number of pairs}}$. This later point is important since for large separations there are many fewer samples, and the resulting correlation values are noticeably noisier. The x coordinate is chosen not to be the center of the bin but is chosen to be the mean of the separations for the pairs in the bin. For most bins the mean of the separations in the bin is very nearly the center of the bin, but for the zero bin the mean of the separations in the bin is about half the width of the first bin. Using an x value of zero for the zero bin causes the fit to undershoot $f(0)$, which is an important value. Figure 24 through Figure 35 and Table 14 through Table 16 show the results of fitting $f(x)=a \cdot \exp(-x/b)+c$ to the correlations at specified separation distances for separations in the horizontal, vertical, and temporal. The exponential decay fits the data very well for RUC and TW for horizontal separations and also fits fairly well for TW for vertical separations. The fit to the RUC error correlations vs. vertical separations is not as good. The RUC data for temporal separations show a distinct harmonic signal superimposed on the exponential decay. A function of the form $f(x)=a \cdot \exp(-x/b)+c+d \cdot \cos(2\pi(x-e)/f)$ is fit in addition to the simple exponential decay for the temporal correlations, and the results are in Figure 36 and Figure 37 and in Table 17.

The primary parameter desired in this analysis is b , the correlation length for wind field errors. The correlation length is the distance at which the exponential decay portion of the error correlation drops to $1/e$. The parameter c accounts for correlations which are constant over all separations, and if c is not nearly zero, it plays an important role in the correlation of errors. If the errors in RUC and TW are known perfectly, $f(0)$ would be exactly one; errors in precisely the same location are equal and hence perfectly correlated. However, the values used to estimate errors (MDCRS-modeled wind) have errors due to errors in MDCRS. Also, this analysis considers the pairs to have separations in only one dimension. However, the remaining separations, while small, are not zero and they add additional errors. Just as noted earlier, the more accurate the modeled wind field, the greater the adjustment to account for these errors; the value $a+c=f(0)$ accounts for these errors.

The value $f(0)$ is related to the variance of the errors in the modeled winds and the variance in the errors in the MDCRS, where the errors in the MDCRS include the small-scale winds captured due to the small aircraft separations which are treated as being zero. The relationship is given in equation (9). The term $f(0)/(1-f(0))$ is sensitive to errors in the estimation of $f(0)$, especially for values of $f(0)$ that are near one. Solving for either error variance term also relies on the estimation of the other error variance term. For these reasons, a direct measurement of the variance in the model errors is preferred. Assuming aircraft errors and model errors are independent, equation (9) can be rearranged, with some work, to give equation (10), which relates the variance in the model errors with the variance of the values (MDCRS-model), which are directly measured.

$$\text{var}(\text{model errors})/\text{var}(\text{MDCRS errors}) = f(0)/(1-f(0)) \tag{9}$$

$$\text{var}(\text{model errors}) = f(0) \cdot \text{var}(\text{MDCRS-model}) \tag{10}$$

The correlation in errors, after accounting for the errors in the MDCRS and the errors from the small separations that are treated as being zero, is then

$$f(x) = (1-c) \cdot \exp(-x/b) + c \tag{11}$$

for separations in one dimension. Note that if c is not nearly zero, b alone does not give a good measure of how fast the correlation gets small.

In actual practice, CTAS computes time-of-flight along trajectories that exist over some time period and extend over some horizontal distance and, generally, extend over some vertical distance as well. Because of this, the errors will decorrelate as a function of all three separations. A three-dimensional fit to the data is not done, but the expected result is that the errors in the three dimensions are not strongly correlated, and the product of the three correlation functions provides a good approximation to the actual correlation function of all three separation variables. Conflict detection and resolution require time-of-flight for trajectories over time periods of 10 minutes to 20 minutes, or about 120 km to 240 km at a flight speed of 200 m/s (about 400 knots). Calculation of metering requires time-of-flight over time periods of 20 minutes to 40 minutes. Flights descend from cruise at approximately 300 mb to the TRACON at about 500 mb. Following the discussions of the correlation lengths in each individual dimension, results for 4 three-dimensional trajectories are given: level flight of 10 minutes, descending flight of 10 minutes, level flight of 20 minutes, and descending flight of 20 minutes.

As seen in Figure 24 through Figure 27, the fits of the exponential decay to the correlations as a function of horizontal separation are quite good. The associated parameters are given in Table 14. The correlation lengths for RUC are 311 km for u and 363 km for v . The addition of recent MDCRS data reduces these values to 231 km for u and 241 km for v . The reductions in the correlation length are substantial, averaging about 100 km, and the error correlation lengths for TW are approximately the length over which CTAS computes metering. As expected, the increased accuracy of TW is evident in the lower value of $f(0)$.

As seen in Figure 30 and Figure 31, the fits of the exponential decay to the correlations as a function of vertical separation are fairly good for the TW data, although the data are not as clean as for the horizontal separations. The fits of the exponential decay to the RUC data are not as good (Figure 28 and Figure 29). In particular, the data for the v component of RUC are roughly linear in the range 0–300 mb where the data have the smaller error bars and the resulting fit has little curvature, i.e., a long correlation length. The parameters associated with the fits are given in Table 15. The correlation lengths for RUC are 153 mb for u and 273 mb for v . The addition of recent MDCRS data reduces these values to 69 mb for u and 66 mb for v . These lengths are in the range of what is operationally significant for CTAS, with the error correlation lengths for TW being much less than the vertical distance over which CTAS computes time of flight. Again, the increased accuracy of TW is evident in the lower value of $f(0)$.

As seen in Figure 32 through Figure 35, the fits of the exponential decay to the correlations as a function of temporal separation are quite good for the TW data. The fits of the exponential decay to the RUC data are good, roughly in the range of 0–400 minutes, which covers the time domain of interest for CTAS. After this range, a harmonic signal is seen in the RUC data. The parameters associated with the fits are given in Table 16. The correlation lengths for RUC are 156 minutes for u and 284 minutes for v . Unlike in the vertical separation case, the longer correlation length for the RUC v component does not seem to be due to a poor fit of an exponential decay model. The addition of recent MDCRS data reduced these values to 32 minutes for u and 43 minutes for v . CTAS computes trajectories on time scales up to 40 minutes, so this reduction is also operationally significant. The increased accuracy of TW is evident in the lower value of $f(0)$, although $f(0)$ is larger than in the other cases.

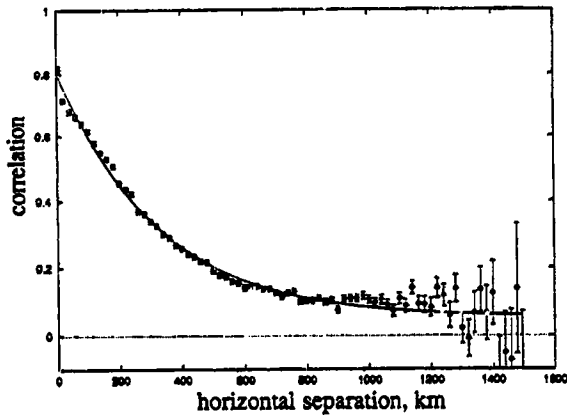


Figure 24. RUC error correlation vs. horizontal separation. U component. Three parameters.

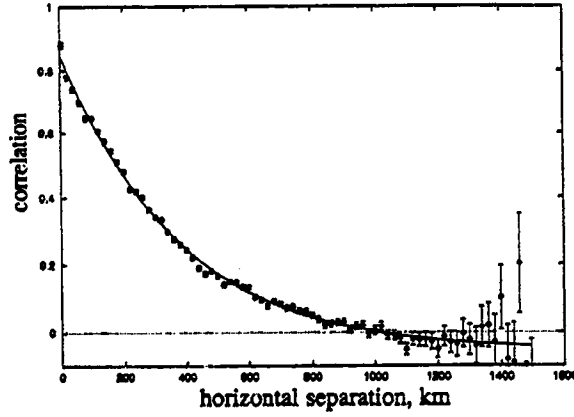


Figure 25. RUC error correlation vs. horizontal separation. V component. Three parameters.

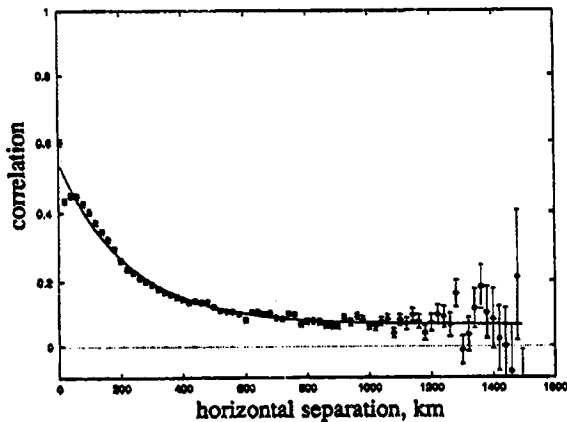


Figure 26. TW error correlation vs. horizontal separation. U component. Three parameters.

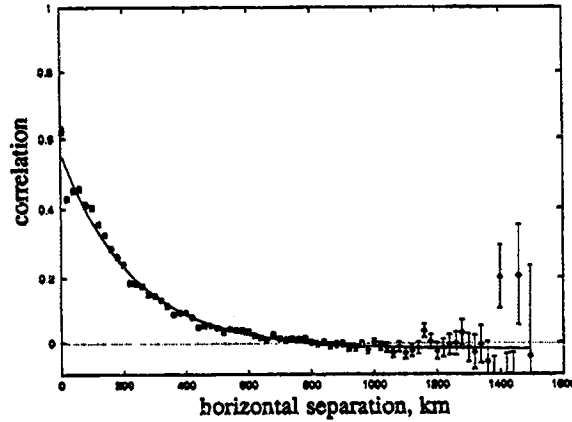


Figure 27. TW error correlation vs. horizontal separation. V component. Three parameters.

Table 14.
Fit Parameters for Error Correlation vs. Horizontal Separation

variable	RUC u	RUC v	TW u	TW v
a	0.75	0.91	.48	.58
b (km)	311	363	231	241
c	0.05	-.06	.07	-.02
f(0)	0.80	0.85	0.54	0.56

Given the harmonic signal evident in the RUC correlation as a function of temporal separation data, a function of the form $f(x) = a \cdot \exp(-x/b) + c + d \cdot \cos(2\pi(x-e)/f)$ is fit to the RUC and TW data (Figure 36, Figure 39, and Table 17). While the harmonic signal is most evident at greater temporal separations than are of interest for CTAS, the resulting fit is slightly better even at shorter time scales and should give slightly better estimates of the RUC temporal correlation length. The harmonic signal is likely due to the diurnal cycle. However, the period f is not 1440 minutes (24 hours); although the first peak in the RUC data is at about 1400 minutes. This may be due to not fitting an entire cycle —

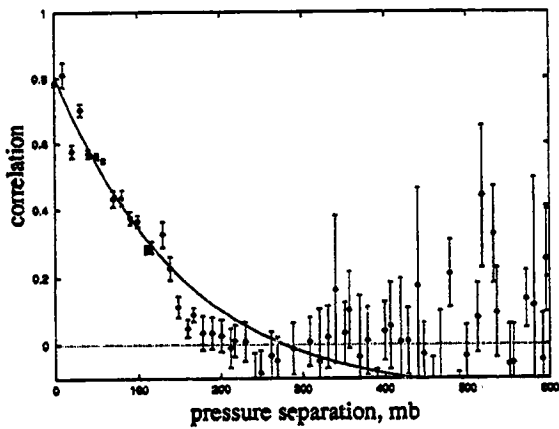


Figure 28. RUC error correlation vs. pressure separation. U component. Three parameters.

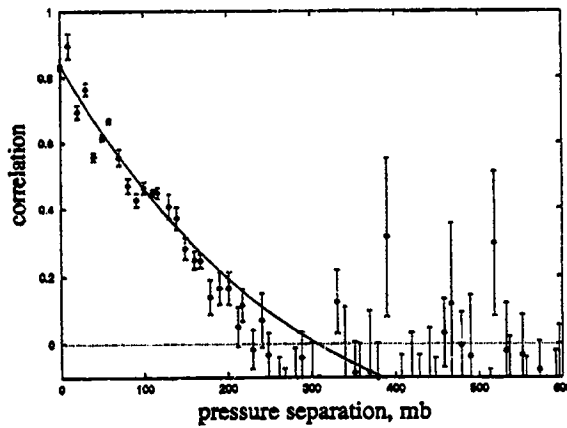


Figure 29. RUC error correlation vs. pressure separation. V component. Three parameters.

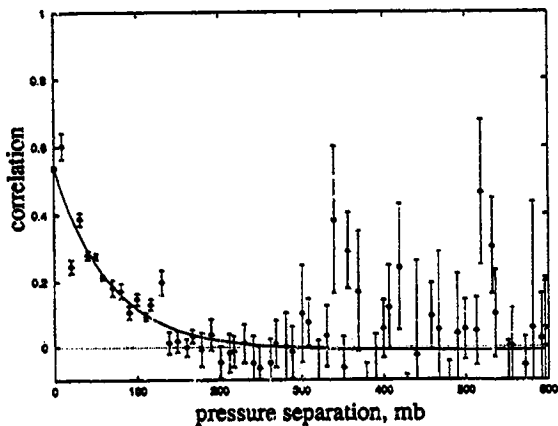


Figure 30. TW error correlation vs. pressure separation. U component. Three parameters.

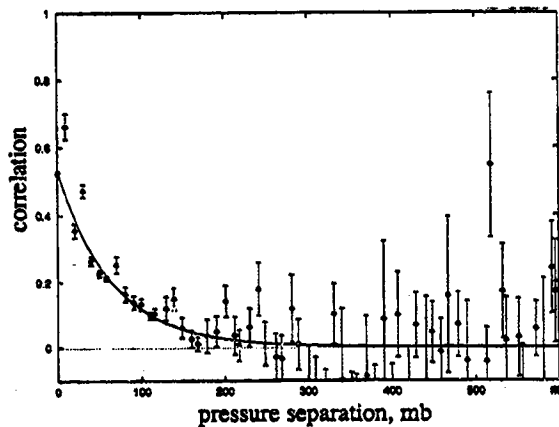


Figure 31. TW error correlation vs. pressure separation. V component. Three parameters.

Table 15.
Fit Parameters for Error Correlation vs. Pressure Separation

variable	RUC u	RUC v	TW u	TW v
a	0.96	1.25	0.55	0.53
b (mb)	153	273	68.7	66.0
c	-.16	-.41	-.01	0.00
f(0)	0.81	0.84	0.54	0.53

in the data. This new function provides a slight reduction in the RUC temporal correlation lengths to 141 minutes for the u component and 254 minutes for the v component; the TW temporal correlation lengths are largely unchanged.

The results in Table 18 show correlations for different nominal trajectories that correspond to conflict calculations performed by CTAS. The correlation of RUC u and v errors for horizontal separations (Δh) of 120 km are the same despite the fact that u and v have rather different values for b.

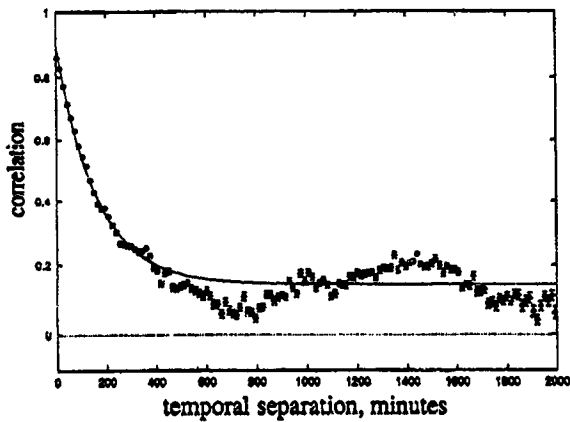


Figure 32. RUC error correlation vs. temporal separation. U component. Three parameters.

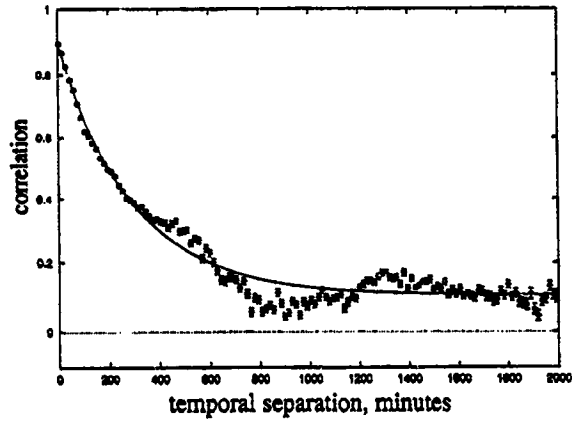


Figure 33. RUC error correlation vs. temporal separation. V component. Three parameters.

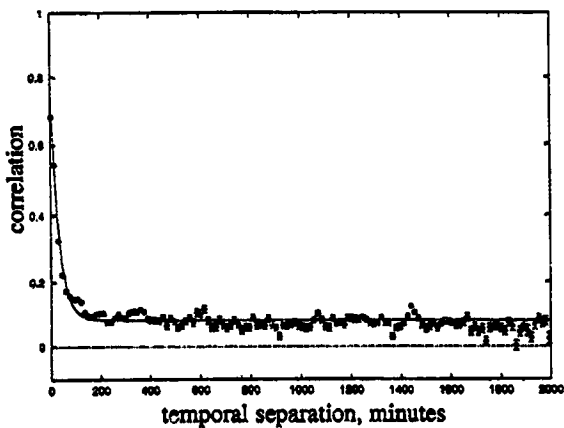


Figure 34. TW error correlation vs. temporal separation. U component. Three parameters.

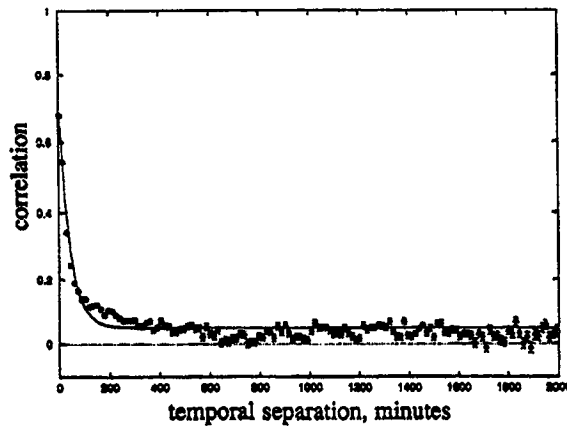


Figure 35. TW error correlation vs. temporal separation. V component. Three parameters.

Table 16.
Fit Parameters for Error Correlation vs. Temporal Separation

variable	RUC u	RUC v	TW u	TW v
a	0.76	0.79	0.69	0.67
b (minutes)	156	284	32.1	42.6
c	0.14	0.10	0.08	0.05
$r(0)$	0.90	0.90	0.77	0.72

They are also the same for a horizontal separation of 240 km. This is due to the fact that 120 km and 240 km are relatively small compared to the corresponding correlation lengths and due to the differing values of c . The TW values of b for horizontal separations are somewhat smaller than for RUC, and the correlations for TW errors are about 0.10 less than for the corresponding RUC errors. The RUC correlations for the nominal separations in the vertical are roughly the same despite the mismatch in b for the two wind components due to the mismatch in the parameter c . Since the vertical separations 100 mb and 200 mb are relatively large compared to the corresponding correlation

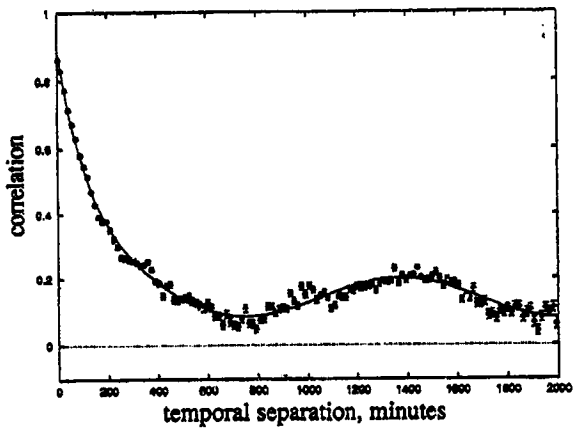


Figure 36. RUC error correlation vs. temporal separation. U component. Six parameters.

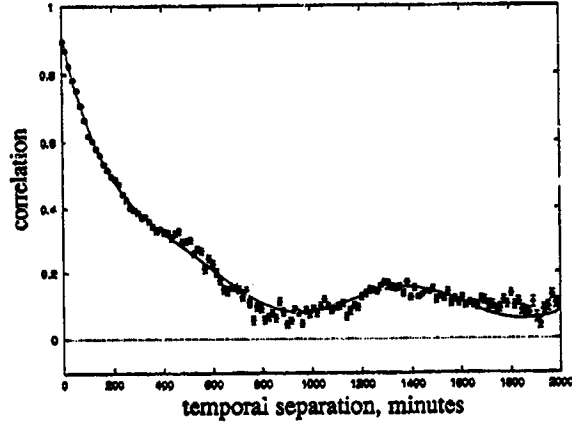


Figure 37. RUC error correlation vs. temporal separation. V component. Six parameters.

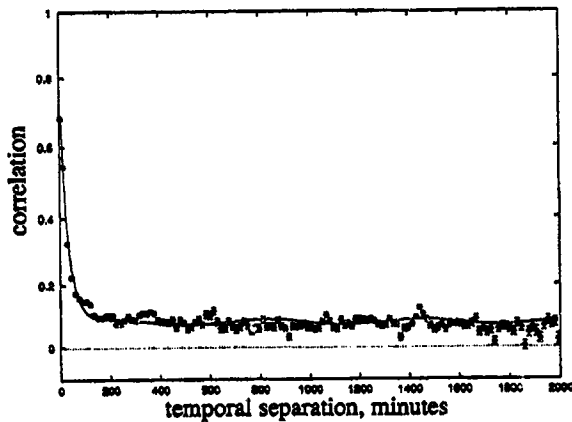


Figure 38. TW error correlation vs. temporal separation. U component. Six parameters.

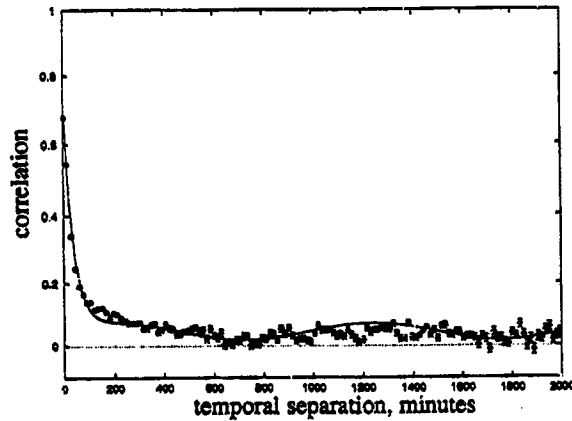


Figure 39. TW error correlation vs. temporal separation. V component. Six parameters.

Table 17.
Fit Parameters for Error Correlation vs. Temporal Separation
Using Six Parameters

variable	RUC u	RUC v	TW u	TW v
a	0.70	0.86	0.70	0.69
b (minutes)	141	254	32	38
c	0.14	0.10	0.08	0.04
d	0.06	0.05	0.01	.03
e (minutes)	97	447	204	208
f (minutes)	1275	935	626	1033
$r(0)$	0.90	0.91	0.77	0.74

lengths, the decrease in the correlation of errors is much greater for the nominal vertical separations than for the other dimensions. The decrease in the correlation of TW errors for vertical separations is much greater than for RUC. The correlations for RUC errors at the nominal temporal separations are again nearly the same, 0.66 vs. 0.68, and 0.44 vs. 0.46, despite the largely different values of b

due to the fact that 10 or 20 minutes is very small relative to the corresponding correlation lengths. The RUC errors are nearly completely correlated for a separation up to 20 minutes.

For a flight in the cruise phase, both the horizontal and temporal correlations apply jointly. For a descending or ascending flight, all three correlations apply. The error correlation is assumed to be the product of the two or three individual error correlations that apply. In level flight, the addition of the extra MDCRS reduces the error correlation by about 0.20, or by 1/3 for a 10-minute flight segment and by 1/2 for a 20-minute flight segment. The correlations are much smaller for both RUC and TW for trajectories that are descending (or ascending). For a 10-minute descending flight segment, the RUC errors are moderately correlated while the TW errors are only slightly correlated. For a 20-minute descending flight segment, the RUC errors are slightly correlated while the TW errors are essentially uncorrelated.

Table 18.
Correlation of Errors for Nominal Separations Using Equation (11)
 The Δh , Δp , and Δt columns are for separations in one dimension only.
 The next two columns are for level flight and for descending flight.

variable	$\Delta h=120$ km	$\Delta p=100$ mb	$\Delta t=10$ min	level	descending
RUC u	0.70	0.44	0.95	0.66	0.29
RUC v	0.70	0.57	0.97	0.68	0.39
TW u	0.62	0.23	0.75	0.47	0.11
TW v	0.60	0.22	0.80	0.48	0.11
variable	$\Delta h=240$ km	$\Delta p=200$ mb	$\Delta t=20$ min	level	descending
RUC u	0.49	0.15	0.90	0.44	0.07
RUC v	0.49	0.27	0.94	0.46	0.12
TW u	0.40	0.05	0.57	0.23	0.01
TW v	0.36	0.05	0.64	0.23	0.01

The RMS errors in the modeled winds can be estimated using equation (10), along with the estimates for $f(0)$ and the RMS error values from table Table 8 (which are uncorrected for MDCRS errors). The resulting error estimates are thus corrected for the MDCRS errors. The model RMS errors are estimated for the values of $f(0)$ calculated for horizontal separations, vertical separations, and temporal separations, and they are given in Table 19. Only the results for the three parameter fits are shown; the results for the six parameter fits are very nearly equal to the results from the corresponding three parameter fits. The estimates of the RMS errors are very close to those given earlier (RMSE 2 in Table 9 and Table 19). The value RMSE 2 is chosen for inclusion here since it is computed using the same separation limits and thus is an independent estimate of the same quantity. The estimates of the RUC RMS errors are very close to each other, spanning a range of 6.12–6.39 m/s for the vector error. The estimates of the TW RMS error are fairly close together, spanning a range of 3.79–4.47 m/s for the vector error.

Table 19.
Comparison of 60 km RUC and 10 km TW
After Correction for MDCRS Errors Using Equation (10)

RMSE raw and RMSE 2 are from Table 9, RMSE h, RMSE v, and RMSE t are from applying equation (10) using the f(0) values for horizontal, vertical, and temporal separation, respectively. Only the three parameter fits are used.
 Values are in m/s.

variable	RMSE raw	RMSE 2	RMSE h	RMSE v	RMSE t
TW u error	3.63	3.08	2.67	2.67	3.18
TW v error	3.69	3.09	2.76	2.69	3.14
TW vector error	5.18	4.37	3.84	3.79	4.47
RUC u error	4.62	4.20	4.14	4.15	4.39
RUC v error	4.91	4.48	4.53	4.50	4.65
RUC vector error	6.74	6.14	6.14	6.12	6.39

•

•

•

•

5. CONCLUSIONS

5.1. Baseline Performance and Benefits from Adding MDCRS to RUC

Computed over the entire one-year data set, the RMS vector difference and median vector difference between RUC and the MDCRS reports is 6.74 m/s and 4.99 m/s, respectively. Incorporating recent MDCRS via the ITWS TW algorithm reduces these values to 5.18 m/s and 3.64 m/s, respectively. Correcting the RMS values for the errors in the MDCRS measurements gives estimates for the RUC and TW RMS vector errors of 6.12 m/s – 6.39 m/s and 3.79 m/s – 4.47 m/s, respectively. Given that vector errors of 7 m/s – 10 m/s (approximately 10 knots – 15 knots of headwind error) are significant to CTAS, the addition of recent MDCRS via the TW algorithm provides a significant improvement in the on-average wind field accuracy.

Perhaps more important than the on-average performance is the distribution of large errors. This is addressed in part by examining the 90th percentile vector errors. The 90th percentile RUC and TW vector differences with MDCRS are 10.18 m/s and 7.85 m/s, respectively. These values cannot be corrected for MDCRS errors as done with the RMS errors. But the actual 90th percentile wind field errors are expected to be somewhat smaller. The addition of the recent MDCRS reports to the RUC wind field is seen to significantly reduce the magnitude of the 90th percentile vector errors. The distribution of large errors is also examined via a cumulative probability plot. From this plot it is seen that 28 percent of the RUC vector errors are greater than 7 m/s, and this is reduced to 14 percent by the addition of the recent MDCRS data. It is seen that 11 percent of the RUC vector errors are greater than 10 m/s, and this is reduced to four percent by the addition of the recent MDCRS data.

Large errors are especially detrimental to CTAS if they are sustained over a large portion of the grid and over a long period of time. As an initial investigation of this issue, the 25th percentile, 50th percentile, and 75th percentile errors are computed on an hourly basis on the one-year data set. The results for the 50th percentile hourly vector error show that out of the 7023 hours in the data set there are 829 hours when the hourly median RUC wind vector error is 7 m/s or more. This means that if CTAS were operating during these hours, half of the wind values that CTAS was using have vector errors of 7 m/s or more. Adding recent MDCRS data to RUC reduces this number of hours to 124. There are 46 hours in the data set when the hourly median RUC wind vector error is 10 m/s or more, and adding recent MDCRS reduces this number of hours to 1. The 25th percentile hourly RUC vector error is greater than 7 m/s for 42 hours (i.e., there are 42 hours when 75 percent of the MDCRS are reporting winds that differ from RUC by 7 m/s or more), and the addition of recent MDCRS reports reduces this to 5 hours. The 75th percentile RUC vector error is greater than 15 m/s for 45 hours (i.e., there are 45 hours when 25 percent of the MDCRS are reporting winds that differ from RUC by 15 m/s or more), and the addition of recent MDCRS reduces this to 8 hours. If these very large errors are concentrated along one or more flight paths, they may represent a serious problem for en route DSTs that generate clearance advisories. The addition of recent MDCRS data to the RUC wind fields provides a very large reduction in large sustained errors.

Another factor in whether or not wind field errors are detrimental to CTAS is their correlation. In computing aircraft time-of-flight along a trajectory, errors that are highly correlated tend to add together when computing time-of-flight, and errors that are not highly correlated tend to cancel. All else being equal, the wind field with the least correlation among errors will provide the smallest trajectory errors. Examining the correlation of errors for level flight over 20 minutes at 400 knots

shows that errors in the RUC winds have correlation coefficients of approximately 0.45, and the addition of recent MDCRS reduces these coefficients to 0.23. The correlation of errors for a descending flight over 10 minutes at 400 knots shows that errors in the RUC winds have correlation coefficients in the range of 0.29 – 0.39, and the addition of recent MDCRS reduces these coefficients to 0.11. Quantifying the effects of the differing error correlations on trajectories is outside the scope of this study.

United Airlines increased the frequency of their MDCRS reports from May through August of 1997. This allows the study of TW wind field errors vs. number of MDCRS reports, where the number of MDCRS reports is varied from less than the current normal to greater than the current normal. Ten days were chosen for this study. The results show that relative to the current normal level of MDCRS, the extra MDCRS reports reduce the TW RMS vector error by about 0.3 m/s and reduce the TW 90th percentile vector error by about 0.5 m/s. This is considered to be a significant improvement.

5.2. Factors Useful in Real-Time Estimation of Error Magnitude

The errors in both the RUC wind fields and the TW wind fields are seen to increase with increasing wind speed, in part due to an underestimation of wind speed which increases with increasing wind speed. The relationship between the magnitude of the wind error and wind speed is seen by computing wind field errors for different wind speeds and also by comparing the errors computed by month with the monthly mean wind speed. The TW system, as part of its wind field estimation, produces an estimate of the error variance for each estimate of the wind. A relationship is shown to exist between the magnitude of the actual errors in the TW wind field and the TW estimates of the error variance. This relationship is seen by plotting the RMS vector error vs. TW estimate of the RMS vector error. It is also seen by comparing the errors computed by altitude with the mean wind at each altitude and the TW estimate of the RMS vector error at each altitude. The TW vector errors follow the trends in the TW estimates of the RMS vector error more closely than the trends in the wind speed in this comparison.

Different types of weather are also seen to influence wind field accuracy. Altocumulus lenticularis, indicative of mountain waves, is associated with a decrease in wind field errors while precipitation, towering cumulus, and thunder are associated with an increase in wind field errors. Precipitation provides the best signal for increased wind field errors of the four simple weather types studied. The combinations of thunder and towering cumulus and thunder and precipitation are also examined. The combination of thunder and towering cumulus did not provide a significantly better signal than thunder alone. The combination of thunder and precipitation provided the best signal of increased wind field errors of all the weather types and combinations.

5.3. Possible Future Work

This study points to a number of possible improvements to the TW system. The RUC forecast fields along with the current data can be used to produce short-term forecasts of the winds. Improving the error models improves the wind field accuracy and strengthens the relationship between the TW estimate of the errors and the actual errors. The error models used in the TW interpolation can be upgraded to incorporate wind speed. Other weather factors, such as wind field gradients, which are related to measurement representativeness can be incorporated into the error models. Also, the

results on wind speed bias as a function of wind speed can be used to reduce or remove the wind speed bias. The TW analysis or other ITWS algorithms, such as MIGFA[23] could be extended to explicitly incorporate weather, such a frontal passage, which is suspected of being difficult for the current wind prediction/analysis systems.

Further study of the current data set is warranted. An analysis of time-of-flight errors along flight paths would provide a direct link to CTAS performance. The data set can also be used to develop algorithms to predict wind field accuracy in real time. This study could be extended to include other en route sensors such as Doppler wind profiler data. A more detailed study of the relationship between weather phenomena and wind errors could be undertaken.

There are two primary weaknesses in the current study. First, the 60 km RUC will be replaced by the 40 km RUC in the near future. Second, these results do not readily translate to terminal automation because the current study does not utilize Doppler data and because the current study does not analyze the performance of the 2 km resolution TW wind field, both of which are very important in the terminal airspace. These weaknesses will be addressed by extending this study to use the 40 km RUC data, Doppler data, and the full TW system in the Dallas/Ft. Worth (DFW) Center and TRACON.



GLOSSARY

ACLS	Alto cumulus (standing) lenticularis
ATC	Air Traffic Control
ATM	Air Traffic Management
CTAS	Center TRACON Advisory System
DEN	Denver International Airport
DST	Decision Support Tools
FMS	Flight Management System
FSL	Forecast Systems Laboratory
ITWS	Integrated Terminal Weather System
METAR	Aviation Routine Weather Report
mb	millibar
MDCRS	Meteorological Data Collection and Reporting System
MSL	mean sea level
NASA	National Aeronautical and Space Administration
NCEP	National Center for Environmental Prediction
nmi	nautical mile
NEXRAD	NExt generation weather RADar
NOAA	National Oceanic and Atmospheric Administration
NWS	National Weather Service
OI	Optimal Interpolation
PBL	Planetary Boundary Layer
QC	Quality Control
RMS	Root Mean Square
RMSE	Root Mean Square Error
RUC	Rapid Update Cycle
SAS	Statistical Analysis Software
TCU	Towering Cumulus
TRACON	Terminal Radar Approach Control
TW	Terminal Winds

•

•

•

•

REFERENCES

- [1] Denery, D. G. H. Erzberger, "The Center-Tracon Automation System: Simulation and Field Testing," *Proceedings of the advanced Workshop on ATM (ATM 95)*, sponsored by the National Research Council of Italy, Capri Italy; Also published as NASA Technical Memorandum 110366 (1995).
- [2] Seagull Technology, Inc., "Center-TRACON Automation System - Description to Support an Operational Concept Document," 90112-03 (1990).
- [3] Jardin, M.R., and S.M. Green, "Atmospheric Data Error Analysis for the 1994 CTAS Descent Advisor Preliminary Field Test," NASA TM (#TBD), in draft form.
- [4] Williams, D.H. and S.M. Green, "Flight Evaluation of the Center/TRACON Automation System Trajectory Prediction Process," NASA TPA3696, publication pending.
- [5] Benjamin, S., K. Brewster, R. Brummer, B. Jewett, T. Schlatter, T. Smith and P. Stamus, "An Isentropic Three-hourly Data Assimilation System using ACARS Aircraft Observations," *Monthly Weather Review*, 119, 888-906 (1991).
- [6] Benjamin, S. G., K. J. Brundage, P. A. Miller, T. L. Smith, G. A. Grell, D. Kim, J. M. Brown, T. W. Schlatter and L. L. Morone, "The Rapid Update Cycle at NMC," Preprints, *Tenth Conference on Numerical Weather Prediction*, Portland, OR, Amer. Meteor. Soc. (1994).
- [7] Evans, J. E.: Safely reducing delays due to adverse terminal weather. Proc. of the Advanced Workshop on Air Traffic Management ATM95 (to appear), Capri, Italy, Oct (1995).
- [8] Evans, J. E., E. R. Ducot, "The Integrated Terminal Weather System (ITWS)." *Lincoln Laboratory Journal*, Vol. 7, No. 2 (1994).
- [9] Sankey, D. A.: An Overview of FAA-Sponsored Aviation Weather Research and Development, *Fifth International Conference on Aviation Weather Systems*, Vienna, VA (1993).
- [10] Cole, R. E., J. E. Evans, D. A. Rhoda, "Delay Reduction Due to the Integrated Terminal Weather System (ITWS) Terminal Winds Product," *Seventh Conference on Aviation, Range, and Aerospace*, Long Beach, CA (1997).
- [11] Cole, R. E., and F. W. Wilson: The integrated terminal weather system terminal winds product. *Lincoln Laboratory Journal*, Vol. 7, No. 2. (1994).
- [12] Cole, R. E., F. W. Wilson, "ITWS Gridded Winds Product," *Sixth Conference on Aviation Weather Systems*, Dallas, TX (1995).
- [13] Schwartz, B.E. and S.G. Benjamin, "Accuracy of RUC Wind and Aircraft Trajectory Forecasts as Determined from ACARS Observations," report from NOAA/FSL to NASA Ames Research Center, publication pending (1998).
- [14] Brewster, K., S. Benjamin and R. Crawford, "Quality Control of ACARS Meteorological Observations - a Preliminary Data Survey," Preprints, *Third International Conference on the Aviation Weather System*, Anaheim, CA (1989).
- [15] Merritt, M.W., D. Klinge-Wilson, and S.D. Campbell, "Wind Shear Detection with Pencil-beam Radars," *Lincoln Laboratory Journal*, Vol. 2, No. 3 (1989).
- [16] Crum, T.D. and R.L. Alberty, "The WSR-88D and the WSR-88D Operational Support Facility," *Bull. Amer. Meteor. Soc.*, Vol. 74, No. 4, 645-653 (1993).

- [17] Wilson, F.W. and R.H. Gramzow, "The Redesigned Low Level Wind Shear Alert System," *Fourth International Conference on the Aviation Weather Systems*, Paris (1991).
- [18] ASOS Program Office Staff, "Automated Surface Observing System Users Guide – Preliminary," National Weather Service ASOS Program Office, 84 pp. [Available from NWS ASOS Program Office, Silver Spring, MD 20910] (1991).
- [19] Gandin, L.S., "Objective Analysis of Meteorological Fields," Leningrad, translated by Israel Program for Scientific Translations, Jerusalem, 1965 (1963).
- [20] Daly, R., "Atmospheric Data Analysis," Cambridge University Press, Cambridge (1991).
- [21] Armijo, L., "A Theory for the Determination of Wind and Precipitation Velocities with Doppler Radars," *Journal of Atmospheric Sciences*, **26**, 570–573 (1969).
- [22] Luenburger, D.G., *Optimization by Vector Space Methods*, Wiley, New York (1969).
- [23] Troxel, S., R. L. Delanoy, "Machine Intelligent Approach to Automated Gust Front Detection for Doppler Weather Radars," *SPIE Proceedings – Sensing, Imaging, and Vision for Control and Guidance of Aerospace Vehicles*, Vol. 2220, 182–192, Orlando, FL (1994).